5-2012

Assembly and Disassembly of Myofibrils in Dissociated Cardiomyocytes

Honghai Liu
Clemson University, physhhliu@gmail.com

ASSEMBLY AND DISASSEMBLY OF MYOFIBRILS IN DISSOCIATED CARDIOMYOCYTES

A Dissertation
Presented to
the Graduate School of
Clemson University

In Partial Fulfillment
of the Requirements for the Degree
Doctor of Philosophy
Bioengineering

---

by
Honghai Liu
May 2012

Accepted by:
Bruce Z. Gao, Ph.D, Committee Chair
Thomas K. Borg, Ph.D
Delphine Dean, Ph.D
Dan Simionescu, Ph.D

ABSTRACT

Significance

1) We have developed a hybrid TPEF-SHG imaging system with an onstage incubator for long-term living-cell imaging. Using the imaging system, the assembly of myosin filaments onto the myofibrils can be investigated without fluorescently labeling the specific proteins, which enabled us to study the dynamic process of the assembly and dedifferentiation of myofibrils in living cardiomyocytes without labeling any sarcomeric proteins for long time.

2) We observed the addition of new sarcomeres during myofibrillogenesis while neonatal cardiomyocytes were spreading on the substrate for up to 10 hours under the customized TPEF-SHG imaging system. New-sarcomere addition at both the ends and the sides of existing myofibrils and at the interstice of several separated myofibrils have been observed. Mature myofibrils were proposed to act as templates for the myofibrils forming adjacently. Our observation indicates that the assembly of myosin filaments onto a myofibril involves the initial redistribution of Z-body proteins to ultimately form mature Z-discs.

3) We dynamically investigated the dedifferentiation of cultured adult cardiomyocytes. The myofibrils were found to first shrink to shorter the sarcomere length, then the striated structure of myofibrils was wrecked from the cell ends and then to the whole cell. Results suggest that the striated patterns of different sarcomeric components were not affected simultaneously during dedifferentiation. The striated pattern of myosin filaments was

wrecked first, which was followed by the wreck of the striated F-actin pattern, then alpha-actinin.

Value

1) The lateral assembly of myosin filaments onto the current mature myofibrils, and redistribution of Z-bodies while myosin filaments were assembling to the current myofibrils to cause the mature of myofibrils were first observed in our research, and which has extended the understanding on the myofibrillogenesis in cardiomyocytes.

2) Dynamic remodel of myofibrils and redistribution of sarcomeric proteins in the cultured adult cardiomyocyts under dedifferentiation may promote the understanding on the development of cardiomyopathy and provide methods to assess the developing heart diseases.

DEDICATION

This work is dedicated to my parents; my sisters, Hongyun Liu and Hongxiang liu; and my wife, Yumei Zhao.

ACKNOWLEDGMENTS

I would like to acknowledge my advisor, Dr. Bruce Gao. I had a previous degree in science of physics and materials. But I didn't have any knowledge of biomedicine and experience of engineering before I came to Clemson. Dr. Gao was the one who introduced me to the field of biomedicine and encouraged me to practice different techniques and principles of engineering. He has given help to my life in US as much as, if not more than, in my academic research. His way to organize the projects taught me that cooperation and patience are the most important thing in scientific research and which will benefit my career life in the future.

I would like to acknowledge my committee, Dr. Thomas K. Borg, Dr. Delphine Dean, and Dr. Dan Simionescu for their time, guidance and patience.

I would like to acknowledge Dr. Martine Laberge for all her assistance to my degree program in Clemson.

I would like to acknowledge Ms. Jenny Bourne and Ms. Cassie Gregory, for the friendship and help they gave to me. Jenny provided me a lot of assistance in composing manuscripts for publication. Cassie was always ready to offer me research advice and assistance.

I would like to acknowledge Ms. Maria Martin for her irreplaceable assistance, without which I would not have finished my program in Clemson.

Finally, I would like to acknowledge all the members in the Biophotonics Lab, for their cooperation and friendship.

TABLE OF CONTENTS

Page

TABLE OF CONTENTS

(Continued)

Page

LIST OF FIGURES

LIST OF FIGURES (Continued)

Figure Page

LIST OF FIGURES (Continued)

Figure Page

LIST OF FIGURES (Continued)

Figure Page

LIST OF FIGURES (Continued)

Figure Page

LIST OF FIGURES (Continued)

Figure Page

LIST OF FIGURES (Continued)

Figure Page

CHAPTER ONE

INTRODUCTION

As the basic unit of the functional structure for the contraction of cardiomyocytes, sarcomeres play central role in myofibrils and are related to many heart diseases. Mutations in sarcomeric proteins may induce cardiomyopathies [1, 2]. Sarcomeric proteins normally assemble together to play physiological function as integral functional groups, such as Z-discs, thick filaments and thin filaments, etc. Mutation in anyone of those sarcomeric proteins may impact the normal functions of groups in which the protein is involved, such as that in thick filaments [3-7], thin filaments [8, 9] and Z-discs [10, 11]. The impacted functional groups then affect the basic physiological functions of sarcomeres and induce cardiomyopathy. Stimulations that do not affect genes may also induce cardiomyopathies. Such as cardiac hypertrophy induced by pressure overload [12-14], volume overload [15-17], and chemicals [18, 19]; and heart failure caused by chemicals [20]. All the cardiomyopathies are related to abnormity of the cardiac contraction system, which is dependent on the assembly and remodel of myofibrils. Therefore, knowledge on the assembly and remodel of myofibrils in cardiomyocytes, under normal and abnormal physiological environments, is important for understanding the mechanism of cardiomyopathies and developing therapeutic techniques. It has been known that increased diastolic strain causes cardiomyocytes to elongate by adding sarcomeres in series, and continued systolic stress causes cardiomyocytes to thicken by adding sarcomeres in parallel [21]. However, more efforts are still needed to make a

complete understanding on the assembly, the response to stimulus, and the remodel of myofibrils. The assembly (myofibrillogenesis) and disassembly (dedifferentiation) of a myofibril are at the central position of the research.

STRUCTURE OF SARCOMERE

Sarcomere is the functional unit for the contraction of myofibrils. It longitudinally repeats along myofibrils, with each sarcomere connected by a Z-disc at each ends. Three types of filamentous structures are involved in the formation of sarcomeres, they are thin, thick, and titin filaments. The thin filament includes double-strand actin filaments, tropomyosin which binds to the side of adjacent actin filaments along the groove of the helix to stabilize and stiffen the actin filament [22], the troponin complex which is composed of troponin T, troponin C and troponin I. The coordinated interaction among actin, tropomyosin and troponin permits and influences actin-myosin reactions (actomyosin) triggered by Ca^{2+}. The thin filaments are anchored at the Z-discs via their barbed ends, which are capped by CapZ and cross linked by α-actinin. The pointed ends of thin filaments extend toward the middle of the sarcomere, where the thin filamens are capped by Tropomodulin. The thick filaments consist of primarily the protein myosin which are bundled at the coiled rod region and arranged tail-by-tail to form bipolar filaments with myosin heads oriented in opposite directions at the two ends of the filament. The thick filaments are connected with each other by myosin binding protein C (MyBP-C) and myomesin, and aligned at the middle of the sarcomere by titin, which is the third primary filament in sarcomere. Titin spans the half-sarcomere with its N-

terminal at the Z-disc and its C-terminal at the M-line [23, 24]. The section of titin between Z-disc and one end of myosin filament is located in half length of I-band, which contributes to force transmission at the Z-disc and releasing tension in the I band region. The other section of titin is bound with myosin filaments through accessory proteins (myomesin, etc.) to form A-band.

Thin Filaments

Thin filaments contain three types of primary proteins - actin, tropomyosin, and troponin-complex. Actin is the major component of the thin filaments in muscle. An individual actin molecule is an egg-shaped unit formed by coiled single protein chain, called globular actin (G-actin). Under proper conditions, G-actins assemble into fibrous form (F-actin), which is the form that exists in the thin filament in muscle. The thin filaments in striated muscle are highly regulated and precisely specified in length, to overlap optimally with the thick filaments for efficient myofibril contraction.

Tropomyosin is a molecule of rod-shaped (~40nm long) and containing two strands of tropomyosin molecules that wound diametrically opposed along the actin filaments. Tropomyosin is located in the groove between the two strands of F-actin in the thin filament. Each tropomyosin molecule is in contact with seven actin units.

Troponin-complex includes three proteins: troponin I, troponin T and troponin C. Troponin I , in coordinated with tropomyosin, regulates the interactions between actin

and myosin. When a cardiomyocyte is in relaxing state, troponin I binds tightly to actin filament in a conformation that causes tropomyosin to block the myosin-binding sites of the actin filament. Troponin binds to tropomyosin to form a troponin-tropomyosin complex and mask the interaction between myosin and actin.

Nebulette is an isoform of the protein nebulin and expressed in cardiac muscle. Nebulette is identified in the primary cultures of chicken embryonic cardiomyocytes [25]. Nebulette is involved in early myogenesis and myofibrillar organization in cardiomyocytes [26]. Research has found that nebulette is essential for the assembly and contractile function of myofibrils [27]. Mutation of nebulette is associated with dilated cardiomyopathy [28]. Nebulette interacts with many thin filament-associated and Z-disc–associated proteins [29], and it is also important for the maintenance of tropomyosin, troponin and the length of thin filament [30].

Tropomodulin is a protein that binds and caps the pointed end of actin and regulates the length of actin filaments in muscle and non-muscle cells. Through combining with Leiomodin2, tropomodulin caps the pointed ends of the sarcomeric thin filaments in cardiac muscle, and plays important role in myofibril assembly and thin filament length regulation [31].

Leiomodin is a muscle-specific F-actin-nucleating protein that is related to tropomodulin at the pointed end of F-actin [31]. Overexpression or depletion of leiomodin dramatically

affects the structure and organization of sarcomeres. Overexpression of leiomodin in embryonic chick cardiomyocytes displaced tropomodulin from the pointed ends of thin filaments and led to the elongation of the thin filaments [32], while depletion/knockout of leiomodin causes the cardiomyocytes lacking organized sarcomeres, and makes the Z-disc protein α-actinin concentrating in small spots, rather than the typical striated pattern that observed in normal cells [33]. All these results suggest that leiomodin plays a role in sarcomere assembly and organization.

CapZ, located in the Z-disc, is a protein that caps the barbed end of actin filaments in muscle cells. The CapZ obtained its name because of its presence at the Z-disc of the sarcomere [34] and each CapZ molecule caps one barbed end of thin filament at Z-disc [35]. Research suggested that CapZ may first be localized to the Z-disc before it nucleates the actin filaments to cause the thin filaments mature [36].

Thick Filaments

The thick filaments primarily consist of myosin molecules, which are bundled at the coiled rod region and arranged tail-by-tail to form bipolar filaments with myosin heads oriented in opposite directions at the two ends of the filaments. The thick filaments are connected with each other by myosin binding protein C (MyBP-C) and myomesin and are aligned at the middle of the sarcomere by titin, which is the third primary filament in a sarcomere. Titin spans the half-sarcomere with their amino termini at the Z-disc and their carboxyl termini at the M-line [23, 24]. The section of titin between the Z-

disc and one end of myosin filament is located in half length of the I-band, which contributes to force transmission at the Z-disc and resting tension in the I-band region. The other section of titin interacts with myosin filaments through accessory proteins (myomesin, etc.) to form the A-band.

Myosin is a family of ATP-dependent motor proteins and are well known for their role in muscle contraction and involvement in other motility processes of eukaryotic cells. The myosin-related motility is carried out through myosin's interaction with actin filaments. Myosin constitutes a large superfamily of proteins [37], among which superfamily, muscle myosin II is the myosin type that is responsible for producing muscle contraction in muscle cells [38]. Each muscle myosin II molecule contains two heavy chains (the heads of myosin II), four light chains, and a tail of the elongated molecule that is a coiled coil wounded by two alpha-helical chains. The long coiled-coil tails of the individual myosin molecules join together with titin molecule, assisted by accessory molecules (myomesin, etc.), forming the thick filaments of the sarcomere and defining the A-band region. The head domains of myosin molecule stick out from the side of the thick filament, produce forces by "walking" along the adjacent actin-based thin filaments in response to the proper chemical signals [39].

M-band (or M-line) is the name of the structure that appears as a series of dark lateral lines at the center of the A-band. The location of the M-band implies that it is needed for the regular packing of thick filaments [40]. It has been suggested that M-band plays

important roles in myofibrillogenesis during the nascent thick filaments are assemble and aligned onto regular hexagonal lattice [41, 42]. The M-band contains two principal proteins for the role of M-bridges, which were originally named as myomesin [43, 44] and M-protein [45, 46]. The M-band bridges ensure the regular packing of myosin filaments, which is similar to Z-discs that anchor the actin filaments, are very important for the stability of sarcomere during muscle contraction. At M-band, the centers of myosin filaments are crosslinked into a mechanically stable network that involves titin, myomesin [47], and obscurin [48], with the obscurin acting as a linker to the sarcoplasmic reticulum (SR) [49]. Several proteins including myomesin-1, myomesin-2 (M-protein) [44], myomesin-3 [50], obscurin [48], muscle-type creatine kinase (MM-CK) [51] and the C-terminal fragment of titin [52] are localized in the M-band. A new heart- and muscle-specific protein, myomasp, has recently been proved to be a previously unrecognized component of an M-band–associated signaling pathway that regulates cardiomyocyte gene expression in response to biomechanical stress [53].

Myomesin is a protein found in the M-band of sarcomeres in association with M-protein. It is the principal thick filament crosslinking protein, analogous to alpha-actinin in the Z-disc [54], and thought to be involved in anchoring myosin filaments to titin [48, 55]. Studies on myofibrillogenesis have shown that myomesin becomes localized in its characteristic pattern simultaneously with the appearance of the earliest sarcomeres [56]. The elastic function of myomesin has been found through AFM technique [57]. Single molecule mechanical experiments showed that embryonic myomesin isoform may

increase extensibility [57, 58], and the myomesin filament can be stretched to about 2.5-fold its original length by reversible unfolding [59]. Those results suggested that, similar to titin, myomesin is also a molecular spring.

Obscurin is a sarcomeric protein found in both skeletal and heart muscles, predominantly related with the M-band in mature myofibrils. It was initially discovered as a ligand of titin in Z-disc [60, 61]. Obscurin has been proposed to play an indispensable role in the assembly and organization of myosin into regular A-bands during cardiac myofibrillogenesis [62, 63].

Myosin binding protein C (MyBPC) is a thick filament protein in sarcomeres and known to interact with all the three primary filaments in sarcomeres: myosin and actin filaments [64-66], and titin [65]. Based on chromosome-related research, three MyBP-C isoforms have been identified: cardiac, slow skeletal, and fast skeletal (cMyBP-C, sMyBP-C, and fMyBP-C) [67, 68]. MyBP-C is believed to play two major roles in the organization of sarcomeres: regulating organization and stabilization of thick filaments; and modulating the formation of cross-bridges between myosin and actin through direct interacting with both filamentous systems [69, 70].

Z-disc

Z-disc is a fine dense region in sarcomeres appearing under Transmission Electron Microscopy (TEM). Z-discs form the boundaries between sarcomeres in striated

muscles. Z-disc originates from alpha-actinin-centered mini-bodies [71] and finally becomes a crosslinked complex consisting lots of proteins. As the lateral boundary between sarcomeres, Z-disc is the anchoring plane of thin (actin) filaments. Titin and actin filaments from opposing sarcomere halves crosslinked through tight interactions with α-actinin [72, 73]. The intermediate filament desmin, which connects neighboring myofibrils to form well-aligned muscle bundles [74-76], is also connected with Z-discs, through the accessory protein plectin [77]. The association of plectin with Z-discs has been proved to be an early event in the lateral alignment of myofibrils that precedes the formation of the inter-myofibrillar cytoskeleton of desmin [78]. Besides the structural role of Z-discs that they integrate sarcomeres together, Z-discs are also involved in mechanical sensitivity system [79] and intra-/inter- cellular signalling pathways [79-81].

ASSEMBLY OF SARCOMERIC PROTEINS ONTO SARCOMERES

Myofibrillogenesis is the process that all the sarcomeric proteins, thin/thick filaments, alpha-actinin and other sarcomeric accessory proteins are assembled to form myofibrils. Myofibrillogenesis is essential for the understanding of heart-muscle formation and remodel in myocardium hypertrophy. However, a complete model that can be used to describe the entire myofibril-formation has not been built yet. One of the most unclear issues in myofibrillogenesis is how new sarcomeres are added to the current mature myofibrils. It has been accepted that subunits of the sarcomeres assembled separately before constructed into mature sarcomeres [82, 83]. Several models have been proposed to describe how these separately formed subunits are assembled onto mature

myofibrils (See the articles [84-86] and the references cited therein). The main points of those models can be described as: (1) *template model* that stress fiber-like structures were considered as templates or scaffolds to recruit the components of the future myofibrils, such as dense components of the Z-band (I-Z-I body-like complex), and thick filaments, for the assembly of myofibrils; (2) the *"stitching" model* in which I-Z-I bodies, the future I-Z-I bands, were formed independently from myosin filaments and then stitched together with thick filaments by titin to promote the assemble of mature myofibrils [87-89]; (3) *premyofibril model* proposed three distinguishable stages (premyofibrils to nascent myofibrils and then mature myofibrils) to describe the assembly and maturation of myofibrils. Non-muscle myosin IIB plays important role in the early stages of myofibril assembly by assembling thin filaments and Z bodies, the precursor of Z-discs, to form aligned premyofibrils. Non-muscle myosin IIB then will be replaced by muscle myosin II in the later stages, which promotes the maturation of myofibrils [90, 91].

Models of Myofibrillogenesis

Stress Fiber Template Model

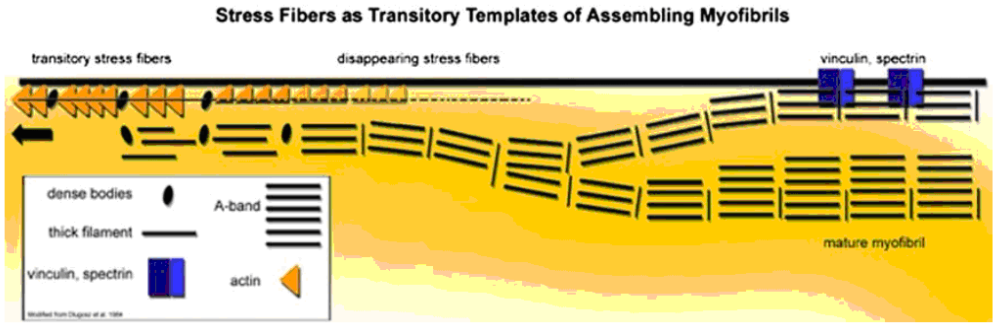

Figure 1.1 Stress fiber template model [85]

In this model, it is proposed that the components of the future myofibril, including dense components of the Z-band, thin and thick filaments, are recruited to the surfaces of stress fibers or stress fiber-like structures in the developing muscle cell (Figure 1.1), with each stress fiber-like structure serving as a temporary template for the elements necessary to form myofibrils. At the completion of assembly, the old stress fiber template disappears and whose components then reassemble into new stress fibers and serve as a template for the assembly of new myofibrils. It is now known that the stress fiber-like structures in muscle cells are composed of a number of muscle specific proteins, such as alpha-actinin, tropomyosin, troponins, and tropomodulin, with nonmuscle or cytoplasmic myosin II the only nonmuscle protein isoform envolved. A potential problem in this template model, as mentioned by Sanger et al. , is that the stress fibers themselves are sarcomeric, and are presumably formed in the absence of a template for their own assembly. The sarcomeric bands of the stress fiber-like structures are also smaller than the 2~2.5 μm mature myofibril sarcomeric sizes, so it is difficult to see how they would provide the template spacing information for myofibrils.

Stitching model

The stitching model was first proposed by Holtzer et al. . They postulated that I-Z-I bodies and thick filaments assemble independently. Titin molecules stitch together the scattered I-Z-I bodies and thick filaments into elongating mature myofibrils (Figure 1.2). Myofibrils were then predicted to elongate through assembling thick filaments and I-Z-I

bodies to the ends of the current myofibrils [92]. This model was initially proposed for myofibrillogenesis in cardiac muscle cells [92], then extended to skeletal muscle cells [88]. Nonmuscle myosin II was not detected in association with the I-Z-I bodies in cardiac muscle cells [92].

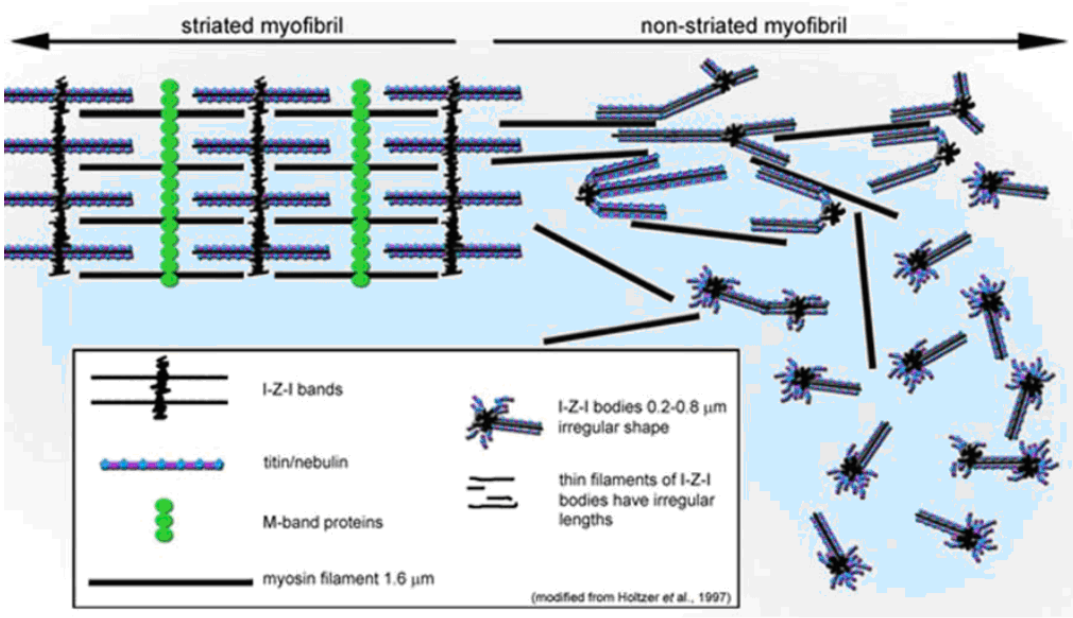

Figure 1.2 Stitching model [85]

Premyofibril model

The premyofibril model (Figure 1.3) was first proposed through analyzing the formation of myofibrils in the spreading embryonic chick cardiomyocytes [90]. The premyofibril model describes myofibrillogenesis in three continuous stages: premyofibrils to nascent myofibrils and to mature myofibrils. The premyofibrils are composed of periodic appearing mini bodies that connected by nonmuscle myosin IIB

and titin at the spreading edges of cardiomyocytes. Those mini bodies are composed of alpha-actinin (Z-bodies) and will mature into Z-discs in late stages.

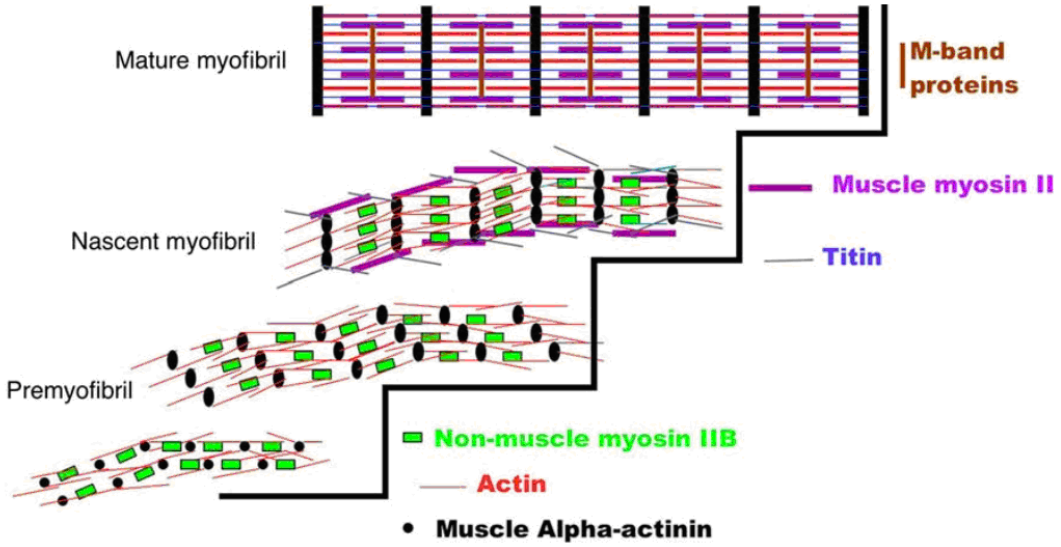

Figure 1.3 Premyofibril model [85]

Non-muscle myosin II filaments interdigitate with actin filaments that contain muscle isoforms of troponins and tropomyosin. The barbed ends of the actin filaments are embedded in the Z-bodies of the premyofibrils. In the earliest steps, the premyofibrils associate at the level of the Z-bodies. Muscle myosin II then begin to assemble onto the premyofibrils via substituting the nonmuscle myosin IIB to promote the premyofibrils to evolve to a stage termed nascent myofibrils, then reach the final mature myofibril stage when all the nonmuscle myosin IIB has been replaced by muscle myosin II. The muscle myosin II is in a continuous linear pattern along the nascent myofibrils while it is immuno-fluorescently stained with antibody, which is possibly caused by the overlap of thick filaments. In the progression from nascent myofibrils to mature myofibrils, the Z-

bodies transform from aligned mini bodies to Z-lines or Z-bands, the muscle myosin II filaments align into A-bands, and non-muscle myosin II is no longer detected at this stage. It is unclear how nonmuscle myosin IIB is replaced by muscle myosin II during nascent myofibril stage. M-band proteins are present in the A-bands of the mature myofibrils, and may be responsible for the final alignment of the thick filaments. Based on the results obtained from the research on GFP-labeled alpha-actinin in living cardiomyocytes, Sanger *et al.* [85] proposed that in living cells myofibrils did not elongate by the serial addition of sarcomeres, but by deposition of premyofibrils that grow and fuse laterally with existing myofibrils to result in elongated myofibrils. They claimed that these observations of living cells were incompatible with both stress fiber template model and stitching model, both models being based on studies of fixed and stained cells.

Premyofibril model is currently widely accepted and consistent with most of the published experimental results. However, three problems still have not been resolved in the current model: 1) the initial step of myofibrillogenesis, or what factors may ignite the the construction of premyofibrils? 2) How can the myofibrils be aligned in the same direction along the axis of cardiomyocytes, or what's the factors that determine the orientation of the myofibrils? 3) How the new sarcomeres are added to the current myofibrils to elongate or thicken the myofibrils?

Through reviewing the published reports, Sparrow and Schöck [71] appended an initial step to extend the premyofibril model, which suggested that integrin, a cell membrane embedded molecule, might be the starting point of myofibrillogenesis.

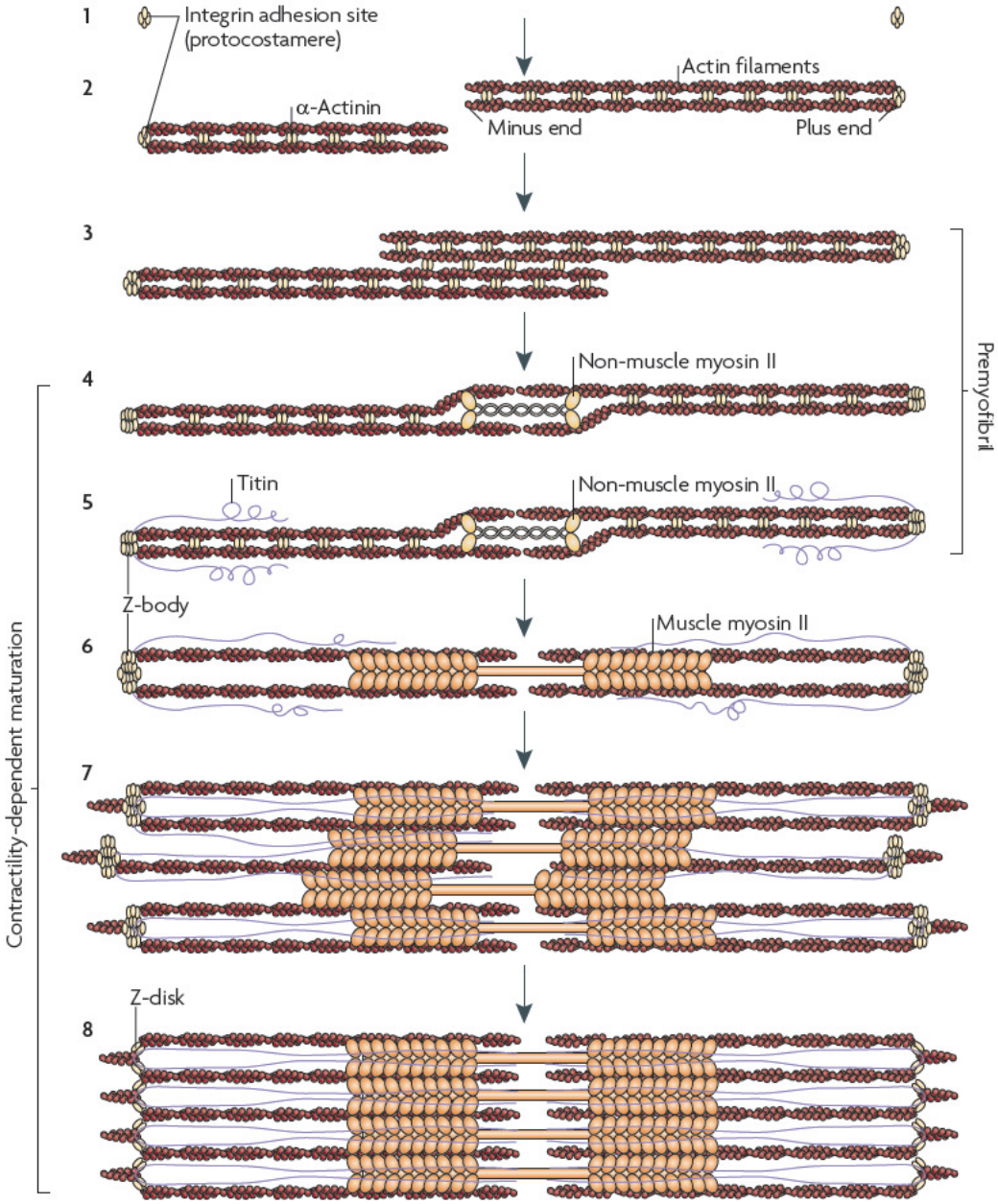

Figure 1.4 Extended premyofibril model [71].

Extended premyofibril model

Figure 1.4 describes the basic steps of the extended premyofibril model. First, the integrin adhesion sites (protocostameres) form at random positions along the muscle cell to polymerize actin filaments (step 1 and 2). When the actin filaments connecting different protocostameres get overlapped in opposing polarity, those actin filaments will fuse through α-actinin-mediated crosslinking (step 3). The α-actinins in the overlapped area of the laterally fused actin filaments are substituted by the incorporated non-muscle myosin II (step 4). Then titin and more α-actinin are incorporated into the Z-bodies (step 5). Bipolar muscle myosin II filaments are then incorporated into the premyofibril to form nascent myofibrils (step 6). The correct space between the two neighboring Z-bodies (the length of the future mature sarcomere) along the orientation of the actin filaments is mediated by both titin and actin filaments, until the length of actin filaments maturates into the final length of the thin filaments in mature sarcomere(step 7). The Z-bodies are now connected and coalesced to their neighboring Z-bodies perpendicular to the orientation of the actin filaments to form the mature Z-discs, through contractility-dependent maturation (step 8).

Chaperone Proteins Involved in Myofibrillogenesis

The description on myofibrillogenesis in aforementioned models is focused on assembly of central sarcomeric components, such as thin and thick filaments, alpha-actinin. However, in the recent research, more efforts have been put on the transient proteins playing the role of scaffold to assist assembling the central contractile

sarcomeric components and the accessory proteins that bind those contractile sarcomeric components together at sarcomeric functional groups such as Z-disc and M-line. N-RAP, as scaffolds close to the cell periphery, participates in assembly of α-actinin and actin to form I-Z-I bodies, the precursors of Z-discs in mature myofibrils, which occurs in the early steps of myofibrillogenesis [93]. The formation of nascent myosin filaments was found to be associated with the chaperone proteins Hsc70 and Hsp90 before their incorporation into sarcomeres [94]. Nonmuscle myosin IIB has been suggested to be involved into myofibrillogenesis in the premyofibril stage, and then replaced by muscle myosin II in later stages via some mechanisms not clear [71, 86]. Recent research found that nonmuscle myosin IIB played a role in cardiomyocyte spreading, and the protein levels of nonmuscle myosin IIB and N-RAP were tightly linked in cardiomyocytes [95]. Krp1 was found to promote the adjacent thin periodic myofibrillar structures fusing laterally to form wide mature myofibrils [93]. Krp1, N-RAP, Hsc70 and Hsp90 are all transiently associated with myofibrillar structures to promote specific steps in the myofibril assembling pathway. Obscurin is a component of mature myofibrils, and which was thought to link the sarcoplasmic reticulum through interaction with ankyrin 1[96]. Obscurin plays a role in promoting the integration of thick filaments with I-Z-I structures, with titin is associated with the myosin filaments along their length. Obscurin mediated incorporation of myosin filaments has been found to occur downstream of N-RAP-mediated assembly of α-actinin and actin, but upstream of Krp1-mediated lateral fusion of fully formed thin myofibrils [93].

DEDIFFERENTIATION OF CARDIOMYOCYTES

Since viable adult ventricular cardiomyocytes were dissociated and cultured [97], the primary cultured adult cardiomyocytes have been used in the research of cardiology and cardiopathology as a model of myocardium [98-100]. However, the fresh dissociated adult cardiomyocytes undergo dedifferentiation while they are cultured in vitro. When dissociated adult cardiomyocytes are cultured at substrates, their rod-shape morphology becomes round and then they spread again at the surface of the substrates with their rod-shape morphology totally lost [101]. During which process, myofibrils were found to break down and rebuild [102] through studies by means of electron microscopy [103, 104] and immunofluorescence microscopy [104, 105]. Using antibodies to myosin, titin, actin and alpha-actinin, those sarcomeric proteins were found to become disorganized into amorphous form in various shapes of cardiomyocytes [105]. However, a complete understanding of the breakdown and rebuild of myofibrils in cultured adult cardiomyocytes depends on the knowledge from the study on myofibrillogenesis in embryonic and neonatal cardiomyocytes.

The adult cardiomyocytes under dedifferentiation lose their rod-shape morphology and the striated myofibril structure. And accordingly, their normal physiological functions change [98, 106-109]. Dissociated cardiomyocytes exhibit stable contractile performance with maintained capacity to respond to inotropic stimulus within short time, and have been applied to investigate intrinsic and extrinsic influences on the contractility of left ventricular cardiomyocytes in human beings [110]. However, research has demonstrated that measuring contractile properties of cardiomyocytes may not be a

reliable method in assessing cultured cardiomyocytes [111], since the current under cell membrane may change in short time due to the detubulation of the cultured adult cardiomyocytes [111-113]. The losing rate of T-tubule (detubulation) is species dependent [114]. The detubulated rat myocytes can be acutely paced even after 72 h in culture, whereas mouse cardiomyocytes fail to follow pacing after only 24 h in culture. The change of dissociated adult cardiomyocytes in morphology and physiological functions weakens the advantages of the cells as ideal in-vitro model of the cardiomyocytes in myocardium. Therefore, preventing the dedifferentiation of the dissociated adult cardiomyocytes is necessary when the cells are in-vitro studied as a substitution of in-vivo cardiomyocytes. Efforts have been made to build culture models of adult cardiomyocytes, with the morphology [115], contractile function [116], signaling system [117, 118], and other in-vivo characters of the dissociated adult cardiomyocytes being preserved for longer time.

Doesn't like the disadvantages mentioned above, dedifferentiated cardiomyocytes were considered to be in an adaptive state [119], and the dedifferentiation of cardiomyocytes may also be an advantage which enables the cardiomyocytes to survive under unfavorable circumstances [120, 121]. Further study shows that limited dedifferentiation may stimulate the zebrafish cardiomyocytes re-enter the cell cycle and regenerate muscle cells in the amputated hearts [122].

Adult mammalian cardiomyocytes have been considered to be terminally differentiated. Recent studies indicated that partial dedifferentiation can also facilitate the proliferation of mature adult cardiomyocytes in myocardium [123, 124].

Dedifferentiation of cultured adult cardiomyocytes that is similar to in-vivo dedifferentiation of adult cardiomyocytes was found can be induced by co-culturing the dissociated adult cardiomyocytes with cardiac fibroblast [125]. Therefore, co-culture of cardio- myocytes and fibroblasts can be an important tool for investigating possible triggers for the progression of dedifferentiation in vivo, which may promote the study on the regeneration of injured heart muscle. However, a recent study postulated that dedifferentiation of cardiomyocytes initially protects stressed hearts by reducing contractile force but fails to support the cardiac structure and function upon continued activation[126]. Therefore, the initial benefit of cardiomyocyte dedifferentiation in situations of acute myocardial damages will turn into a major burden in chronic disease.

Most of the pathological evolutions of cardiac function, if not all, is related with the assembly, disassembly and remodel of myofibrils. Understanding the detailed features on the disassembly of sarcomeric components of myofibrils while cardiomyocytes are under dedifferentiation will provide us the ability to precisely distinguish the stages or degrees of the cardiomyocyte dedifferentiation, which will promote our understanding on the mechanism of cardiamyopathies and development of therapeutic techniques for heart diseases.

CURRENT PROBLEMS

According to the aforementioned discussion, two questions are still remained on the understanding of myofibrillogenesis and dedifferentiation of cardiomyocytes. One is that how new sarcomeres are added during myofibrillogenesis, the other one is that

what's the temporal sequence that different sarcomeric proteins are disassembled from myofibrils during dedifferentiation. The way that new sarcomeres are added has been considered to be the direct cue to understand the mechanism of cardiac hypertrophy, since cardiomyocytes elongate in response to increased diastolic strain by adding sarcomeres in series, and thicken in response to continued systolic stress by adding filaments in parallel [127]. However, the different components assembling into new sarcomeres are not added to the existing myofibrils simultaneously. Different sarcomeric components are assembled onto the existing myofibrils successively in time order, as that described in aforementioned models. The assembly of thick filaments was believed to be one of the last events leading to the maturation of sarcomeres [128, 129], which is also where the major difference between the aforementioned models for myofibrillogenesis is located, that is how myosin filaments are assembled into the nascent myofibrils. Therefore, investigation on the assembly of myosin filaments may promote the understanding on myofibrillogensis and conciliate the divarication among the current models. Immunocytological research on the assembly of myosin filaments has improved our understanding on myofibrillogenesis[91]. The disadvantage of immunofluorescence method is that the fluorescently labeled myosin proteins will fluoresce but not distinguish whether the proteins have been assembled onto myosin filaments or not.

Second harmonic generation (SHG) is intrinsic to a specific structure and the SHG signal has been found to arise from the coiled rod region of myosin thick filaments [130], which enables the study of dynamical assembly of a myofibril without any protein labeling [130-132]. Through combing TPEF and SHG (TPEF-SHG) technique, more

structural information can be obtained from a cardiomyocyte [133, 134], which is ideal for tracking how specific sarcomeric proteins are assembled onto the myofibrils during myofibrillogenesis. Dynamic sarcomere contractions in a cardiomyocyte were recorded for up to several minutes using SHG [131], and the cardiomyocyte remained alive during imaging. However, myofibrillogenesis (i.e., the addition of new sarcomeres) is a process that spans hours to days. Normal physiological conditions (temperature, humidity, pH value, etc.) and appropriate laser power are necessary to maintain normal physiological processes inside the cardiomyocytes while myofibrillogenesis is recorded. Therefore, an incubating system that provides the required physiological conditions is required in the study of myofibrillogenesis.

Although the structure [135, 136], electro-physiological properties [106] and other cell functions of cardiomyocytes under dedifferentiation have been intensively studied, the dynamical structure change and redistribution of sarcomeric proteins in dedifferentiating adult cardiomyocytes, under mechanical or chemical stimulus, are not known.

RESEARCH OVERVIEW

The Long Term Goal

The long term goal of my research is to build a dynamic model of myofibrillogenesis, which should include the following features:

1) Describe the positions of all the sarcomeric proteins in myofibrils, and the roles those proteins play in sarcomeres and myofibrils;

2) Describe the temporal sequence for the sarcomeric components to assemble onto sarcomeres and myofibrils, and the role of related chaperone proteins play in this process;

3) Simulate the responding process of myofibrils to various (mechanical, electrical and chemical, etc.) stimuli;

The Goal In Our Current Research

The goal is to visualize the addition and disassembly of myosin filaments to and from the current mature myofibrils, respectively. To achieve this goal, we focus the research on the following aims:

Aim 1 Build a hybrid TPEF-SHG imaging system, and combine the imaging system with an onstage incubator, in which cardiomyocytes can be cultured under the TPEF-SHG imaging system while the dynamic process of myofibrils are studied in live cell culture.

Aim 2 Determine how myosin is assembled onto the myofibrils during myofibrillogenesis. The pattern of myosin filaments represented by the SHG signal will be monitored through the SHG channel of the imaging system, the dynamic change of which pattern will be recorded through the time lapse at specific intervals.

Neonatal cardiomyocytes are applied since fresh dissociated neonatal cardiomyocytes are in dedifferentiated status and redifferentiate while they are spreading the surface of the substrate, where myofibrillogenesis appears. The results from the TPEF-SHG imaging system are compared and analyzed with that from the immunocytological experiments, with the sarcomeric proteins fluorescently labeled and

the images of which acquired from a Nikon Eclipse T*i* confocal system. Relationship between the myosin filaments and other sarcomeric proteins during myofibrillogenesis will be analyzed.

Aim 3 Determine how myosin is disassembled from the myofibrils during dedifferentiation of cultured cardiomyocytes. Same image acquiring procedures in Aim2 are repeated. In this aim, fresh dissociated adult cardiomyocytes are applied. The disappearance of the striated structure of myofibrils during dedifferentiation is analyzed. The redistribution of sarcomeric proteins during dedifferentiation of cultured adult cardiomyocytes is studied. The relationship between myosin filaments and other sarcomeric proteins during dedidifferentiation is studied.

Based on the research results, we propose a model to describe how the myosin filaments are assembled into the sarcomere and how orientation of myofibrils is regulated during the formation of myofibrils, as well as the dynamic process of the dedifferentiation of cultured adult cardiomyocytes and the disassembly of sarcomeric proteins.

Innovation of the research

We have developed a hybrid TPEF-SHG imaging system with an onstage incubator for long-term living-cell imaging. Using the imaging system, the assembly of myosin filaments onto the myofibrils can be investigated without fluorescently labeling the specific proteins, which enabled us unique ability in studying the dynamic process of

the assembly and dedifferentiation of myofibrils in living cardiomyocytes without labeling any sarcomeric proteins for a prolonged period.

Significance of the research

1) We found new-sarcomere addition at both the ends and the sides of existing myofibrils and at the interstice of several separated myofibrils have been observed. Mature myofibrils were proposed to act as templates for the myofibrils forming adjacently. Our observation indicates that the assembly of myosin filaments onto a myofibril involves the initial redistribution of Z-body proteins to ultimately form mature Z-discs. Our research illumines the assembly of myosin filaments onto the myofibrils, which is lacked in the previous research.

2) We found that the striated patterns of different sarcomeric components were not affected simultaneously during dedifferentiation of adult cardiomyocytes. The striated pattern of myosin filaments was wrecked first, which was followed by the wreck of the striated F-actin pattern, then alpha-actinin.

CHAPTER TWO

BUILD OF ONSTAGE INCUBATOR-COMBINED TPEF-SHG IMAGING SYSTEM

We have developed a hybrid TPEF-SHG imaging system with an onstage incubator for long-term living-cell imaging. Using the imaging system, we observed the addition of new sarcomeres during myofibrillogenesis while a cardiomyocyte was spreading on the substrate. The results suggest that our customized TPEF-SHG imaging system with an onstage incubator is an effective tool for investigation of dynamic myofibrillogenesis.

INTRODUCTION

The study of myofibrillogenesis in live cardiomyocytes is essential for understanding heart-muscle formation and remodel [71]. In conventional fluorescence technique, this process inside living cells has been studied by labeling specific molecules with fluorescent protein (FP) technology [137]. However, whether the FP will fluoresce no matter whether it has been assembled onto a structure such as a sarcomere.

Because two-photon excitation fluorescence (TPEF) can be from a specific molecule and second harmonic generation (SHG) is intrinsic to a specific structure, the combination of TPEF and SHG (TPEF-SHG) is ideal for exploring how sarcomeric molecules (tracked by TPEF) [138, 139] are dynamically assembled onto myofibrils (visualized by SHG) [130-132]. Compared with corresponding single-photon excitation microscopy, the double wavelength requirement of TPEF and SHG can achieve a deeper

penetration inside biological materials[140]. Because both TPEF and SHG require high excitation power, which is distributed only within a very small volume confined at the focal point, TPEF and SHG can provide higher 3D resolution than conventional single-photon excitation microscopy [142-144].

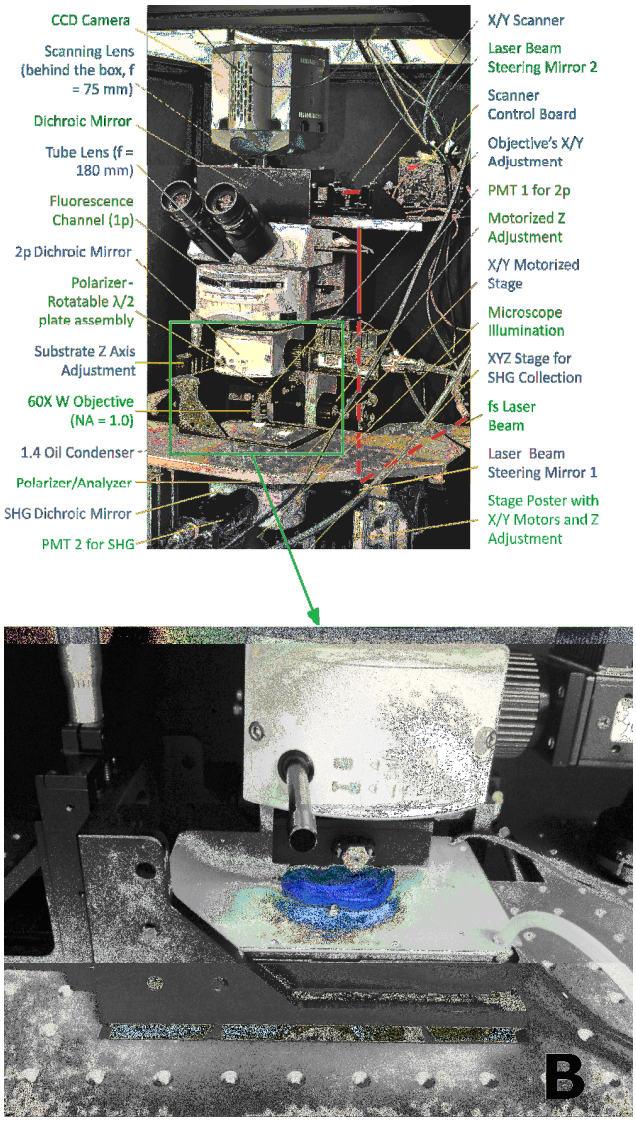

Figure 2.1 The schematic of the TPEF-SHG hybrid microscope: (A) the imaging system and (B) the onstage incubator mounted on the imaging system

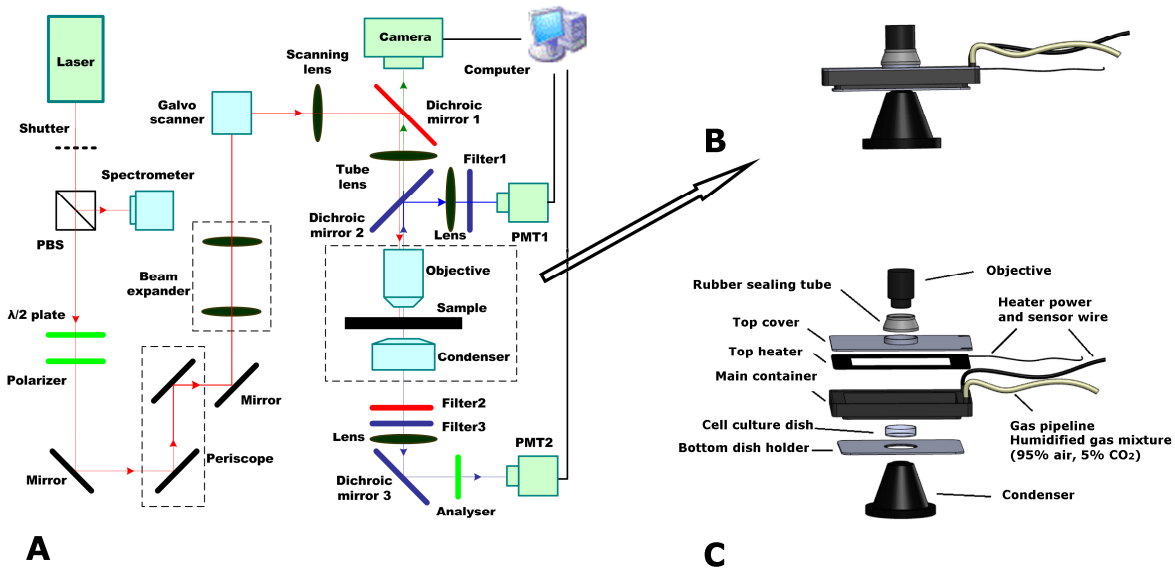

Figure 2.2 Schematic of the hybrid TPEF-SHG microscope with an onstage incubator: (A) Schematic of the imaging system; (B) Location of the onstage incubator; and (C) Components of the onstage incubator.

In the previous report, dynamic sarcomere contraction in a cardiomyocyte was recorded for up to several minutes using SHG technique [131], and the cardiomyocyte remained alive during imaging. However, myofibrillogenesis (i.e. the addition of new sarcomeres) is a process that spans hours to days. Normal physiological conditions (temperature, humidity, pH value, etc.) and appropriate laser power are necessary to maintain normal physiological processes inside the cardiomyocytes while myofibrillogenesis is recorded. Therefore, an incubating system that provides the required physiological conditions is required in the study of myofibrillogenesis.

In this study, we developed a hybrid TPEF-SHG polarization-imaging system combined with an onstage incubator that provides normal physiological conditions to isolated cardiomyocytes during imaging the process of myofibrillogenesis. Here we report the results of the recorded time-lapse images of single living cardiomyocytes while they were spreading on the glass substrate obtained from the onstage-combined TPEF-SHG imaging system.

INCUBATOR-COMBINED TPEF-SHG IMAGING SYSTEM

The TPEF-SHG Imaging System

The real instrumentation of the hybrid TPEF-SHG imaging system with an onstage incubator is displayed in Figure 2.1. A schematic setup of the imaging system is shown in Figure 2.2A. The femtosecond (fs) laser beam from a Ti:Sapphire laser (Tsunami pumped by a 10 W Millennia, Spectra-Physics) was tuned to 810 nm and collimated with optics that also expanded the beam 3 times and enforced the beam's polarization. The expanded beam was directed to the microscope custom-designed and built in our lab using several Olympus microscopic components. The beam was then steered onto the XY scanner (6210H, Cambridge Tech.). After being scanned and passing the scanning lens, the beam was reflected by a dichroic beam splitter and passed the tube lens. The beam then passed the TPEF dichroic beam splitter (FF665, Semrock) and was fed into the back aperture of the objective (W 60X, 1.0NA, Olympus,) to stimulate the sample. The stimulated TPEF signals were delivered through the objective, reflected by the TPEF dichroic beam splitter, and recorded by a photomultiplier tube (PMT1,

H7422p-40, Hamamatsu) with an IR filter (Filter1, FF01-720, Semrock). The SHG signals were collected from the forward direction through an Olympus 1.4 NA oil immersion condenser. The same types of PMT (PMT2) and IR filter (Filter2) were used in addition to a 405 ± 10 nm bandpass filter (Filter3, FF01-405/10-25, Semrock). The microscope's XY stage and the objective were facilitated by motorized control mechanisms (MP-285, Sutter). The microscope was equipped with a ThorLab microscope illumination unit (M530L2) with a polarizer, an EXPO fluorescence-illumination system (X-cite 120Q450), and an Andor EM-CCD camera (DU-888E-C00-#DZ) so that it could be used individually as a standard polarized microscope or conjunctionally as a conventional fluorescence microscope.

The lateral scan for 3D imaging was achieved with a pair of orthogonal galvanometers, which bidirectionally raster-scanned the fs laser beam to construct the sectional image. To implement high speed scanning, the turning regions of the triangle waves were smoothed by our custom-designed waveform. The laser scanning, data acquisition (PCI6115, NI), and the optical-shutter switch were controlled using custom-built, Labview-based software developed in our lab. The scanning range was calibrated using a standard-resolution target (Fluorescent USAF 1951, Edmund Optics). The resolution was estimated by scanning a 0.2-μm fluorescent bead, imaging it through the TPEF channel, and fitting the data to the theoretical-point-spread function. The lateral resolution was estimated to be 0.47 μm, and the axial resolution was estimated to be 1.2 μm. The scanning speed was 4 second/frame (spf, 512×512 pixels), and the data were acquired from both channels simultaneously; different frames acquired in one single

image-acquisition trial were saved in an image virtual stack. The image virtual stack was then processed by ImageJ software (http://rsbweb.nih.gov/ij/).

The Onstage Incubating System

An electric CO_2 microscopic stage incubator (H301-TC1-HMTC, 2GF-MIXER, Okolab) was incorporated into the TPEF-SHG imaging system (Figure 1B, 2B). The glass-bottom culture dish that was used for cardiomyocyte culture was mounted on the onstage incubator during real-time imaging of living neonatal cardiomyocytes. The temperature inside the incubator was maintained at 37ºC, and a mixture of CO_2 (5%) and air (95%) was passed through a humidifying module and pumped into the incubator. The gap between the objective lens and the top cover of the onstage incubator was sealed with a rubber sealing tube to maintain a stable temperature inside the incubator and to minimize leakage of the gas mixture.

PREPARATION OF THE CELL SAMPLES

Neonatal Cardiomyocytes

Three-day-old neonatal rats were euthanized by decapitation according to procedures approved by Clemson's IACUC. The heart was isolated and minced into 1 mm^3 pieces with scissors. The tissue pieces were digested with enzyme solution (0.14mg/ml trypsin-NO EDTA in PBS solution) overnight and then shaken at 75 rpm in the collagenase solution (PBS with 1 mg/ml Collagenase II, GIBCO; 0.24 unit/ml Neutral Protease, Worthington) for 1.5 hours. The fibroblasts were removed from the cell

solution using an adhesive assay by incubating the cell solution in a 1000-mm^2 flask with culture medium (DMEM, HyClone; 20% Fetal bovine serum, HyClone; 1% Penicillin/Streptomycin, Fisher Scientific). The cardiomyocytes were diluted to a concentration of 100k cells/ml. One ml of cell solution was seeded into a 3-mm culture dish with a glass bottom coated with laminin (20 μg/ml). The cells were cultured in a conventional incubator (37 ºC and 5% CO_2). The culture medium was changed after 24 h to remove dead cells and then was changed every 2 days.

Adult Cardiomyocytes

Four-week-old adult Sprague–Dawley rats were euthanized according to procedures approved by Clemson's IACUC. Heparin was injected (45 mg/kg) and it normally takes about 15 minutes for the heparin to take effect. Then, sodium pentobarbital was intraperitoneally injected (0.5ml/100g). After the anesthetization takes effect so that the rat lose consciousness and roll over on its side, the chest cavity of the rat was surgically opened and the aortic arch, the anterior vena cava and postcaval vein were cut quickly. At least 5 mm length of the aortic arch was left at the isolated heart. The heart was perfused from the aortic arch with perfusion buffer (NaCl,113mM; KCl, 4.7mM; KH2PO4, 0.6mM; Na2HPO4, 0.6mM; MgSO4, 1.2mM; Phenol red, 0.032mM; NaHCO3, 12mM; KHCO3, 10mM; HEPES, 10mM; Taurine, 30mM; 2,3-Butanedione monoxime (BDM), 10mM; Glucose, 5.5mM) for 5 min at 12 ml/min. Then the perfusion buffer was replaced by the digestive buffer (Perfusion buffer, Collagenase type II (Invitrogen), 1.4mg/ml; Neutral Protease (Worthington), 12u/50ml; Trypsin (SIGMA),

0.14mg/ml; CaCl2, 30uM) and the heart was perfused for 30 min at a flow rate of 12 ml/min. Once enzyme digestion of the heart was complete, the ventricle was cut in a 100×15 mm^2 dish containing 5 ml of digestion buffer and gently minced into small pieces (<1 mm^3) with fine forceps. The cell suspension was transferred into a 50-ml polypropylene conical tube. The tube was agitated with 5 ml perfusion buffer (37^oC) combined with cell suspension for a final volume of 40 ml. The cells were then allowed to settle down by gravity for 2 minutes, followed by the supernatant being transferred into a new 50-ml tube. Another 40 ml perfusion buffer was added into the original tube and the above procedures were repeated until very few tissue blocks were left in tube. The collected supernatant was centrifuged for 3 minutes at 500 rpm. The supernatant was removed from the centrifuged tube carefully. The pellet was resuspended into a 50-ml tube with 40 ml fresh perfusion buffer and agitated gently for 10 times. The collected cell solution was centrifuged for 3 minutes at 500 rpm. The supernatant was removed from the centrifuged tube carefully. Fresh perfusion buffer (20 ml) was added to the tube containing cell pellet. The cell solution was agitated gently for 10 times to resuspend the cells. The resuspended cells were then experience calcium reintroduction: adding 10 µl $CaCl_2$ (10 mM), 100 µl $CaCl_2$ (10 mM), 200 µl $CaCl_2$ (10 mM), 60 µl $CaCl_2$ (100 mM) and100 µl $CaCl_2$ (100 mM), consecutively with a 4-min interval. Then, the tube was centrifuged for 3 minutes at 500 rpm. The supernatant was removed, and the resuspended cells in culture medium (DMEM, 1% penicillin/streptomycin, 20% Fetal Bovine Serum) (50k cells/ml) will be used for cell culture.

IMAGING PROCEDURES

The cultured cells were pretreated in two ways before the imaging procedure: Immunocytological staining of myofibrillar components and living cell membrane staining with DiO dye.

Immunocytological Staining

For imaging alpha-actinin-labeled cells, the cells were first fixed by immersion in absolute ethanol for 30 min at -20ºC, then after their immersion in blocking solution (4% normal donkey serum, 0.02mg/ml Bovine serum albumin, 0.05% Triton X-100, dissolved in phosphate buffered saline), the following procedures were applied: primary alpha-actinin antibody (monoclonal alpha-actinin antibody from mouse, Sigma-Aldrich) and secondary antibody (Alexa Fluor 488 goat anti-mouse IgG, Invitrogen) to label alpha actinin, and Alexa Flour 488 phalloidin (Invitrogen) to label the F-actin. The stained cells were then mounted onto coverslides with mounting solution containing DAPI (Invitrogen).

Living Cell Membrane Staining

The cell membrane was stained with DiO (Invitrogen) before imaging: the serum-culture medium in the culture dish was removed. The cells were washed with warm PBS solution and then rinsed again with serum-free medium (DMEM, 1% penicillin/streptomycin). Then 1 ml DiO solution (5 µl DiO per ml serum-free medium) was added to the culture dish, and the cells were incubated in the dark at 37 ºC for 40

minutes. The DiO solution was removed from the culture dish, and the cells were washed 3 times with serum-free medium. Then fresh culture medium with serum was added to the culture dish.

Imaging Process Under TPEF-SHG System

After the cardiomyocytes were cultured for 1-5 days, the culture dish was moved from the conventional incubator to the TPEF-SHG imaging system. The signals from the TPEF and SHG channels were collected, and the 2D/3D images of the selected cells were reconstructed using ImageJ software.

The cell to be imaged was first identified via the fluorescence channel of the imaging system. Then the cells were excited by the 810-nm fs laser beam. The TPEF and SHG signals from the sample were collected simultaneously through two different channels. A 2D image of the cell was reconstructed from the signals acquired from both channels and displayed on the monitor. The focus was adjusted to find the SHG image of the best quality. Time-lapse images were acquired from both channels and saved at designated time intervals into a virtual stack.

The parameters of the onstage incubator were set to physiological conditions when living cells were imaged. Although no energy is absorbed during generation of second harmonics[145], the incident laser may still damage cardiomyocytes [146]. Therefore, when living cells are imaged under the system, the average power of the incident fs laser beam needs to be adjusted carefully. Strong power may kill the cardiomyocytes within very short time (Figure 2.3). In our experiments, an incident-laser

power of 2.8 mW (adjusted by a pair of polarizers) was proved not to damage the cultured neonatal cardiomyocyte at Day 1~5. When fixed and stained cells were imaged, the onstage incubator was turned off, and the average power of the incident fs laser beam was adjusted to ensure the best image quality was obtained. The virtual stack was then processed by ImageJ software. (http://rsbweb.nih.gov/ij/)

RESULTS AND DISCUSSION

3D adult cardiomyocyte images were reconstructed from both TPEF (green) and SHG (red) z-stacks. Images of the sarcomere structure obtained with non-purely polarized (polarizer was placed in front of the laser) and purely polarized (polarizer was placed immediately before the objective) excitation beam were acquired and reconstructed, which demonstrated that the sarcomere image obtained with SHG method was very sensitive to the polarization state of the excitation laser beam (Figure 2.4). Changing the scanning area at the sample or optically zooming in/out may change the resolution of the acquired image, optically zooming in may increase the resolution of the acquired image and provide more details about the samples (Figure 2.5). However, since the orientation of myofibrils in the cultured cardiomyocytes is randomly distributed, the signals from the striated features that do not parallel with the orientation of the polarizer will be weakened. Therefore, we used non-purely polarized setup for the excitation laser beam in our research.

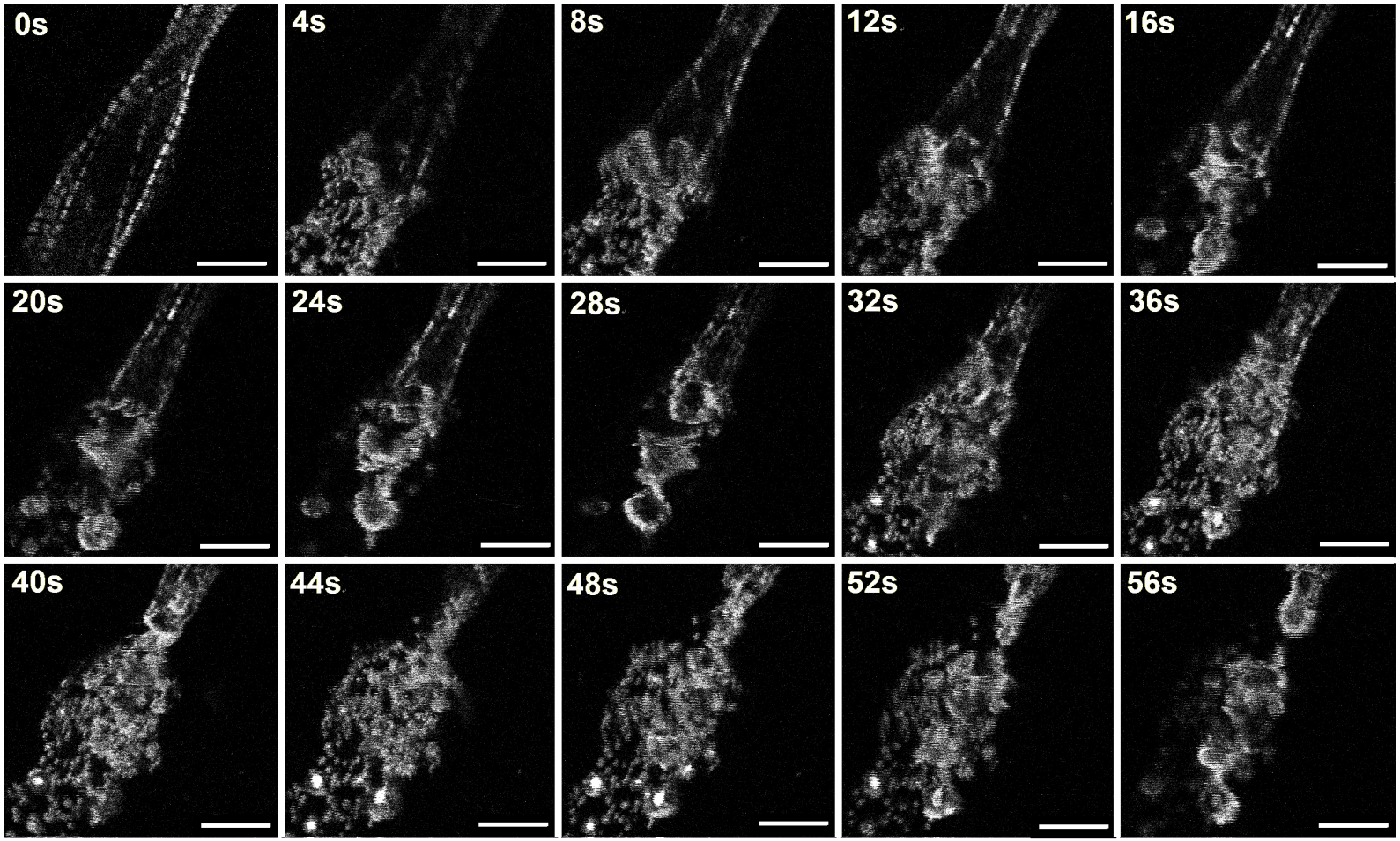

Figure 2.3 The changing process of the sarcomere structure while a cardiomyocyte (day-5) was dying after the cell was exposed to the incident fs laser beam of 8mW for 60s. The time before cell was dying is labeled as 0s. (Scale bar: 10 μm)

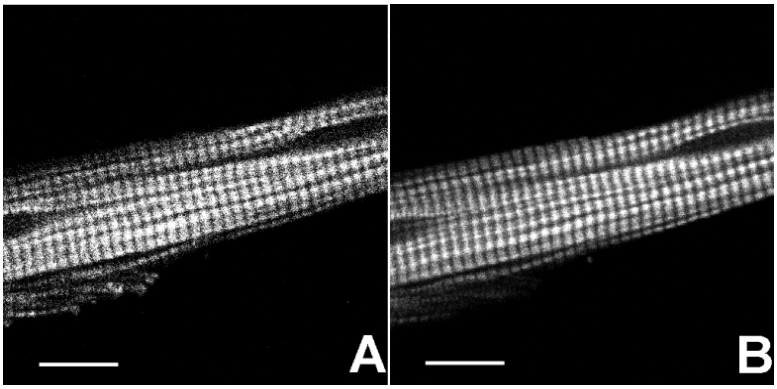

Figure 2.4 Sarcomeric structure of an adult cardiomyocyte acquired by the SHG technique with A) non-purely polarized excitation laser beam and B) fully polarized excitation laser beam (Scale bar: 10μm).

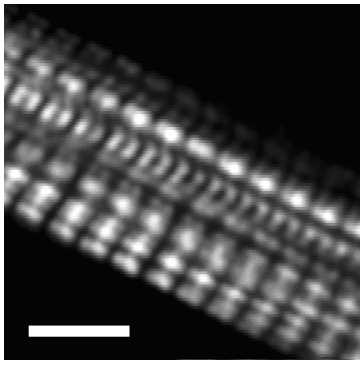

Figure 2.5 Sarcomeric structure of an adult cardiomyocyte acquired by the SHG technique with purely polarized excitation laser beam (Scale bar: 5μm).

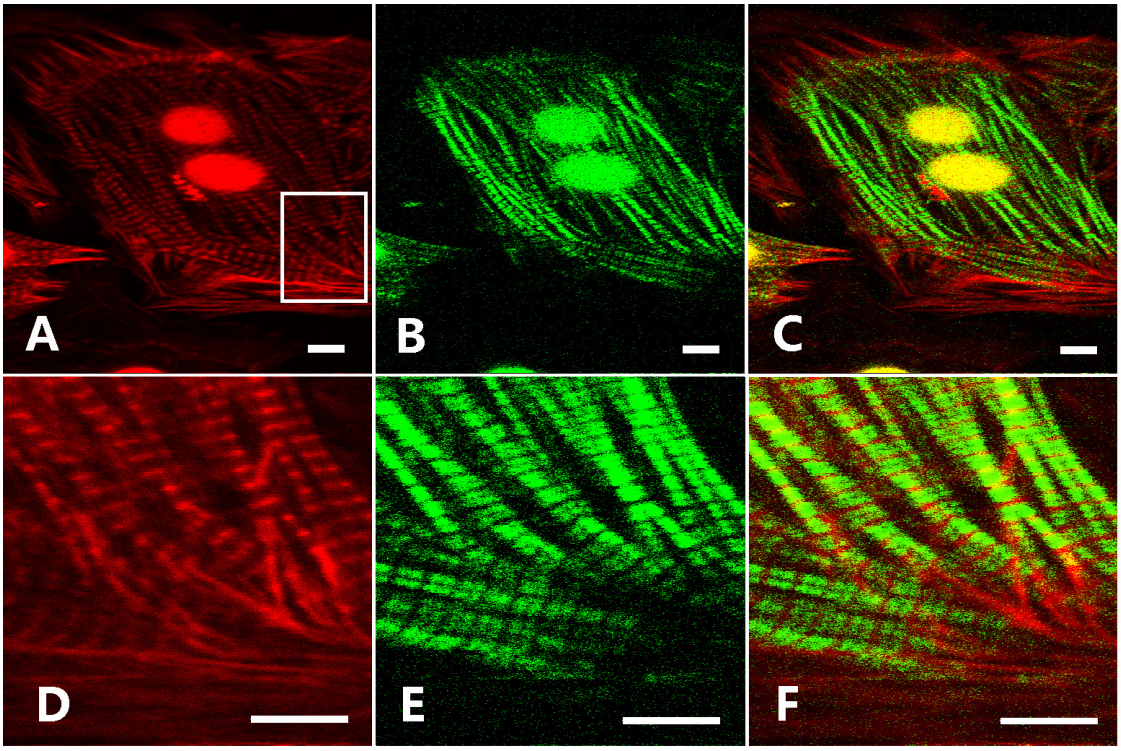

Figure 2.6 The sarcomeric structure of a neonatal cardiomyocytes cultured in vitro at Day 4. The F-actin (Red) pattern was acquired from the TPEF channel, and the myosin filament pattern (Green) was acquired from the SHG channel. The square-circled area of the cell in (A) was optically magnified during data acquisition (D, E and F). (scale bar: 5μm)

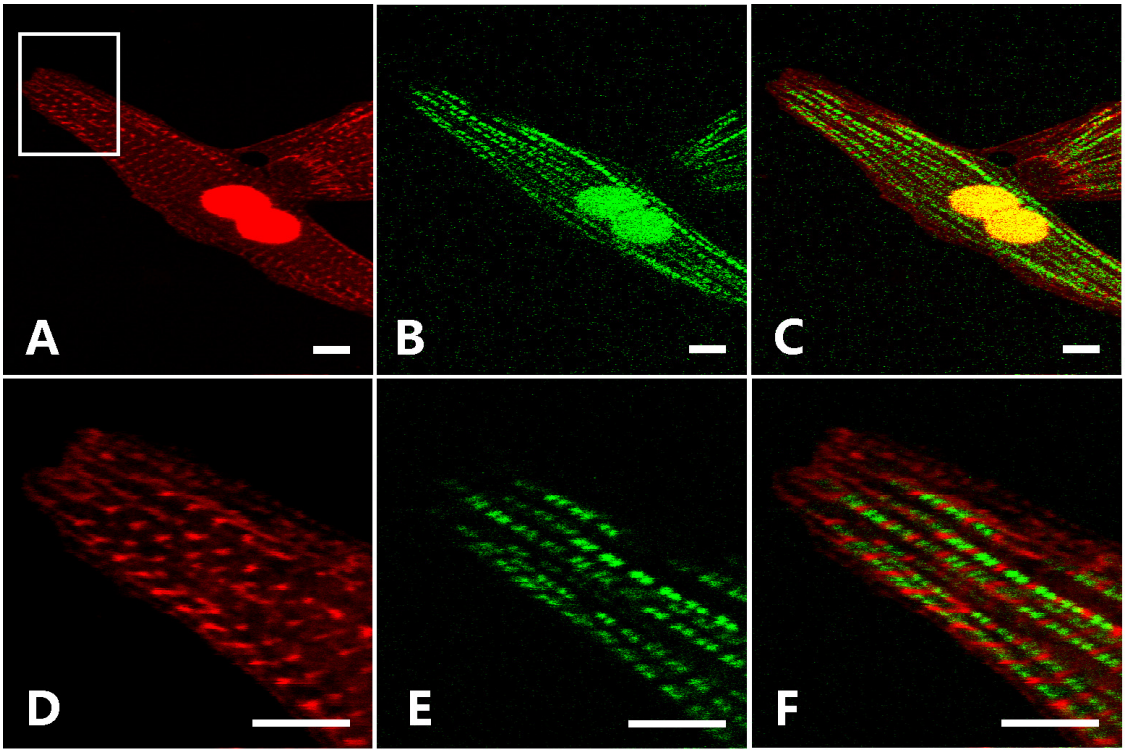

Figure 2.7 The sarcomeric structure of a neonatal cardiomyocytes cultured in vitro at Day 1. The alpha-actinin (Red) pattern was acquired from the TPEF channel, and the myosin filament pattern (Green) was acquired from the SHG channel. The square-circled area of the cell in (A) was optically magnified during data acquisition (D, E and F).

(scale bar: 5μm)

Immunocytological Stained Cardiomyocytes

The reconstructed 2D images of the fixed neonatal cardiomyocytes with F-actin and alpha-actinin labeled are displayed in Figure 6 and Figure 7, respectively. More details at the square-circled area are displayed through optically zooming into the area (Figure 2.6, D~F, and Figure 2.7, D~F). The 3D images of a cardiomyocyte reconstructed

from the z-stack image sequence are displayed in Figure 2.8. The slices of the reconstructed 3D images show that the internal structural features and the relationship between F-actin and SHG-represented myosin filaments can be clearly demonstrated, which proves that the TPEF-SHG imaging system is powerful to the study of sarcomeric structure.

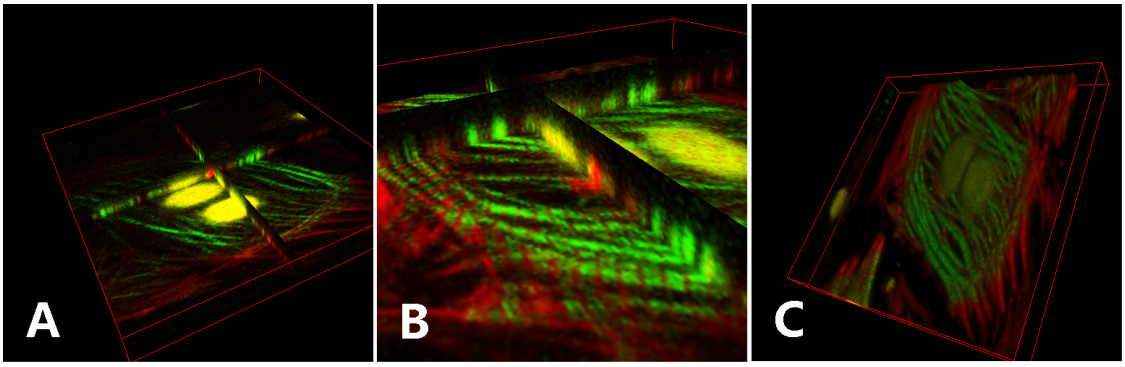

Figure 2.8 3D image construction of a neonatal cardiomyocyte (the cell in Figure 6) displayed as orthoslice (A~B) and volume (C). F-actin is shown in red and the pattern of the SHG signal is shown in green.

Living Cardiomyocytes With Membrane Stained

The topology of the cell membrane and the sarcomeric structure of a living neonatal cardiomyocyte were clearly demonstrated by the images acquired from the TPEF and the SHG channels, respectively (Figure 2.9, A and B). Combination of the cell membrane and the sarcomeric structure images displayed the connection of the sarcomeric structure with the cell membrane (Figure 2.9, C). It is known that the fresh dissociated neonatal cardiomyocytes are round-ball shape, and after 3-day's culture at collagen coated substratum, the cells become thinner and redifferentiate when the

myofibrils are reconstructed. The relationship between cell membrane and sarcomeric structure of spreading cardiomyocytes can be clearly displayed in the reconstructed 2D images. The result shows that while a neonatal cardiomyocyte is spreading at the surface, the spreading of cell membrane is not immediately followed by mature myofibrils, which morphology is different from the fresh isolated living adult cardiomyocytes (Figure 2.10). To demonstrate the spatial relationship between the cell membrane and the sarcomeric structure, the 3D image of a living adult cardiomyocyte was reconstructed from the z-scanning image stacks including the cell membrane and the sarcomeric structure via ImageJ software (http://rsbweb.nih.gov/ij/) (Figure 2.11). The cross-section of the reconstructed 3D cell image showed that the sarcomeric structure was well embedded into the cell membrane.

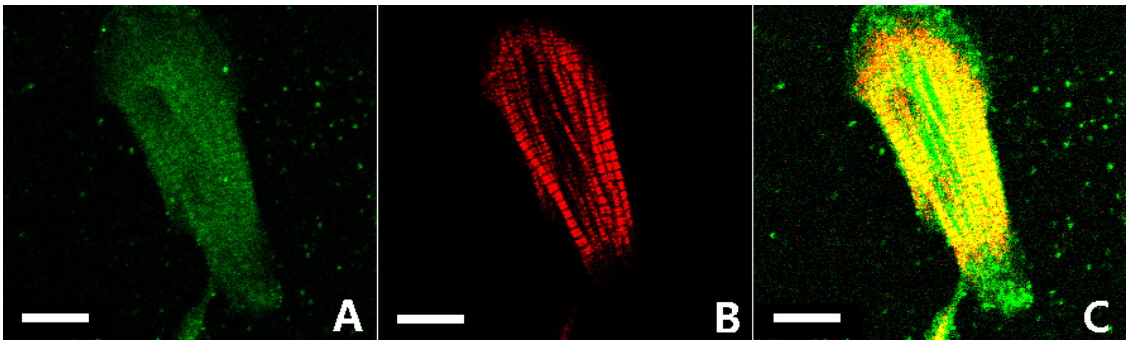

Figure 2.9 2D image of freshly isolated neonatal cardiomyocyte (Day 3): (A) TPEF image of a live cardiomyocyte with DiO-stained membrane (green); (B) Simultaneous SHG image of the same cell, showing sarcomeric structure (red); and C) Combination of images A and B (Scale bars: 10 μm), showing the relationship between the frontier cell membrane and the myofibril tip.

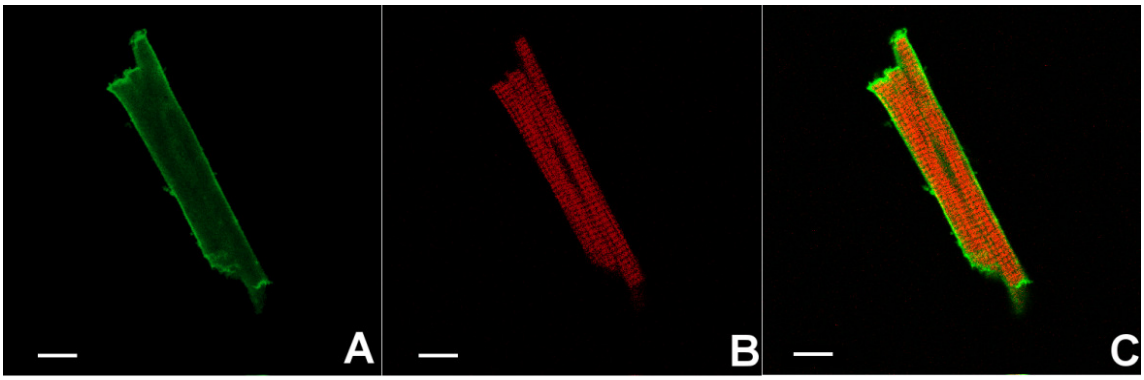

Figure 2.10 2D image of freshly isolated adult cardiomyocytes: A) TPEF image of a live myocyte with DiO stained membrane (for better color contrast, the DiO stained cell membrane was displayed green); B) simultaneous SHG image of the same cell, showing sarcomeric structure (red); and C) Combination of images A and B (Scale bar: 10 μm).

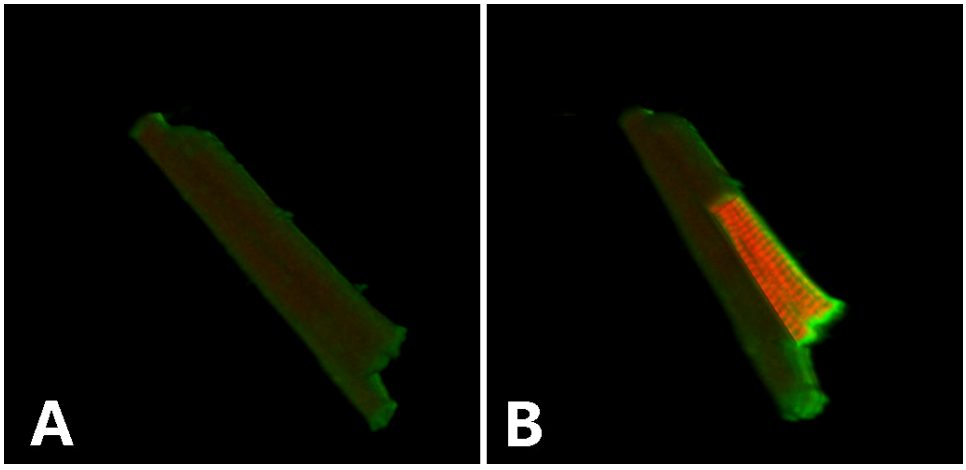

Figure 2.11 3D image of the sarcomere structure in a living adult cardiomyocyte reconstructed from both TPEF (green) and SHG (red) image stacks.

Growth Of Myofibrils In Living Neonatal Cardiomyocytes

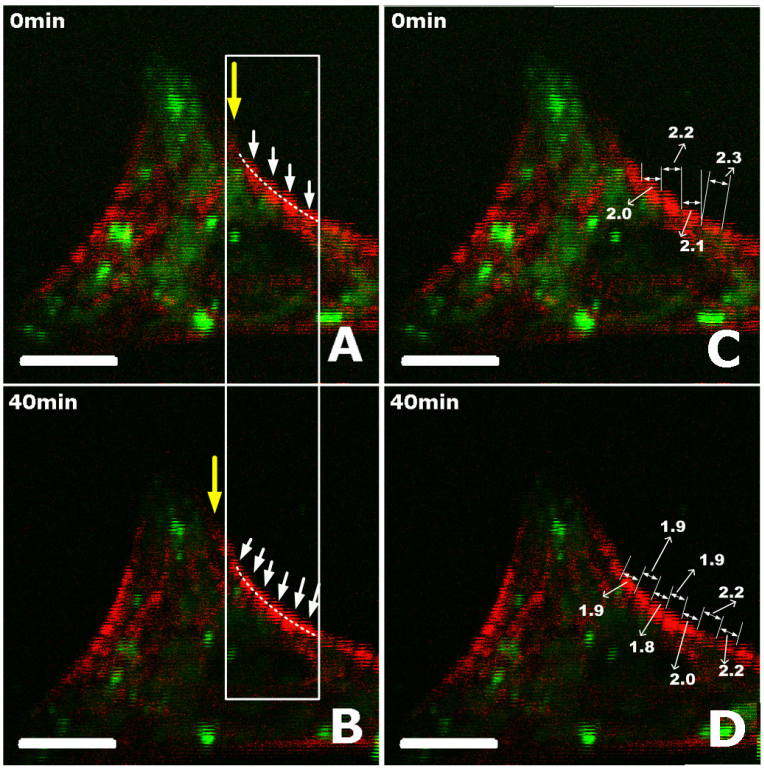

Figure 2.12 Addition of new sarcomeres during myofibril growth. DiO-stained cell membranes acquired through the TPEF channel are green; myofibrils detected by SHG are red. A and C are identical TPEF-SHG overlapped images acquired at 0 min. B and D are identical TPEF-SHG overlapped images acquired 40 minutes after the initial image. In A and B, each white arrow denotes one sarcomere; the white box in A and B shows the addition of two new sarcomeres at 40 minutes. In C and D, sarcomeric length (μm) is shown. In the area denoted by the long arrows in A and B, the SHG signal shows that striated sarcomeric structure has not yet developed. The scale bars represent 10 μm.

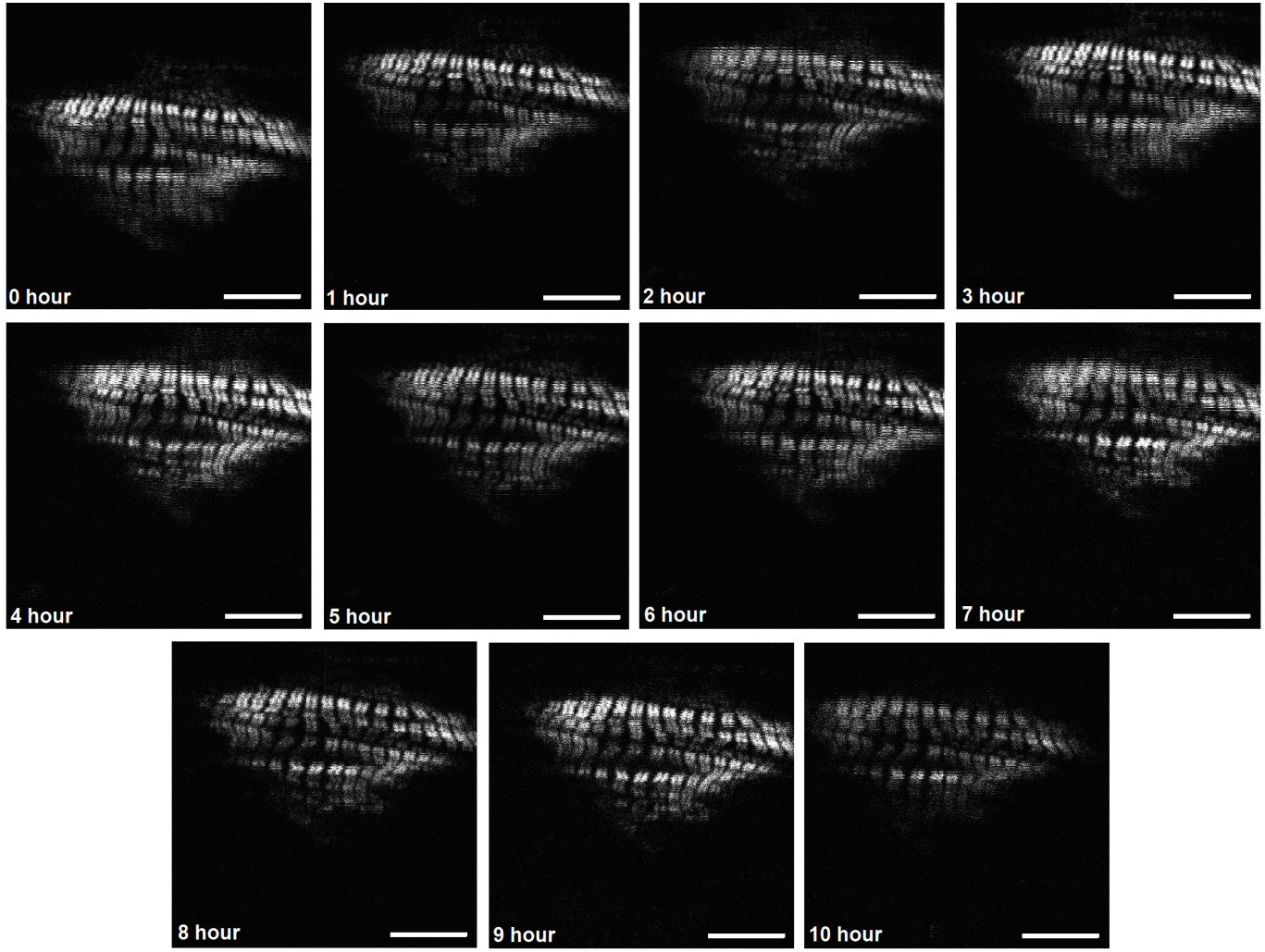

Figure 2.13 The sarcomere structure of a single neonatal cardiomyocyte (day-5) acquired via SHG signals. With well controlled cell culture conditions, the cell was cultured and imaged up to 10 hours, without apparent sarcomere structure change.

Figure 2.12 shows TPEF-SHG overlapped, time-lapse images of a myofibril structure from a cardiomyocyte on the Day 1 in culture. These images were acquired when the mature myofibrils (red) had not extended to the tip of the filopodia (green) while the cell was spreading on the substrate. Each sarcomere is indicated by a white arrow. After 40 minutes of onstage incubation, two additional sarcomeres appeared inside the white rectangle. The two series of white dots, which denote the loci of the myofibrils at the cell boundary, form two different inward curves respectively in Figure 2.12, A and B, exhibiting the rotation of the sarcomeres in 40 minutes. The length of the sarcomeres indicated in Figure 2.12, A and B by white arrows was estimated using ImageJ software and denoted in Figure 2.12, C and D. The displayed loci and indicated sarcomere lengths in Figure 2.12 demonstrate that the space required by the newly added sarcomeres was gained from rotation and shrinkage of the existing sarcomeres. Although there were no striated sarcomeric structures at the tip of the myofibril (the area denoted by the long arrows in Figs. 2.12, A and B), the detection of SHG signals demonstrated that myosin heavy chain bundles existed in this area [130] before being assembled into myofibrils to form the striated sarcomeric structure. This is consistent with previous research, which showed that muscle myosin bundles form separately from the formation of other myofibril components [83, 147] before the assembly of the sarcomeric structure.

Research from Russell's group has shown that under static stretch, the addition of new sarcomeres can happen within 1-4 hours [148]. This finding was obtained by analyzing results from fixed cells with labeled sarcomeric proteins at different time points during myofibril remodeling under static stretch. In our experiments, the rate of SHG

imaging was 4 spf; cells remained physiologically active for at least ten hours (see chapter 3). Using our system, we were able to record the addition of two new sarcomeres that occurred within 40 minutes while the cardiomyocyte was spreading on the substrate. Thus, our imaging system could be used to explore the addition of a new sarcomere in a single cardiomyocyte during cardio- myofibrillogenesis and remodeling. We should note here that due to the non-uniform distribution of the culture conditions (temperature, nutritious, etc.) inside a culture dish, the growing speed of myofibrils may be different in different cells. Figure 2.13 shows that no apparent myofibril growth/remodel appeared in a neonatal cardiomyocyte within a period of 10-hours' culture in the onstage incubator.

CONCLUSION

Our study demonstrates that customized TPEF-SHG imaging system including an onstage incubator is effective in real-time study of long-term structural changes in cardiomyocytes. We observed the addition of new sarcomeres to the mature myofibrils that occurred within a short time. The results demonstrate that our imaging system could be a useful tool for investigating the prolonged process of myofibrillogenesis of a single cardiomyocyte. More results on the process of myofibrillogenesis or dedifferentiation of cardiomyocytes will be discussed in the following chapters.

CHAPTER THREE

ASSEMBLY OF MYOSIN FILAMENTS ONTO MYOFIBRILS IN LIVE NEONATAL CARDIOMYOCYTES OBSERVED BY TPEF-SHG MICROSCOPY

Utilizing a customized onstage incubator-combined two-photon excitation fluorescence (TPEF) and second harmonic generation (SHG) imaging system, we studied the dynamic process of assembly of contractile myosin filaments onto myofibrils in a live cardiomyocyte culture during myofibrillogenesis. We report the dynamic process of the formation of myofibrils in neonatal cardiomyocytes during 10 hours of onstage incubation. We observed new-sarcomere addition at both the ends and the sides of existing myofibrils and at the interstice of several separated myofibrils, during which mature myofibrils may act as templates for the myofibrils forming adjacently. Our observation indicates that the assembly of myosin filaments onto a myofibril involves the initial redistribution of Z-body proteins to ultimately form mature Z disks.

INTRODUCTION

Understanding myofibrillogenesis, the process that assembles all protein components of a sarcomere and connects the sarcomeres to form myofibrils, is essential for understanding heart-muscle formation, development, and remodeling in response to physiological stimulation. It is also critical to understanding cardiac regulation in response to mechanical-loading conditions: Increased diastolic strain causes cardiomyocytes to elongate by adding sarcomeres in series, and continued systolic stress

causes cardiomyocytes to thicken by adding sarcomeres in parallel [127]. Although the contractile components, such as actin and myosin filaments, and the structural components such as the titin of a sarcomere (Figure 3.1) are known to be synthesized separately before being assembled to form a mature sarcomere [149, 150], a model that describes the entire formation process has not been established. Several models have been proposed to describe how the sarcomeric components are assembled onto mature myofibrils [84, 86]: (1) template model—stress fiber-like structures are thought to play the role of template or scaffold for assembly of myofibrils [151]; (2) stitching model—sarcomeric components are thought to be assembled at the end of an existing myofibril by adding I-Z-I bodies and myosin filaments alternately [87]; and (3) premyofibril model—the formation of myofibrils is thought to undergo three stages: premyofibrils, nascent myofibrils, and mature myofibrils. The three stages are distinguished by the substitution of muscle myosin II for nonmuscle myosin IIB and the maturation of Z-discs from Z-bodies [152]. In the premyofibril stage, nonmuscle myosin IIB is interdigitated with alpha-actinin-containing Z-bodies. In the nascent myofibril stage, muscle myosin II is substituted for nonmuscle myosin IIB; this continues toward the mature myofibril stage, when all the nonmuscle myosin IIB has been replaced by muscle myosin II.

The sarcomeric components are not added simultaneously to the existing myofibrils; instead, different components are assembled successively on the existing myofibrils, as described in the models above. The addition of myosin filaments is believed to be one of the final events in the process that leads to sarcomeric maturation [56, 128, 153]. The major difference among the myofibrillogenetic models lies in how the

initial assembly of myosin filaments onto myofibrils is explained in each model. Immunocytochemistry research based on myosin-filament staining has enhanced our understanding of myofibrillogenesis [154]. The disadvantage of this method is that the image of the immunofluorescently labeled myosin proteins does not distinguish whether the proteins have been assembled onto myosin filaments.

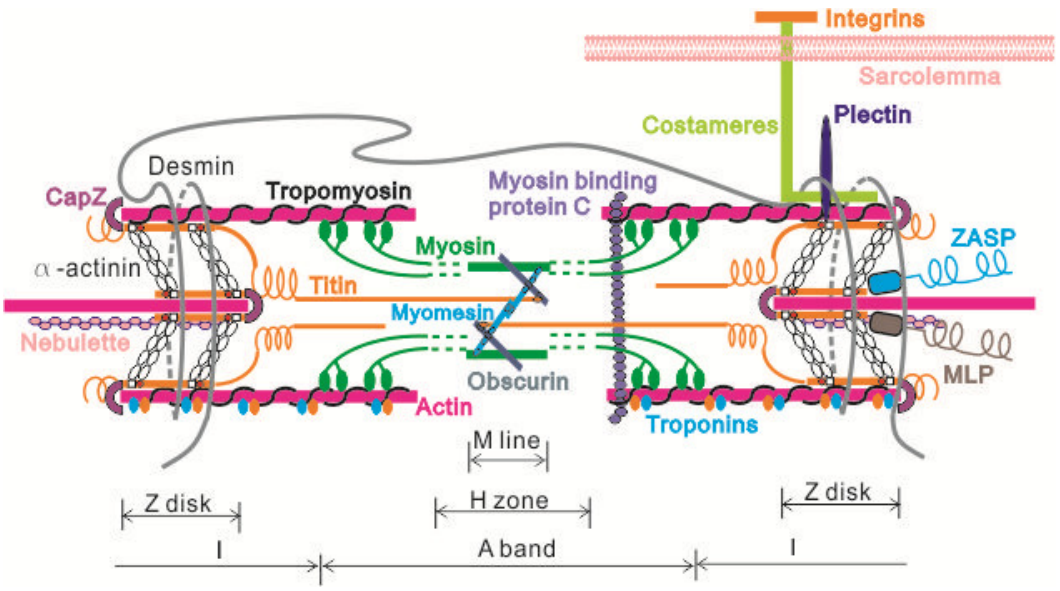

Figure 3.1 Schematic of sarcomeric structure

Second harmonic generation (SHG) stimulated by a femtosecond (fs) laser beam is intrinsic to a specific structure. Because the SHG signal from cardiomyocytes arises from the coiled-rod region of myosin filaments [130], dynamic assembly of myosin filaments onto a myofibril may be studied without protein labeling [155]. Through the combination of two-photon excited fluorescence (TPEF) and SHG (TPEF-SHG), additional structural information can be obtained from a cardiomyocyte [133, 134]; this

microscopic technique is ideal for tracking how specific sarcomeric proteins are assembled onto myofibrils during myofibrillogenesis. Since myofibrillogenesis is a process that spans hours to days, we have developed a hybrid TPEF-SHG imaging system with an onstage incubator that provides normal physiological conditions to isolated cardiomyocytes [155]. Here, we report the dynamic process of the formation of myofibrils in neonatal cardiomyocytes during 10 hours of onstage incubation. Because the concepts described in the premyofibril model best describe our observation, they will be adopted in our explanation of the experimental results.

METHODS AND PROCEDURES

TPEF-SHG Imaging System With An Onstage Incubator

The construction of the TPEF-SHG imaging system with an onstage incubator is described in our previous publications [155, 156]. The exciting fs laser beam was tuned to 810 nm. The sample was scanned repeatedly, and the images were acquired continuously at the rate of 4 seconds per frame (spf) in each image-acquisition trial. Approximately 10-20 frames were recorded in one virtual stack. When live cells were imaged under the system, the average power of the incident fs laser beam was set to 2.8 mW. The parameters of the onstage incubator were set to physiological conditions. When fixed and stained cells were imaged, the average power of the incident fs laser beam was adjusted to ensure that the best image quality was obtained, and the onstage incubator was turned off. The virtual stack was then processed by ImageJ. (http://rsbweb.nih.gov/ij/)

Primary Culture of Neonatal Cardiomyocytes

Three-day-old neonatal rats were euthanized by decapitation according to procedures approved by the Clemson University Institutional Animal Care and Use Committee. The cardiomyocytes were dissociated from myocardial tissue with trypsin, collagenase, and neutral proteinase as previously described [157], chapter 2]. The cardiomyocytes were diluted to a concentration of 100 K cells/ml. One ml of cell solution was seeded into a 35-mm culture dish with a glass bottom coated with laminin (20 µg/ml). The cells were cultured in a conventional incubator (37 ºC and 5% CO_2). The culture medium (including 20% fetal bovine serum) was changed after 24 h to remove dead cells and then was changed every 2 days.

Pretreatment Of The Cells Before The Imaging Process

For imaging live cells, the cell membrane was live-stained with DiO (Invitrogen) as previously described [155], then the culture dish with the stained cell culture was placed into the onstage incubator of the TPEF-SHG imaging system. The cell to be imaged was first identified via the fluorescence channel of the imaging system, and then the SHG signal was collected from the SHG channel of the imaging system. For imaging alpha-actinin-labeled cells, the cells were first fixed by immersion in absolute ethanol for 30 min at -20ºC, then after their immersion in blocking solution (4% normal donkey serum, 0.02mg/ml Bovine serum albumin, 0.05% Triton X-100, dissolved in phosphate buffered saline), the following were applied: primary alpha-actinin antibody (monoclonal alpha-actinin antibody from mouse, Sigma-Aldrich) and secondary antibody (Alexa Fluor

488 goat anti-mouse IgG, Invitrogen; Rhodamine donkey anti-mouse IgG, Millipore) to label alpha actinin, and Alexa Flour 488 phalloidin (Invitrogen) to label the F-actin. The stained cells were then mounted in mounting solution containing DAPI (Invitrogen). Nikon Eclipse Ti confocal microscope was applied for multichannel fluorescence-image acquisition.

RESULTS

Figure 3.2 (modified from Figure 2.12) demonstrates the growth of myofibrils in onstage cultured cardiomyocytes (40 min incubation). Mature sarcomeres are represented by striated patterns collected from the SHG channel. The number of sarcomeres in the rectangle-enclosed myofibril increased from 4 (Figure 3.2A) to 6 (Figure 3.2B). We did not capture the procedure by which two new sarcomeres were added.

A separation area located at the boundary of multiple mature-myofibril segments was found in a cardiomyocyte selected from a culture that was incubated for one day (Figure 3.3, arrow-a). We observed the process in which this separation area was filled with newly developed sarcomeres. To demonstrate the structural difference before and after sarcomeres were added to this separation area, we analyzed (through ImageJ software) the grey value of this area at two representative stages selected from the time-lapse sequence. In Figure 3.3E and 3.3F, the separation area surrounded by the rectangles shows the two additional sarcomeres in immature and mature stages, respectively. The grey-value plots clearly demonstrate that irregular peaks appeared at the area where sarcomeres were initially immature, and striated peaks with two tips (characteristic of

mature sarcomeres [145] appeared at the same area. Before the mature sarcomeres formed in the separation area, we noted that when the contraction wave was propagating from one segment to the others across this separation area, a propagation perturbation appeared at this separation area (data not shown). However, after matured sarcomeres filled the separation area, the contraction wave propagated from one end of the myofibril to the other end without perturbation. Therefore, the separation area (Figure 3.3D, arrow-a) appears to be the interstice where the divided myofibril sections unite into a single mature myofibril. The time-lapse image sequence (Figure 3.3G) demonstrates that during the maturation of the immature sarcomeres at the separation area, the assembly of myosin filaments to the sarcomeres progressed laterally from one side of the sarcomeres to the other side.

SHG signals were detected in the area indicated by arrow-b at the beginning of the experiment (Figure 3.3A), but no apparent striated-fibril structure could be distinguished. After onstage incubation for 90 minutes, a striated fibril structure gradually became distinguishable between the middle of the cell body and the edge of the cell body (Figure 3.3B). Since the SHG signal is emitted by the bundled myosin filaments [130], our time-lapse observation demonstrated the time sequence of myosin-bundle formation, accumulation, and addition to a myofibril. For example, it was observed that the fibril length increased longitudinally with onstage incubation time (Figure 3.3, A~D and I~J). A similar phenomenon was observed at the area indicated by arrow-c (Figure 3.3, A~D). A dynamic myosin-filament addition similar to that seen at the area indicated by arrow-a in Figure 3.3 was also found at the area indicated by arrow-c, where a new myofibril was

added adjacent to the existing myofibrils during a 10-hr time-lapse observation of SHG. Notably, as the myosin filaments were being assembled onto the new myofibrils indicated by arrow-c, the direction of assembly of of myosin filaments in a single sarcomere was from the adjacent mature myofibrils outwards.

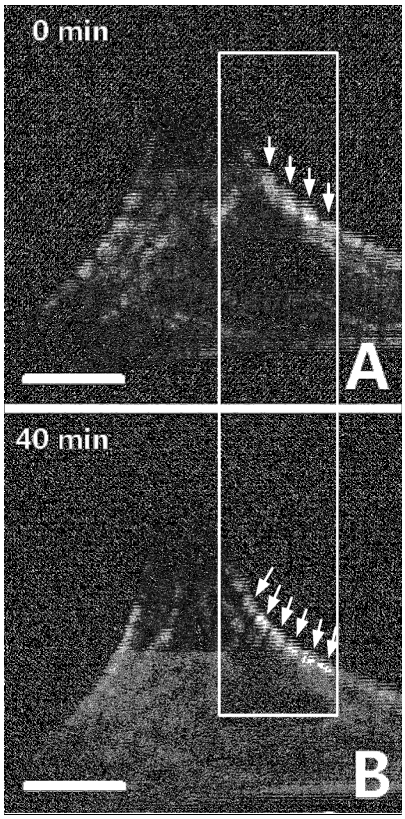

Figure 3.2 Addition of new sarcomeres during myofibril growth. A: an SHG image acquired at 0 min. B: the SHG image acquired at the same location 40 minutes after image A. Each white arrow denotes one sarcomeric unit; two new sarcomeres were added in the interval between image acquisitions. (scale bar: 10μm)

Alpha-actinin has been recognized as the central protein in the early stage of myofibrillogenesis . The images displayed in Figure 3.2 and Figure 3.3 show only myosin filaments. To reveal how the myosin filaments are related to alpha-actinin during the formation and growth of myofibrils, we fixed the in vitro-cultured neonatal cardiomyocytes at Day 1 and immuofluorescently labeled the alpha-actinin. We then collected the fluorescence signal that represented the distribution of alpha-actinin from the TPEF channel of our imaging system and simultaneously collected the SHG signal that represented the distribution of myosin filaments from the SHG channel. Then alpha-actinin and myosin-filaments images were reconstructed, given different colors, and combined.

Since our imaging system has only one TPFE channel, we employed a multichannel confocal microscope to record the cell nucleus, alpha-actinin, and F-actin in one fluorescence image, and then inserted the myosin-filament image that was recorded from the same cell with our TPEF-SHG imaging system (Figure 3.4A~3.4E). To ensure the insertion would accurately maintain the relationship among alpha-actinin, F-actin and myosin filaments during myofibrillogenesis, an image-matching operation was performed to linearly transform the TPEF-SHG image so that the alpha-actinin image obtained from the TPEF channel would perfectly overlap that obtained from the multichannel confocal microscope. Consequently, the correspondingly transformed myosin-filament image (Figure 3.4D) from the SHG channel of the TPEF-SHG system would be under the same coordinate system as the other multichannel confocal images (Figure 3.4A~3.4C).

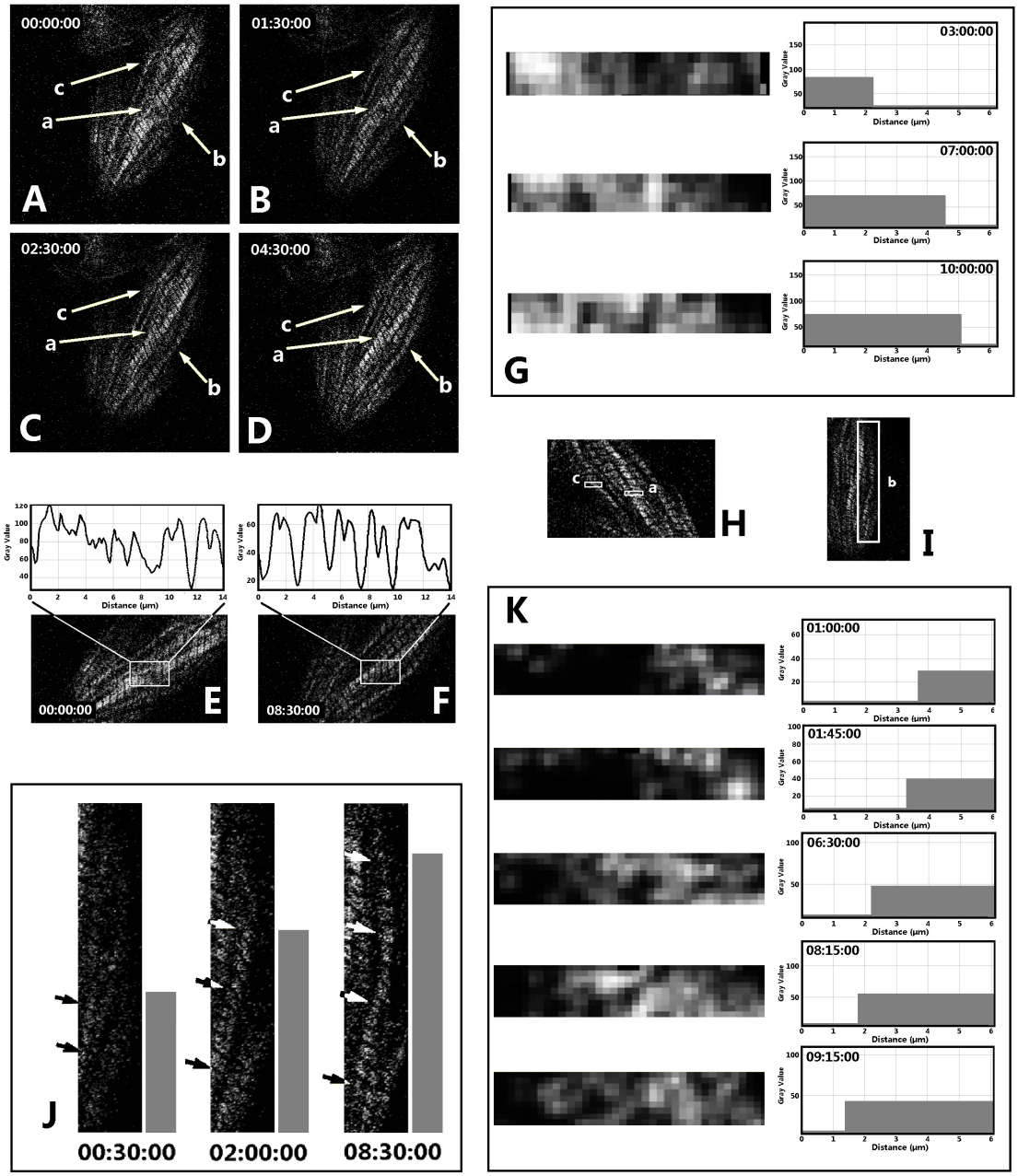

Figure 3.3 The assembly of myosin filaments and the growth of myofibrils in a live-cell culture. The images were collected from the SHG channel. The dynamic process was detected at areas a, b, and c (white arrows). A-D: The myofibril structure at different time

(Figure 3.3, continued)

points. E and F: The gray values of the SHG image indicated by arrow-a at 0 min and 510 min are plotted against the axial distance before and after new sarcomere addition. The images of the cell are presented in (E) and (F) with a rotation angle relative to those in A-D to make the plot's X-axes consistent with those of the images. G and K: The time-lapse sequence of the gray-values (against the lateral distance) in the areas indicated by inserted rectangles-a and -c in the SHG image shown in H. The corresponding horizontal bars were obtained by selecting a threshold gray value (e.g., 1/3 peak value) and binarizing the gray-value images accordingly to demonstrate the lateral extension of sarcomeres from one side to the other. Similarly, the time-lapse images in J demonstrate the axial growth of a myofibril indicated by the inserted rectangle-b in I.

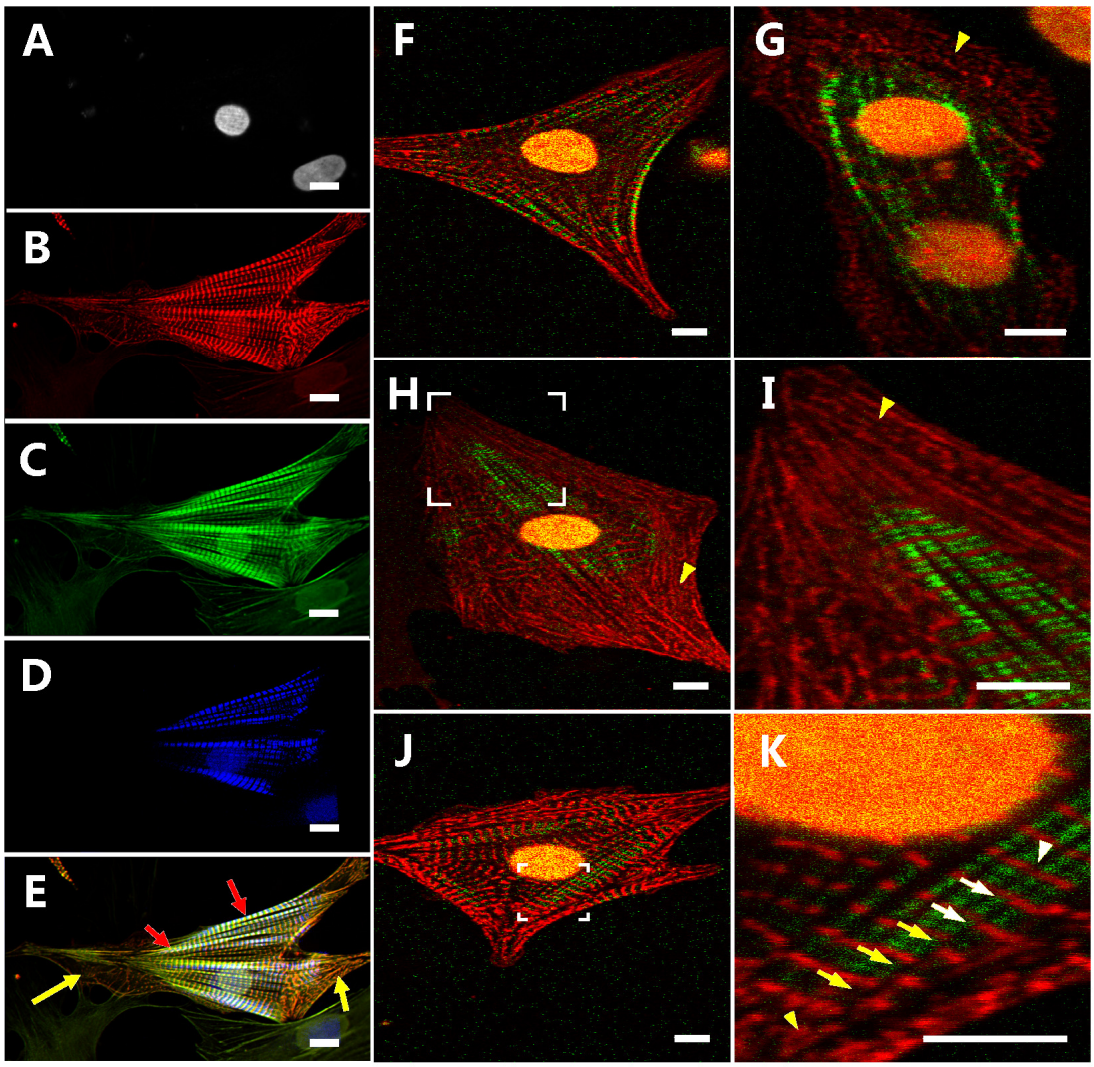

Figure 3.4 The myofibril structure of the cardiomyocytes cultured in vitro at Day 3. A, B and C: images of the nucleus, alpha-actinin, and F-actin, fluorescently labeled by DAPI, alpha-actinin antibody, and phalloidin, respectively, obtained with a Nikon T*i* confocal microscope. D: image of myosin filaments obtained from the SHG channel of our TPEF-SHG imaging system. E: Combination of A-E. (see text for details). F-K, TPEF-SHG images of alpha-actinin (red) and myosin filaments (green). The cells were fixed and

(Figure 3.4, continued)

alpha-actinin was fluorescently labeled. The alpha-actinin pattern was acquired in the TPEF channel, and the myosin filament pattern was acquired in the SHG channel. F: A cell in which the mature sarcomeres first appeared in the middle of the myofibrils at the cell edge. G and J: Cells in which the mature sarcomeres first appeared in the center of the cell. H: A cell in which the mature sarcomeres appeared in the center of the cell and in the middle of the myofibrils at the cell edge. I: Magnification of the area surrounded by the white bracket in H. The yellow arrowheads in G, H, and I point to the short-term Z-bodies of premyofibrils. K: Magnification of the area surrounded by the white bracket in J: The white arrowhead indicates the adjacent Z-discs in neighboring mature myofibrils, which were connected and merged completely. The white arrows point to the Z-discs in adjacent myofibrils; these were connected, but smooth Z-lines passing through adjacent myofibrils had not yet appeared. The yellow arrows point to a striated structure that had appeared in the myofibril, but the length of the sarcomeres had yet to be adjusted to make the Z-discs connect with those in adjacent mature myofibrils to form long Z-lines. The yellow arrowhead point to an area where no striated structure was found (premyofibrils). (scale bar: 10μm)

The results show that 1) in the cell periphery (yellow arrows in Figure 3.4E), alpha-actinin and F-actin form I-Z-I structures, which are consistent with the description in the premyofibril model (the distance between Z-bodies in premyofibrils is 0.3~1.4 μm.) The combined image (Figure 3.4E) also supports our point of view that the alpha-actinin images (pointed by the yellow arrowheads in Figure 3.4G, 3.4H, and 3.4I, and green arrows in Figure 3.5B) that are obtained from the TPFE-SHG imaging system and arranged as dotted strips represent premyofibrils [56, 128, 129, 152]; 2) as premyofibrils transition towards striated mature myofibrils, myosin filaments start to appear, which is consistent with the description of the nascent myofibril in the premyofibril model; 3) the detected myosin filaments are distributed mainly in the central area of the cells or in the middle section of the myofibrils at the boundary of the cells (Figure 3.4F~3.4H, and 3.4J).

In the area where myosin filaments were dense (white arrowhead in Figure 4K), Z-discs in adjacent myofibrils were connected and had merged to form long smooth Z-lines through several myofibrils. In the area where myosin filaments were not dense (white arrows in Figure 3.4K), Z-discs in adjacent myofibrils were connected, but smooth Z-lines passing through adjacent myofibrils had not formed. In the area where myosin filaments were assembled at even lower density (yellow arrows in Figure 3.4K), striated structures had appeared in the myofibrils, but the length of the sarcomeres had not adjusted to allow the Z-discs to connect with the Z-discs in adjacent mature myofibrils to form long Z-lines. In the area of the myofibrils where no myosin filaments were detected, no striated structure was found (yellow arrowhead in Figure 3.4K, green arrows in Figure 3.5B). The results suggest that the assembly of myosin filaments to a sarcomere is

important in the rearrangement of Z-bodies in premyofibrils to form mature Z-discs. The transition from premyofibril to mature myofibril was observed to start with a low density of assembled myosin filaments on the sarcomere structure, but the maturation of sarcomeres and the formation of Z-lines were accompanied with a dense assembly of myosin filaments. Furthermore, in the area where myosin filaments began to assemble onto the myofibrils, the premyofibrils were cleaved by the assembled myosin filaments (Figure 5B, indicated by yellow arrow). When more myosin filaments assembled to the myofibrils, the cleaved premyofibrils became even thinner (Figure 3.5B, blue arrow) and finally disappeared totally when more myosin filaments were added (Figure 3.5B, red arrow).

When myosin filaments began to assemble onto the myofibrils at the place where a mature Z-disc would appear, the alpha-actinin-represented premyofibril extended laterally, but no cleavage of the fibrillar alpha-actinin pattern was found (Figure 3.5B, yellow arrowhead). This differed from the future A-band area where cleavage appeared (Figure 3.5B, yellow arrow). When more myosin filaments had assembled, the extended alpha-actinin cluster became thinner along the myofibril direction and elongated along the direction of the future mature Z-discs (Figure 3.5B, white arrow) until, when enough myosin filaments assembled onto the sarcomere, the alpha-actinin cluster became as thin as that of mature Z-discs. The cluster then connected with the adjacent mature Z-discs in neighboring myofibrils (Figure 3.5B, red arrow head). We observed that in the area where two cells connected, Z-discs labeled by alpha-actinin extended laterally out of the

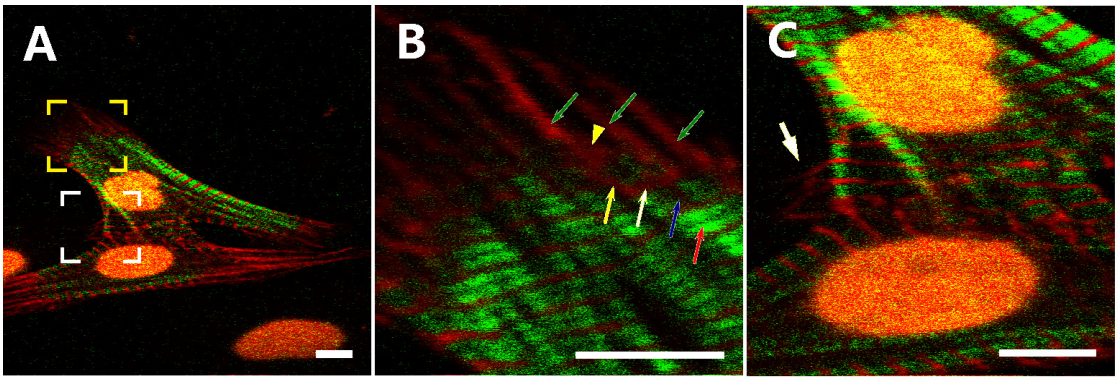

Figure 3.5 The myofibril structure of the cardiomyocytes cultured in vitro at Day 3. The cells were fixed and alpha-actinin was fluorescently labeled. The alpha-actinin (Red) pattern was acquired in the TPEF channel, and the myosin filament pattern (Green) was acquired in the SHG channel. A: The myofibril structure of two connected cardiomyocytes. B: Magnification of the area surrounded by the yellow brackets in (A). Green arrows: premyofibril, no myosin filaments assembled yet; yellow arrow: nascent myofibril—the premyofibril was cleaved by the assembled myosin filaments; yellow arrowhead: lateral extension of the myofibril where the Z-disc will appear in the future; white arrow: immature Z-disc that was thicker than the mature Z-disc; blue arrow: the cleaved premyofibril disappeared at the future A-band area, while more myosin filaments were being assembled to the sarcomere; red arrow: mature sarcomere—the cleaved premyofibril had totally disappeared at the A-band area. C: Magnification of the area surrounded by the white brackets. The white arrow indicates that the Z-discs extended laterally from the mature myofibril at the area where the two cardiomyocytes connected. (scale bar: 10μm)

myofibrils (Figure 3.5C, white arrow); this was different from the typical axial myofibril extension (Figure 3.5B, green arrows).

DISCUSSION

Previously, Yu and Russell reported that when neonatal cardiomyocytes were under static stretch achieved by 10% stretching of the PDMS elastic substrate, rupture appeared within one hour [148]. If new sarcomeres were added between mature sarcomeres in our experiment (Figure 3.2), some sarcomeres must have been broken to make space for the new ones. The cells were cultured on a glass surface, and no stretch was applied to the cells; we found no factors that might induce rupture in the mature myofibrils. Further, 40 minutes appeared to be too brief to allow the rupture of mature sarcomeres and addition of two new sarcomeres. Therefore, we infer that the new sarcomeres shown in Figure 2 were added to the end of the mature myofibrils.

In the template model proposed by Dlugosz et al. [151], the striated myofibril assembly is considered to be directed by a stress fiber-like structure that disappears as the myofibrils mature. The relationship between the molecules that comprise the stress fiber-like structure and the mature myofibrils is not explained in this model. Sanger et al. suggested that the templates should the nascent myofibrils themselves [158]. In Sanger's premyofibril model, the fibril structure of premyofibrils is formed by interdigitating nonmuscle myosin II filaments with actin filaments that contain muscle isoforms of troponins and tropomyosin, with the barbed ends of the actin filaments embedded in the Z-bodies . However, the premyofibril model does not explain the factors that cause those

sarcomeric proteins to align into fibrils and the mechanisms by which those fibrils are oriented.

In their review paper, Sparrow and Schöck proposed a model to extend the premyofibril model [71]. In this extended model, the bonding of Z-bodies to an integrin-dependent cell-matrix adhesion (ICA) was suggested as the starting point of myofibrillogenesis. Many techniques, such as the microcontact-printing technique [159] and the collagen alignment technique [160], have been applied to regulate the shape of cardiomyocytes and the orientation of myofibrils through control of the distribution of ICAs in the cell membrane. The success of these techniques supports the idea that the ICA paves the way for myofibrillogenesis. Our data (Figure 3.3, arrow-b and -c) indicate that, in addition to the alignment of ICAs, mature myofibrils can serve as a template for the alignment of new myofibrils. Our data that show the connection and merger of the Z-discs in adjacent myofibrils (Figure 3.4K) suggest that the templating function may be achieved through alignment of the Z-discs. Results shown in Figure 3.4F and 3.5B also indicate that Z-discs start to appear only when muscle myosin II filaments have been assembled onto the sarcomeric structure. Although these data were from stained cells, our live imaging data from the same type of cell culture (Figure 3.3) suggest that the myofibrillogenetic process we observed is consistent with that reported previously: The mature myofibrils are assembled through lateral fusion of adjacent thin fibrils mediated by Krp1 [93].

The models described in the introduction differ regarding whether new sarcomeres can be added serially to the end of growing or existing myofibrils. In the

premyofibril model, myofibrils are thought to elongate by deposition of premyofibrils that fuse with existing myofibrils by overlapping the tail of one premyofibril with the head of one existing myofibril . This description was based on the distribution of GFP-tagged alpha-actinin in live cardiomyocytes [161], in which the serial addition of myosin filaments along the premyofibrils was not observed. Our alpha-actinin staining images from the TPFE channel obtained simultaneously with our SHG images (Figure 3.4 and 3.5) demonstrate that the assembly of myosin filaments onto the sarcomere occurred later than the formation of premyofibrils and led to the serial maturation of premyofibrils at the tip of the existing mature myofibrils. These demonstrated observations are consistent with that reported in Holtzer's work, although the Holtzer group described their observation using the stitching model of assembling myosin filaments and I-Z-I bodies alternately at the tip of existing myofibrils [85, 88, 92] without formation of a premyofibril structure.

Based on the present results, we propose a model to describe the addition of myosin filaments to the tips of existing myofibrils (Figure 3.6). Initially, the aligned premyofibril (red) is cleaved by the lateral assembly of myosin filaments (green, Figure 3.6, A and B). This lateral addition of myosin filaments proceeds stepwise along the axial direction (Figure 3.6B). During the time when the myosin filaments are assembled onto a developing myofibril, the sarcomere length and the orientation of this myofibril may be affected by the adjacent mature myofibrils (Figure 3.6B); this probably occurs through the connection of sarcomlemma-related proteins such as desmin at the Z-disc area.

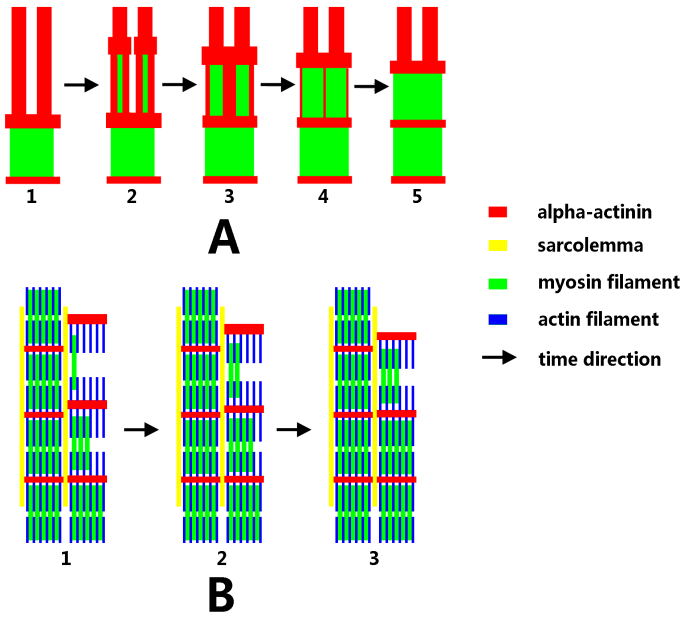

Figure 3.6 Schematic of the lateral assembly of myosin filaments onto myofibrils to mature the sarcomeres. (A) The assembly of myosin filaments cleaves the premyofibrils, rearranges the alpha-actinin to Z-disc area, and removes alpha-actinins from A-band area. The Z-disc becomes thinner during the maturation of the sarcomere. The sarcomere length becomes shorter while myosin filaments are assembling to the sarcomere. (B) The orientation and sarcomere length of the growing myofibril are affected by the adjacent mature myofibril. The myofibril aligns along the mature myofibril, and its Z-discs connect and merge with the adjacent Z-discs in the neighboring mature myofibril. The Z-discs become thinner during the maturation of the myofibril as myosin filaments are assembling to the myofibril.

CONCLUSION

In terms of our data obtained from the neonatal-cardiomyocyte cultures, we conclude that new sarcomere addition can occur at both the ends and the sides of existing myofibrils and at the interstice of several separated existing myofibrils. During the addition of sarcomeres, myosin filaments are assembled onto the myofibril laterally. This lateral addition proceeds stepwise along the axial direction, which plays an important role in the accumulation of Z-bodies to form mature Z-discs and the regulation of sarcomere length during maturation. Finally, our results demonstrate the advantages of our onstage incubator-combined TPEF-SHG imaging system for investigation of myofibril formation in live-cell culture. Additional work is necessary to discover how the related proteins interact with each other while myosin filaments are assembling onto the sarcomere.

CHAPTER FOUR

DISASSEMBLY OF MYOFIBRILS IN ADULT CARDIOMYOCYTES UNDER DEDIFFERENTIATION

Based on TPEF-SHG and immunocytology technique, we studied dedifferentiation of dissociated adult cardiomyocytes. The length change of sarcomere was analyzed during dedifferentiation. We found that myofibrils first shrink to shorten the sarcomere length, the striated structure of myofibrils was wrecked from the cell ends and then to the whole cell. our results suggest that the striated patterns of different sarcomeric components do not disassemble simultaneously during dedifferentiation. The striated pattern of myosin filaments was wrecked first, which was followed by the wreck of the striated F-actin pattern, then alpha-actinin. Our research will promote the understanding on the development of heart diseases and provide methods to assess the developing heart diseases.

INTRODUCTION

The primarily cultured adult cardiomyocytes have been widely used as a cell model of adult myocardium and shown increasing importance in the research of cardiology and cardiopathology . However, the fresh dissociated adult cardiomyocytes undergo dedifferentiation while they are cultured in vitro. The adult cardiomyocytes under dedifferentiation lose their rod-shape morphology and the striated myofibril structure, and accordingly, their normal physiological functions change [98, 106-109],

which weakens the advantages of dissociated adult cardiomyocytes as an ideal in-vitro model of the cardiomyocytes in myocardium. Therefore, prevention of dedifferentiation of adult cardiomyocytes is necessary when dissociated adult cardiomyocytes are in-vitro studied as substitution of myocardium. Efforts have been made to build a culture model of adult cardiomyocytes, with the morphology [117], contractile function , signaling system [117, 118], and etc. of the dissociated adult cardiomyocytes being preserved for longer time.

However, doesn't like the disadvantages mentioned above, dedifferentiation of cardiomyocytes may also be an advantageous function for the survival of cardiomyocytes in infarct border zones [121]. Observations have suggested that dedifferentiated cardiomyocytes represent an adaptive state [119], which enables the cardiomyocytes to survive under unfavorable circumstances [120]. Further study shows that regenerated heart muscle cells in amputated zebrafish heart are derived from the proliferation of differentiated cardiomyocytes that undergoing limited dedifferentiation, which was characterized by the disassembly of their sarcomeric structure, detachment from one another and the expression of regulators for cell-cycle progression [122].

Recent studies have indicated that dedifferentiated mature mammalian adult cardiomyocytes can also facilitate the proliferation of cardiomyocytes in myocardium, which confers a degree of stemness to the cells, including the expression of c-kit and the capacity for multipotency [123, 124]. Understanding of detailed features on the disassembly of sarcomere components of myofibrils while cardiomyocytes are under dedifferentiation will provide us the ability to precisely distinguish the stage or degree of

the cardiomyocyte dedifferentiation, which will promote the understanding on regeneration of the heart in diseases such as cardiac infarct [121].

Although the structure [135, 136], electro-physiological properties [106] and other cell functions of cardiomyocytes under dedifferentiation have been intensively studied, the dynamical structure change and redistribution of sarcomeric proteins of fresh-dissociated adult cardiomyocytes under dedifferentiation are lack. A recent emerged imaging technique based on second harmonic generation (SHG) and two-photon excitation fluorescence (TPEF) have shown the advantages of intrinsic high-resolution and high-contrast in biomedical research [143] and specifically, the study on dynamic remodel of myofibrils [155].

TPEF can be from a specific molecule that gives off fluorescence and thus can be used for investigating the arrangements of sarcomeric components in the myofibrils [138, 139]. SHG is a coherent nonlinear optical phenomenon that originates from polar molecules organized in noncentrosymmetric structures, such as the coiled rod region of myosin filaments in cardiomyocytes [130]. The characteristic of SHG enables us to study the specific structure without labeling any proteins and keep the cells living. The combination of TPEF and SHG (TPEF-SHG) can provide more structural information in a cardiomyocyte [133, 134], which is ideal for tracking how specific sarcomeric proteins are rearranged in relatively to myofibrils during dedifferentiation of the adult cardiomyocytes. The double wavelength and high excitation power requirement of TPEF and SHG can achieve a deeper penetration inside biological materials with higher 3D resolution than conventional single-photon excitation microscopy [142, 143].

In the previous research, dynamic sarcomere contractions in a living cardiomyocyte have been recorded for up to several minutes through SHG technique [131]. However, dedifferentiation of adult cardiomyocytes is a process that spans hours to days. Normal physiological conditions (temperature, humidity, pH value, etc.) are necessary to maintain the normal physiological processes inside the cardiomyocytes while the dedifferentiation process is recorded. Therefore, an incubating system that provides the required physiological conditions is required. We have developed a hybrid TPEF-SHG imaging system combined with onstage incubator to study the long term physiological process in heart muscle cells (up to 10 hours) [155, 156]. In this paper, we report the applications of our onstage incubator-combined TPEF-SHG imaging system to record the dedifferentiation process of living adult cardiomyocytes. Through combining the results from our customized TPEF-SHG imaging system and normal confocal system, we found that during dedifferentiation, the myofibrils in the dissociated adult cardiomyocytes first shrink to shorter the sarcomere length, and future more, the striated structure of myofibrils was wrecked from the cell ends and then which wreck extended to the whole cell. The results suggest that the striated patterns of different sarcomeric components were not wrecked simultaneously during dedifferentiation, and the end-by-end connection of the adult cardiomyocytes may play an important role in preventing the dedifferentiation of dissociated adult cardiomyocytes. The asynchronism of the wreck of normal pattern of different sarcomeric components provides us a novel way to understand the development of heart diseases and assess the developing heart diseases.

MATERIALS AND METHODS

Microscope System Setup (See chapter 2 for detailed description)

We have developed a hybrid TPEF-SHG polarization-imaging system with an onstage incubator that provides normal physiological conditions (37ºC, CO_2 (5%) and air (95%) with humidity) to dissociated cardiomyocytes during imaging of myofibrillogenesis [155]. The objective of the TPEF channel (60X W Objective) immerges into the culture media in the culture dish, and the condenser (1.4 oil condenser) of the SHG channel is adjusted as close as possible to the surface of the coverglass at the bottom of the culture dish to archive SHG image of best quality. Under this onstage incubator-combined TPEF-SHG imaging system, we have investigated the dynamic process of myofibrils in live neonatal cardiomyocytes for up to 10 hours [155].

Dissociation Of Adult Cardiomyocytes(See chapter 2 for detailed description)

The cardiomyocytes were harvested from the heart of 4-week-old adult Sprague–Dawley rats according to procedures approved by the Clemson University Institutional Animal Care and Use Committee. Detailed procedure has been described in other places[155]. Simply, after heparin injection (45 mg/kg) and anaesthesia (sodium pentobarbital 0.5ml/100g), the heart was removed from thorax and perfused with Ca^{2+}-free perfusion buffer and enzyme solution (30μM Ca^{2+}). Then the heart tissue was gently minced into small pieces (<1 mm^3) with fine forceps, and the tissue solution was agitated with a pipette until most of cells were dissociated from the tissue. After being separated from the undigested tissue in perfusion solution through centrifuge, the collected

cardiomyocytes experienced calcium reintroduction via adding $CaCl_2$ solution gradually, until the concentration of Ca^{2+} in the cell solution arrived at 1mM. Then the cell solution was centrifuged again to remove the perfusion solution and the cells were resuspended with fresh culture media containing 20% fetal bovine serum (FBS). The cells then were diluted into 50k cells/ml for study use.

Cell Culture And Imaging Procedure

The fresh dissociated adult cardiomyocytes were planted into 35mm glass-bottom culture dish coated with laminin (20μg/ml). The planted cells were incubated in a normal incubator for 5 hours to allow the cells attaching to the surface of the glass bottom. Then the culture media in the culture dish was changed very carefully to remove the unattached cells. The culture dish with attached cells was mounted onto the incubated TPEF-SHG imaging system. The cells to be studied were first identified through the polarized normal microscope of the imaging system. Then the cells were excited by the 810-nm femtosecond (fs) laser beam. The TPEF and SHG signals from the sample were collected through the TPEF and SHG channels, respectively. Two 2D images of the cell were reconstructed from the collected TPEF and SHG signals, respectively, and displayed on the monitor for real-time monitoring. The focus was adjusted to find the SHG image of the best quality. Time-lapse images were acquired from TPEF and SHG channels, respectively, and saved alternately in a single image stack at designated time intervals.

In another sample group, the cells were fixed with pure ethanol at day-0 under -20ºC, and then alpha-actinin and F-actin was fluorescently labeled with antibodies and

A488-phalloidin, respectively. In the sample group, the alpha-actinin and F-actin were not labeled in same sample, to make sure the relationship between alpha-actinin (TPEF) and myosin filaments (SHG), or F-actin (TPEF) and myosin filaments (SHG) were clearly demonstrated. After being immersed in mounting solution with DAPI, the fixed samples were mounted to the TPEF-SHG imaging system (onstage incubator removed). The cells to be studied were first indentified via the fluorescence channel of the imaging system. Then the cells were excited by the 810-nm fs laser beam. The TPEF and SHG signals from the samples were collected simultaneously through the two different channels.

In the third sample group, alpha-actinin and F-actin in the fixed cells (day-1) were double-labeled fluorescently with alpha-actinin antibody and A488-phalloidin. The cells were imaged under a Nikon Eclipse T*i* confocal microscope, images of alpha-actinin and F-actin were acquired from different channels simultaneously, for the study of the relationship between alpha-actinin and F-actin.

All the collected raw data of the 2D images was treated and reconstructed using ImageJ software (http://rsbweb.nih.gov/ij/), and edited in Microsoft® paint tool.

RESULTS

The structure change of the myofibrils of the adult cardiomyocytes was investigated in real time while the cells were under dedifferentiation. Figure 4.1 shows the dedifferentiation process of an adult cardiomyocytes on the incubator-combined TPEF-SHG imaging system. The end of the cell became round after 5-hour's incubation

since its dissociation from heart tissue (Figure 1A). The striated structure at the end of the cell was distorted and difficult to distinguish (Figure 4.1A, arrow head) and then totally disappeared after 4-hour's onstage incubation (Figure 4.1E, arrow head). Following the disappearance of striated structure at the cell end, the striated sarcomeric structure at the middle of the cell shrunk (compare the arrow heads and arrows in Figure 4.1A and 4.1D) and then totally disappeared (Figure 4.1E, arrow) after 4-hours' onstage incubation. Although the striated structure of the cell disappeared after 4-hour's onstage incubation, the SHG signal was still detected in the SHG channel (Figure 4.2E), indicates that the bundled myosin filaments still existed inside the cell. The result implies that at the early stage of dedifferentiation, the myosin filaments were rearranged to wreck the striated structure of sarcomeres, rather than disassembled into separated myosin monomers.

To study the change of sarcomere length during dedifferentiation, we rotated the cell in Figure1 in ImageJ software, to make the Z-discs oriented along the vertical direction. The gray value of the striated SHG pattern was measured and plotted in the ImageJ software (Figure 4.2). Figure 4.2A demonstrates that after 5-hour's incubation since the dissociation of the cells, 6 sarcomeres were embraced in the 14μm-long square, and one more sarcomere was embraced in the same square after 3 more hours' onstage incubation (Figure 4.2B), demonstrates that the sarcomeres shrunk during dedifferentiation.

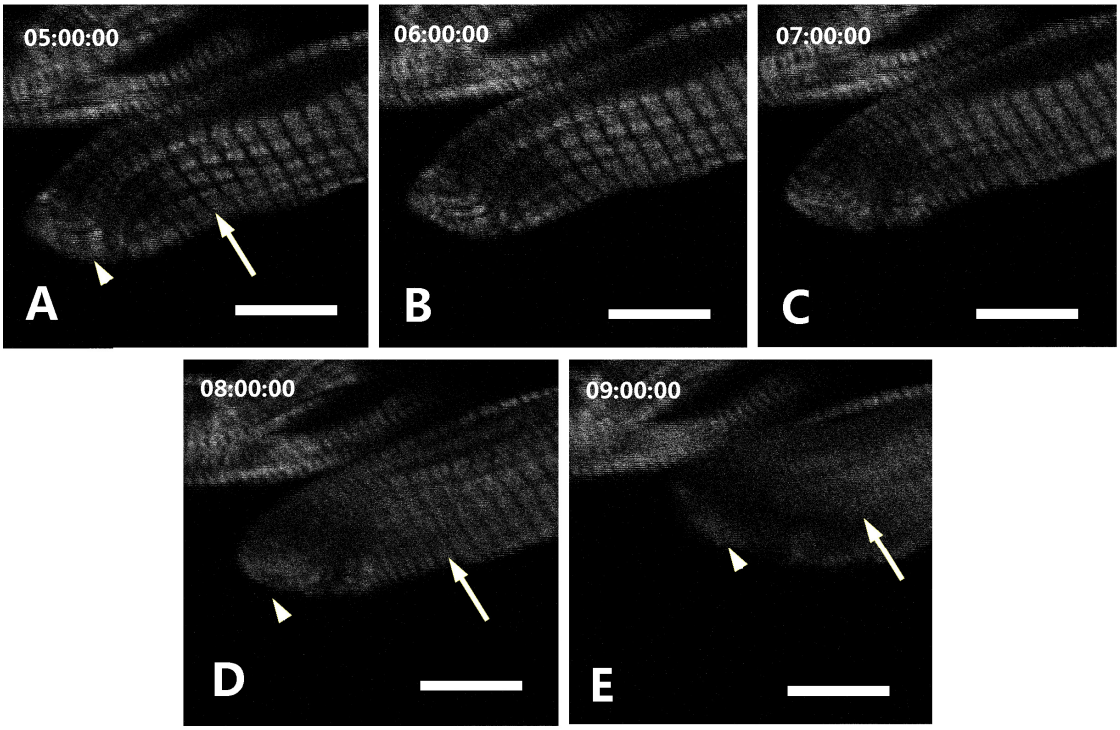

Figure 4.1 Dedifferentiation process of a living adult cardiomyocytes under incubated TPEF-SHG imaging system. Only signal from the SHG channel was collected. The time points (since the dissociation of the cells from the heart tissue) are embedded in hh:mm:ss format. (Scale bar: 10μm)

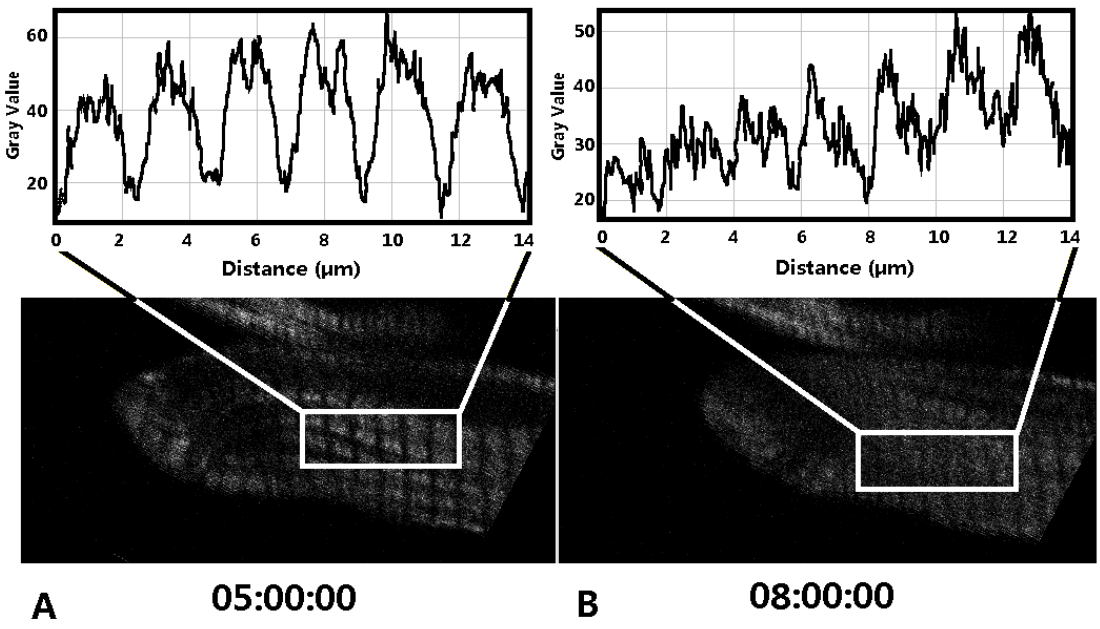

Figure 4.2 Quantification of sarcomeres in a specified area of the dedifferentiating adult cardiomyocyte displayed in Figure 4.1. The image of the cell presented in (A) and (B) was rotated by an angle relative to that in Figure 4.1 to make the plot's X-axes consistent with those of the images. The time points (since the dissociation of the cells from the heart tissue) are embedded in hh:mm:ss format.

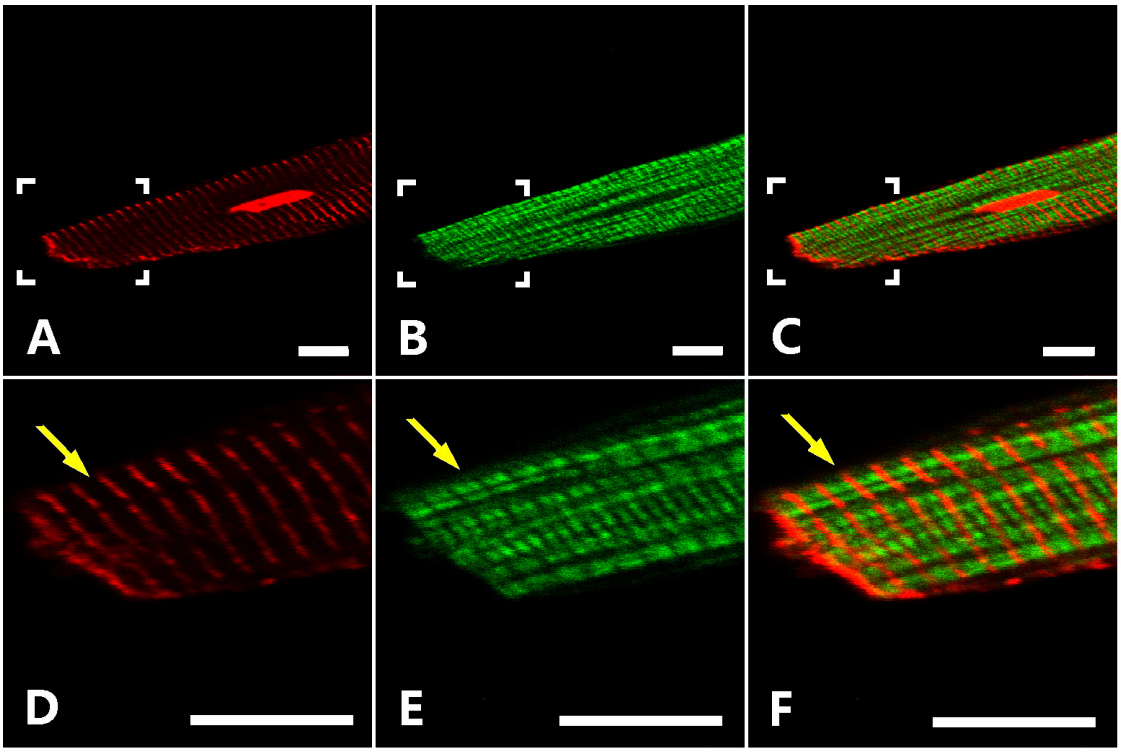

Figure 4.3 The myofibril structure of undedifferentiated adult cardiomyocytes. The cells were fixed and alpha-actinin was fluorescently labeled. The alpha-actinin (Red) pattern was acquired in the TPEF channel, and the myosin filament pattern (Green) was acquired in the SHG channel. D, E and F are magnification of images square-circled area in A, B and C, respectively. (Scale bar: 10μm)

To find out the structure change in molecule level while the adult cardiomyocytes were dedifferentiating, we fixed the cells at day-1, and fluorescently labeled the alpha-actinin and F-actin with antibodies and A488-phalloidin, respectively. The images that describe the distribution of alpha-actinin and F-actin inside the cells under dedifferentiation was rebuilt based on the data collected from the TPEF channel, and

which images were combined with the images describing the myosin filament pattern rebuilt from the data collected from the SHG channel (Figure 4.3~4.5), respectively. Figure 4.3 demonstrates an adult cardiomyocyte before dedifferentiation, where the striated pattern of myosin filaments and alpha-actinin are clearly demonstrated. The sarcomere length indicated by the distance between neighboring Z-discs (Figure 4.3A) is equal through the whole cell. Figure 4.4 demonstrates that, at the end of the cell where dedifferentiation happened, the distribution of alpha-actinin was condensed while the striated pattern was still distinguishable (Figure 4.4A, yellow arrow), but myosin filaments was evanescing (Figure 4.4B, yellow arrow). To clearly study the structure change of myofibrils during dedifferentiation, the areas circled by squares in Figure 4.4A~4.4C were magnified and displayed in Figure 4.4D~4.4F. Figure 4.4D~4.4F demonstrate that at the area where the striated myosin filament pattern was evanescing (yellow arrows), the sarcomere length (distance between neighboring Z-discs) was shorter than that where dedifferentiation was not apparently distinguishable (Figure 4.4D, 4.4E, white arrows). At some dedifferentiating area, the sarcomere length became even shorter than the length of normal A-band (compare the area indicated by the yellow arrow and arrow head in Figure 4.4F). At the area where dedifferentiation happened, although the detection of SHG signal indicated that the myosin filaments still existed, the striated pattern of myosin filaments was difficult to distinguish (Figure 4.4E, white arrow), and even totally disappeared when Z-discs were very close to each other (Figure 4.4E, yellow arrow). Fluorescent phalloidin-labeled F-actin demonstrates similar relationship with myosin filaments (Figure 4.5). The evanescing striated sarcomeric structure at the end of

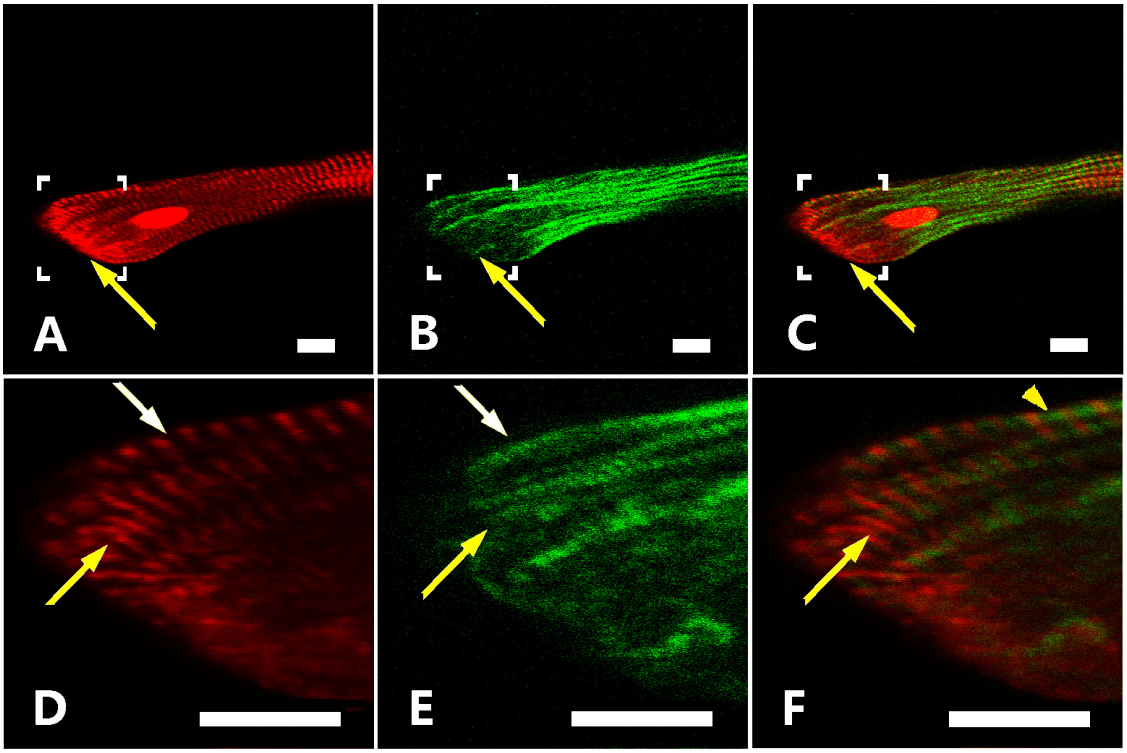

Figure 4.4 The myofibril structure of dedifferentiating adult cardiomyocytes. The cells were fixed and alpha-actinin was fluorescently labeled. The alpha-actinin (Red) pattern was acquired in the TPEF channel, and the myosin filament pattern (Green) was acquired in the SHG channel. D, E and F are magnification of images square-circled area in A, B and C, respectively. (Scale bar: 10μm)

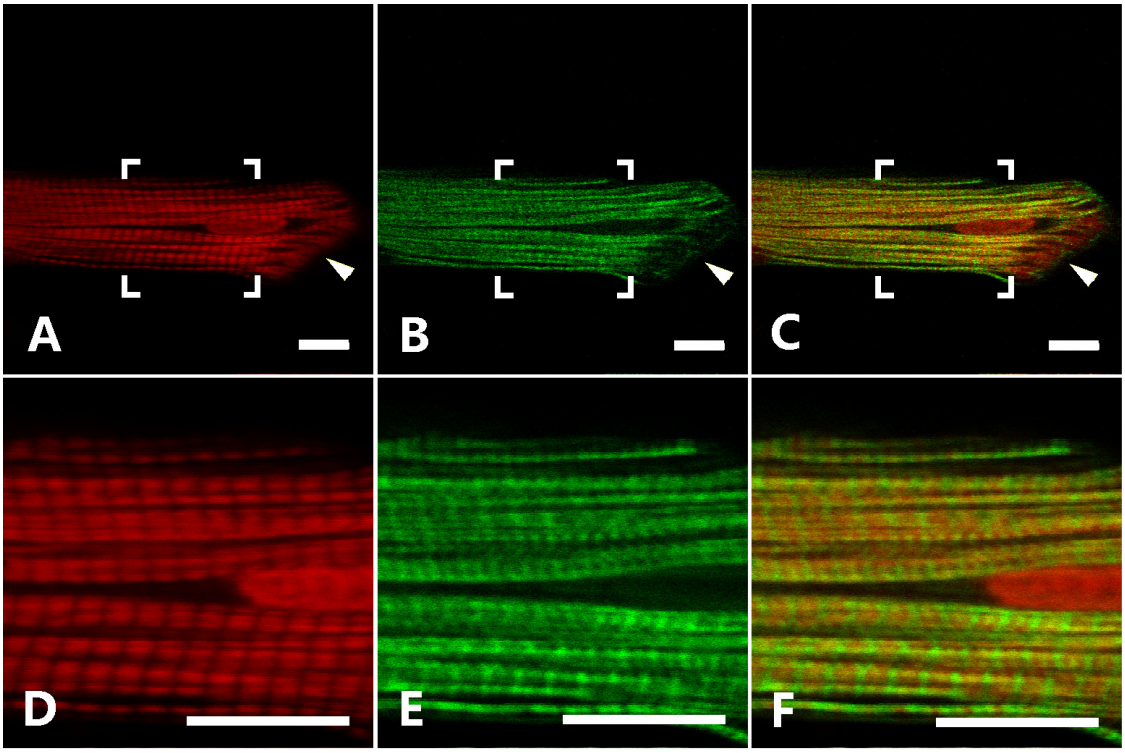

Figure 4.5 The myofibril structure of dedifferentiating adult cardiomyocytes. The cells were fixed and F-actin was fluorescently labeled. The F-actin (Red) pattern was acquired in the TPEF channel, and the myosin filament pattern (Green) was acquired in the SHG channel. D, E and F are magnification of images square-circled area in A, B and C, respectively. The evanescing striated sarcomeric structure at the end of the cell indicated by F-actin (arrow heads) was companied by the evanescing myosin filaments indicated by weakened SHG signal (arrow heads). (Scale bar: 10μm)

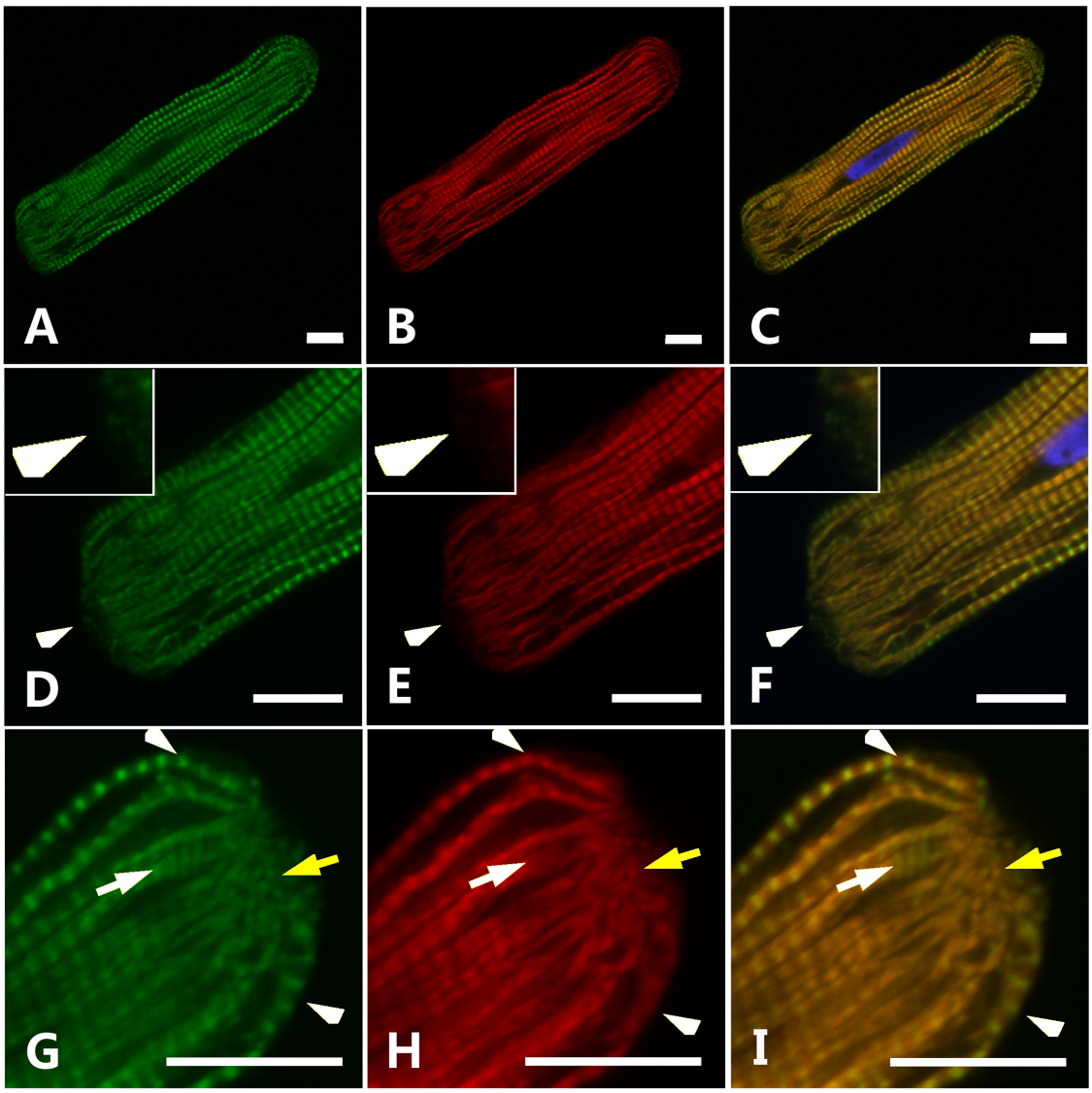

Figure 4.6 The myofibril structure of dedifferentiating adult cardiomyocytes. The cells were fixed at day-1, alpha-actinin (green), F-actin (red) and nuclear (blue) were fluorescently labeled. The images were acquired from a Nikon Eclipse T*i* confocal system. D, E and F are magnification of the lower end of the cell in A, B and C, respectively. The small panels in D, E and F are magnification of the very tip of the cell end. G, H and I are magnification of the upper end of the cell in A, B and C, respectively.

(Figure 4.6, continued)

The white arrow heads in D, E and F indicate the Z-body-like mini bodies with alpha-actinin and F-actin appear together. The white arrows in G, H and I indicate that at some area where striated pattern of F-actin was not distinguishable, the striated pattern of alpha-actinin was still visible. The shrinkage of myofibril causes the wreck of the striated structure of the myofibrils (yellow arrows), while bending of myofibrils do not (white arrow heads). (Scale bar: 10μm)

the cell indicated by F-actin (arrow heads in Figure 4.5A) was companied with weakened SHG signal (Figure 4.5B, arrow head), which suggests the decrease of myosin filaments. At the middle area of the cell (Figure 4.5D-4.5F), although the striated F-actin pattern looked normal (Figure 4.5D) and the SHG signal from myosin filament structure was still strong (Figure 4.5E), the dark gaps between neighboring SHG pattern disappeared, and the A-band area in one sarcomere was difficult to distinguish from that in neighboring sarcomeres (compare Figure 4.3E and Figure 4.5E).

It is known that, at the early stage of myofibrillogenesis, F-actin and alpha-actinin assemble into Z-bodies at the areas where close to cell periphery [83]. To find out the relationship between F-actin and alpha-actinin while an adult cardiomyocyte is under dedifferentiation, we fixed the cells at day-1, and labeled alpha-actinin and F-actin fluorescently with alpha-actinin antibody and A488-phalloidin, respectively. The results in Figure 6~7 demonstrate that, at different dedifferentiation stages, overlap of the stained alpha-actinin and F-actin patterns could be found, implying that alpha-actinin and F-actin

were still related during dedifferentiation. However, the distribution of alpha-actinin and F-actin were not exactly the same when dedifferentiation progressed future. At the initial stage of the dedifferentiation (Figure 4.6), the cell ends shrunk and where the patterns of F-actin and alpha-actinin well overlapped (Figure 4.6D~4.6I). However, we can notice that at some area, the striated pattern of F-actin became obscure, while that of alpha-actin was still distinguishable (Figure 4.6G~4.6I, white arrows), implies that the striated structure of F-actin may be impaired before that of alpha-actinin. At areas where myofibrils shrunk along their axis, striated structure disappeared and the alpha-actinin and F-actin randomly distributed as small dots (Figure 4.6G~4.6I, yellow arrows), while at areas where myofibrils were bending because of dedifferentiation, striated structure was still visible (Figure 4.6G~4.6I, white arrow heads). These results suggest that shrinkage of myofibril along the axis is more likely to impair the striated structure of the myofibrils and induce dedifferentiation. It is interesting to notice that, at the very tip of the dedifferentiating end of the cell, alpha-actinin and F-actin appeared together as mini dots and spread at the substrate away from the cell (Figure 4.6D~4.6F, white arrow heads), which is very similar to the Z-bodies in premyofibrils during myofibrillogenesis [90], while no such mini dots were found at the cell surface where striated structure were clearly visible and no dedifferentiation appeared. This result implies that the redifferentiation is more likely to appear where dedifferentiation happens while adult cardiomyocytes are cultured and spread at the substrates.

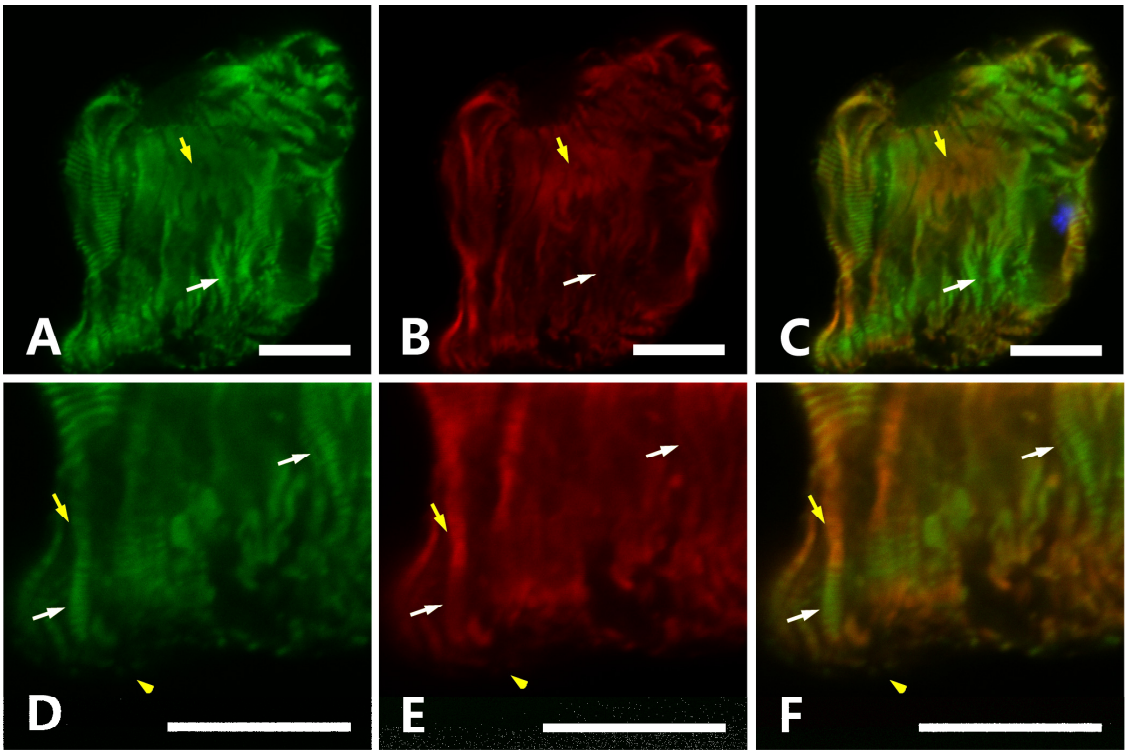

Figure 4.7 The myofibril structure of dedifferentiating adult cardiomyocytes. The cells were fixed, alpha-actinin (green), F-actin (red) and nuclear (blue) were fluorescently labeled. The images were acquired from a Nikon Eclipse T*i* confocal system. D, E and F are magnification of the lower part in A, B and C, respectively. The yellow arrows indicate that at the areas where F-actin was heavily stained, the alpha-actinin was lightly stained. The white arrows indicate that at the areas where alpha-actin was heavily stained, the F-actin was lightly stained. The yellow arrow heads indicate the Z-body-like mini bodies with alpha-actinin and F-actin appear together. (Scale bar: 10μm)

In future dedifferentiated adult cardiomyocytes, the patterns of alpha-actinin and F-actin were still overlapped, but the distribution of the staining density of the two proteins was different (Figure 4.7). At some areas where alpha-actinin was heavily stained, F-actin was relatively lightly stained (Figure 4.7, white arrows), or vice versa (Figure7, yellow arrows). At the very tip of the cell end where dedifferentiation happened, Z-body-like mini bodies appeared (Figure 4.7, yellow arrow heads). These results future imply that although alpha-actinin and F-actin were still related during the dedifferentiation of adult cardiomyocytes, they intend to redistribute separately, and combined together to form Z-body-like mini dots at the cell periphery where redifferentiation might appear.

DISCUSSION

The dedifferentiation was found to first appeared at the ends of the fresh dissociated adult cardiomyocytes (Figure 4.1 and 4.6). At the area where dedifferentiation appeared, the sarcomere length became shorter, and the striated sarcomere structure disappeared gradually. The results demonstrate that the striated pattern of myosin filament (A-bands) was wrecked by the rearrangement of the myosin filaments. That the striated pattern of alpha-actinin (Z-discs) and F-actin (thin filaments) were still visible implies that different sarcomeric components do not disassemble synchronously during. The results suggest that myosin filaments disassemble from the mature sarcomere before Z-discs and actin filaments disassemble.

In the myocardium, the cardiomyocytes connect with their neighboring cardiomyocytes end-by-end through the intercalated discs. The existence of intercalated discs assures that a single sarcomere is under pulling forces exerted at the Z-discs of its both ends while a cardiomyocyte is contracting and relaxing during systole and diastole, respectively. But the condition is different for the dissociated adult cardiomyocytes. The intercalated discs are broken while the cardiomyocytes are dissociated from the myocardium. Therefore, no end-by-end connections exist between different cells, which causes that, at most time, the pulling forces exerted at both ends of the sarcomere is inequivalent and the direction of the resultant force points to the middle of the cell. For the sarcomeres close to the ends of the cell, because there are more sarcomeres at the close-to-cell-middle side of the specified sarcomere than that close to the end side, the resultant force to the sarcomeres at the cell ends is larger than that to the sarcomeres at the cell middle, which leads to lower internal stress at the titins in the sarcomeres at the cell ends, and causes those sarcomeres are more difficult to get relaxed after contraction, which results the impaired contracting function of the sarcomeres and causes the sarcomeres at cell ends become shorter and shrink to cell middle. It has been found that contraction is helpful in preserving the function and structure of dissociated cardiomyocytes [141]. Therefore, the contracting function-impaired sarcomeres close to the cell ends may lead to the dedifferentiation starts from the ends of the dissociated adult cardiomyocytes, as displayed in Figure 1. Based on the above discussion, contracting function of the sarcomeres at the middle area of the cell may also be impaired and weakly affect the striated structure at the middle of the cell (Figure 4.4 and 4.5). Therefore, the

dedifferentiation of the dissociated adult cardiomyocytes starts from the ends of the cells and then extends to the whole cell.

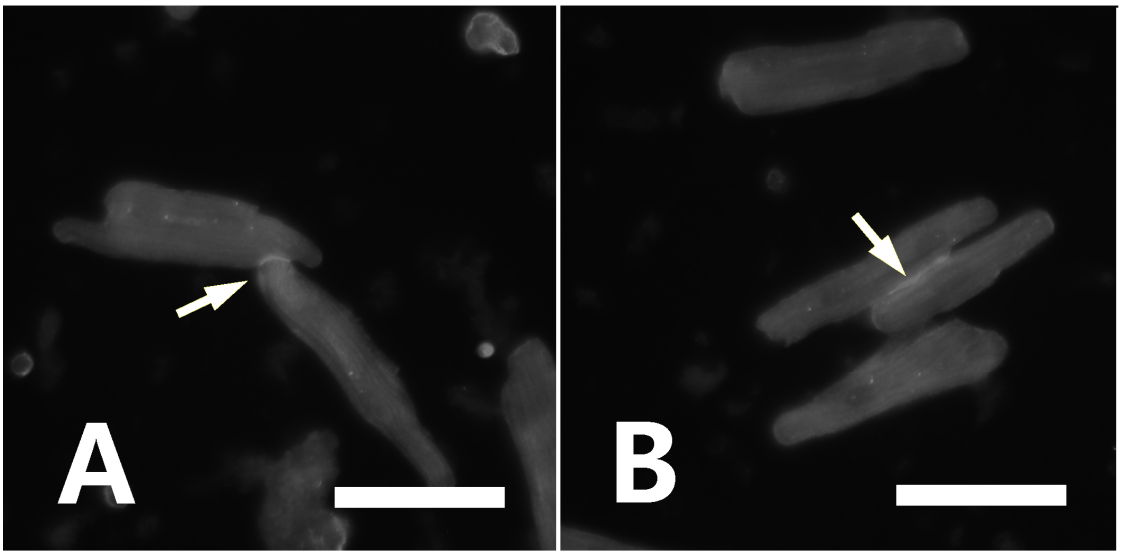

Figure 4.8 N-Cadherin of fresh dissociated adult cardiomyocytes. The arrows indicate the connections labeled by N-Cadherin 2 hours after the cells were dissociated from heart tissue. (scale bar: 50μm)

Alpha-actinin and F-actin were related at the very early dedifferentiating stage of adult cardiomyocytes (Figure 4.6). It seems that the striated structure of F-actin was wrecked before that of alpha-actinin during dedifferentiation (Figure 4.6, white arrows). Since F-actin is filamentous, similar with myosin filaments, the wrecking of the striated pattern of F-actin before that of alpha-actinin may also caused by the shrinkage of myofibrils, which wiped off the gaps between neighboring F-actin filaments along the axis of myofibrils. The different staining density of alpha-actinin and F-actin patterns in some areas (Figure 4.7, white and yellow arrows) implies that some alpha-actinin may

detach from the F-actin filaments and aggregate in other area. Alpha-actinin and F-actin have been found to appear together as mini bodies called "Z-bodies" close to cell periphery in the early stage of myofibrillogenesis while cultured cardiomyocytes are spreading at the substrate [90]. Similar phenomena also appeared at the cell periphery where dedifferentiation happened (Figure 4.6, white arrow heads; Figure 4.7, yellow arrow heads). The result that the Z-body-like mini bodies are close the dedifferentiating area implies that the reassembly of new myofibrils is related with the dedifferentiation of old myofibrils. But whether these Z-body-like mini bodies at the cell periphery are assembled through recruiting the alpha-actinin detached from the previous myofibrils is still unclear.

Based on the discussion above, end-by-end connection is necessary to build an in vitro model of dissociated adult cardiomyocytes that preserves the rod-shape morphology of the adult cardiomyocytes and striated structure of myofibrils for longer time. We have observed in the experiments that N-Cadherin junctions may form when fresh dissociated adult cardiomyocytes contact each other within 2 hours (Figure 4.8). These results encourage us to build an end-by-end connected adult cardiomyocytes culture model in the future through our custom developed laser micropatterning technique [157].

However, we should note that end-by-end connection between dissociated adult cardiomyocytes may not only provide mechanotransduction between the connected cells to maintain the stress equivalence of the sarcomeres, but also transfer chemicals between the cells through formed chemical channels, which may also affect the phonotype

preservation of the adult cardiomyocytes. How the stress equivalence affects the remodel of myofibrils and the phonotype of the adult cardiomyocytes still needs more efforts.

CONCLUSION

Our present research suggests that dedifferentiation happens from the ends of adult cardiomyocytes while the adult cardiomyocytes are cultured in vitro, and the sarcomeres become shorter during dedifferentiation. During dedifferentiation, the striated structure of myofibrils are destroyed, while the striated patterns of different sarcomeric components are not affected simultaneously. The order that the striated patterns of the current investigated sarcomeric components are affected by the dedifferentiation is supposed to be myosin/thick filaments, actin/thin filaments, and then alpha-actinin (the central component of Z-discs). The dedifferentiation of adult cardiomyocytes within short time after dissociation is a big obstacle for the application of dissociated adult cardiomyocytes as a substitution of myocardium. Our results suggest that rebuilding the intercalated discs between dissociated adult cardiomyocytes through end-by-end connection may be a potential culture model of cardiomyocytes for cardiology research. In our future work, the orders that different sarcomere components (alpha-actinin, F-actin, and myomesin, etc.) disassemble from the mature myofibrils will be studied while dissociated adult cardiomyocytes are dedifferentiating.

CHAPTER FIVE

CONCLUSIONS AND PROSPECTIVE

CONCLUSIONS

Several models have been proposed to describe the process of myofibrillogensis, the main divergence among which lies on how myosin filaments are assembled onto the myofibrils. Immunocytology and fluorescence protein (FP) technique have been applied in the previous researches on myofibrillogensis from other groups. Immunocytology technique can provide adequate results for the analysis on the relationship between different sarcomeric components in building a detailed description of sarcomere structure, and determine the time order that different sarcomeric components are assembled onto the myofibrils on the basis of logical analysis. But the lacking of dynamic investigation via immunocytology causes that many detailed features of myofibrillogensis are not able to be noticed and confirmed, such as the maturation of sarcomeres along the current myofibrils proposed in this dissertation (chapter 3). The FP technique allows researchers to track the movement of specific proteins while they are assembling onto the myofibrils in living cells, and enable the researchers to build a dynamic model of myofibrillogenesis [147]. But the shortage of FP technique is that FP-labeled proteins always emit fluorescence and can not enable the researcher to determine whether the FP-labeled proteins have been combined into a specific structure, such as determining the formation of myosin filaments. The SHG technique is developed based on a coherent nonlinear optical phenomenon that second harmonic wave originates from polar molecules

organized in noncentrosymmetric structures, such as the coiled rod region of myosin filaments in cardiomyocytes [130]. The noncentrosymmetric structure-dependent characteristic provides researchers the ability to determine the formation of myosin filaments, because no second harmonic wave emits from single myosin molecule. The SHG technique makes it possible to investigate the dynamic process of myosin filaments onto the myofibrils in living cardiomyocytes. Most of the current researchers who are applying SHG technique in biology study are interested in the analysis of static cellular structure [132, 162] or short term dynamic process in cardiomyocytes [131]. The myofibrillogenesis (or dedifferentiation) of cardiomyocytes is a dynamic process that spans hours to days, normal physiological conditions (temperature, humidity, pH value, etc.) are necessary to maintain normal physiological processes inside the cardiomyocytes while myofibrillogenesis (or dedifferentiation) is recorded.

To meet the requirements of the research, we have combined an onstage incubator with the customized TPEF-SHG imaging system, which enables us to investigate those process in long time while keeping the cells living [155, 156], and obtain the results that can not be acquired through traditional immunocytology and FP techniques. Therefore we can draw conclusions that are currently not able to be made by other groups.

In the research of myofibrillogensis in neonatal cardiomyocytes, we found that new sarcomere addition can occur at both the ends and the sides of existing myofibrils and at the interstice of several separated existing myofibrils. During the addition of sarcomeres, myosin filaments are assembled onto the myofibril laterally, and which lateral addition proceeds stepwise along the axial direction to plays an important role in

the accumulation of Z-bodies to form mature Z-discs and the regulation of sarcomere length during maturation of myofibril. The results also demonstrate that our imaging system is a powerful tool for investigating the prolonged process of myofibrillogenesis of a single cardiomyocyte.

In the research of dedifferentiation of adult cardiomyocytes, based on our results, we propose that dedifferentiation happens from the ends of adult cardiomyocytes while the adult cardiomyocytes are cultured in vitro, with the sarcomeres become shorter. While the striated structure of myofibrils are destroyed during dedifferentiation, the striated patterns of different sarcomeric components are not affected simultaneously. The striated patterns of myosin/thick filaments are destroyed before that of actin/thin filaments, and the following wreck of alpha-actinin (the central component of Z-discs).

PROSPECTIVE OF MYOFIBRILLOGENESIS AND DEDIFFERENTIATION IN CARDIOLOGY RESEARCH

Myofibrillogenesis

Myosin filaments and titin molecules are bound together to form the thick filaments in the middle of sarcomeres by myomesin at M-band [163] and Myosin binding protein-C in the C-zone [70], etc. We have proposed that myosin filaments are assembled laterally to the myofibrils in single sarcomere, but how nonmuscle myosin IIB is substituted by muscle myosin II while myofibrils mature is still unclear.

Sarcomere is probably the most complex molecular structure in human body. Hundreds of proteins are involved during the assembling and remodeling processes of sarcomeres. Heavy efforts have been put into the investigation on the myofibrillogenesis and dedifferentiation of cardiomyocytes in the passed years. Several models on myofibrillogenesis have been proposed for the purpose of describing the sequence that the major sarcomeric structure components are assembled onto myofibrils [85]. The fact is, many chaperone proteins that are not sarcomeric structure components have been involved into the process of myofibrillogenesis. Such as N-RAP [95, 164], UNC-45 [165], and nonmuscle myosin IIB [90, 95], etc. Those chaperone proteins assist the synthesis of sarcomeric structure components and their assembly to myofibrils. Many chemical stimulators [166, 167] and sarcomeric structure proteins [53, 168] are also involved into the signaling path ways to regulate the synthesis of sarcomeric proteins and remodel of sarcomeres. But there is not a model on myofibrillogenesis has currently been proposed to involve the chaperones, chemical and mechanical signaling path ways, and which should be involved in the future model on myofibrillogenesis.

Dedifferentiation of Cardiomyocytes

The structure [135, 136], electro-physiological properties [106] and other cell functions of cardiomyocytes under dedifferentiation [101, 169] have been intensively studied since the viable adult ventricular cardiomyocytes were dissociated and cultured [170, 171]. Dissociated adult cardiomyocytes dedifferentiate to change their phenotype within short time, such as rod-shape morphology and contraction in response to electrical

stimulation [98]. That is a big obstacle for the application of dissociated adult cardiomyocytes as substitution of myocardium. Many efforts have been made to build a cell culture model to preserve the in-vivo phenotype of adult cardiomyocytes for longer time [117, 118, 172], as well as understand the mechanism of dedifferentiation of adult cardiomyocyes [106, 107]. However, a complete model on dedifferentiation of adult cardiomyocytes has not been built yet. To build a detailed description of dedifferentiation of adult cardiomyocytes, the following features should be involved:

1) The factors that may introduce the dedifferentiation of adult cardiomyocytes, which might include chemical and mechanical stimulation to the cells;
2) The path ways that the adult cardiomyocytes respond to the dedifferentiation stimulations;
3) The sequences that different sarcomeric components are disassembled from the myofibrils, in response to the dedifferentiation stimulations;
4) The transition from dedifferentiation status to redifferetiation status;

Observations have suggested that dedifferentiated cardiomyocytes represent an adaptive state [119], which enables the cardiomyocytes to survive under unfavorable circumstances [120], such as the survival of the cardiomyocytes in infarct border zones [121]. Why the dedifferentiation allows the cardiomyocytes survive under abnormal circumstances is unclear, which might be benefitted from the research, as aforementioned, on the factors that may introduce the dedifferentiation of adult cardiomyocytes.

The mammalian adult cardiomyocytes have long been considered to be terminally dedifferentiated and do not proliferate. But the cardiomyocytes in more primitive animals, such as zebrafish, have been proved to dedifferentiate and proliferate to regenerate amputated cardiac muscle [122]. Future more, recent research indicated that dedifferentiation of mammalian cardiomyocytes may also facilitate the proliferation cardiomyocytes and confer a degree of stemness, including the expression of c-kit and the capacity for multipotency [123]. However, how and when the multipotency of dedifferentiated mammalian cardiomyocytes is activated is not known. These research motivate us to comprehensively assess the value of dedifferentiation when dissociated adult cardiomyocytes are applied as substitute for myocardium in our research. The study on dedifferentiation of adult cardiomyocytes can not only promote our work on finding a way to preserve the in-vivo morphology of adult cardiomyocytes in vitro, but also help us to understand how adult cardiomyocytes could be induced into cell cycle to promote the self repair of injured myocardium.

Myofibrillogenesis and dedifferentiation of cardiomyocytes may be the two sides of one coin. Although they look like demonstrating opposite remodel processes in cardiomyocytes, the dedifferentiation and redifferetiation (myofibrillogenesis) may transform from one status to another at specific conditions. Therefore, a unified understanding on myofibrillogenesis and dedifferentiation will help us to comprehensively understand the remodel process of myofibrils and promote the progress on the study of heart diseases.

REFERENCES

1. Kamisago, M., et al., *Mutations in sarcomere protein genes as a cause of dilated cardiomyopathy.* New England Journal of Medicine, 2000. **343**(23): p. 1688-1696.
2. Chang, A.N. and J.D. Potter, *Sarcomeric protein mutations in dilated cardiomyopathy.* Heart Failure Reviews, 2005. **10**(3): p. 225-35.
3. Oldfors, A. and P.J. Lamont, *Thick filament diseases.* Advances in experimental medicine and biology, 2008. **642**: p. 78-91.
4. Oldfors, A., *Hereditary myosin myopathies.* Neuromuscular disorders : NMD, 2007. **17**(5): p. 355-67.
5. Oldfors, A., et al., *Myopathies associated with myosin heavy chain mutations.* Acta myologica : myopathies and cardiomyopathies : official journal of the Mediterranean Society of Myology / edited by the Gaetano Conte Academy for the study of striated muscle diseases, 2004. **23**(2): p. 90-6.
6. Cammarato, A., et al., *Myosin transducer mutations differentially affect motor function, myofibril structure, and the performance of skeletal and cardiac muscles.* Molecular Biology of the Cell, 2008. **19**(2): p. 553-62.
7. Tajsharghi, H., *Thick and thin filament gene mutations in striated muscle diseases.* International journal of molecular sciences, 2008. **9**(7): p. 1259-75.
8. Tardiff, J.C., *Thin filament mutations: developing an integrative approach to a complex disorder.* Circulation Research, 2011. **108**(6): p. 765-82.
9. Mirza, M., et al., *Dilated cardiomyopathy mutations in three thin filament regulatory proteins result in a common functional phenotype.* The Journal of biological chemistry, 2005. **280**(31): p. 28498-506.
10. Frank, D., et al., *The sarcomeric Z-disc: a nodal point in signalling and disease.* Journal of molecular medicine, 2006. **84**(6): p. 446-68.
11. Selcen, D. and O. Carpen, *The Z-disk diseases.* Advances in experimental medicine and biology, 2008. **642**: p. 116-30.
12. Harada, K., et al., *Pressure overload induces cardiac hypertrophy in angiotensin II type 1A receptor knockout mice.* Circulation, 1998. **97**(19): p. 1952-9.
13. Usui, S., et al., *Endogenous muscle atrophy F-box mediates pressure overload-induced cardiac hypertrophy through regulation of nuclear factor-kappaB.* Circ Res, 2011. **109**(2): p. 161-71.
14. Chiang, C.S., et al., *The Ca(v)3.2 T-type Ca(2+) channel is required for pressure overload-induced cardiac hypertrophy in mice.* Circ Res, 2009. **104**(4): p. 522-30.

15. Ruzicka, M., V. Skarda, and F.H. Leenen, *Effects of ACE inhibitors on circulating versus cardiac angiotensin II in volume overload-induced cardiac hypertrophy in rats.* Circulation, 1995. **92**(12): p. 3568-73.

16. Lear, W., M. Ruzicka, and F.H. Leenen, *ACE inhibitors and cardiac ACE mRNA in volume overload-induced cardiac hypertrophy.* The American journal of physiology, 1997. **273**(2 Pt 2): p. H641-6.

17. Turcani, M. and H. Rupp, *Development of pressure overload induced cardiac hypertrophy is unaffected by long-term treatment with losartan.* Mol Cell Biochem, 1998. **188**(1-2): p. 225-33.

18. Zierhut, W. and H.G. Zimmer, *Significance of myocardial alpha- and beta-adrenoceptors in catecholamine-induced cardiac hypertrophy.* Circ Res, 1989. **65**(5): p. 1417-25.

19. Simpson, P., *Stimulation of hypertrophy of cultured neonatal rat heart cells through an alpha 1-adrenergic receptor and induction of beating through an alpha 1- and beta 1-adrenergic receptor interaction. Evidence for independent regulation of growth and beating.* Circ Res, 1985. **56**(6): p. 884-94.

20. Feenstra, J., et al., *Drug-induced heart failure.* J Am Coll Cardiol, 1999. **33**(5): p. 1152-62.

21. Russell, B., D. Motlagh, and W.W. Ashley, *Form follows function: how muscle shape is regulated by work.* J Appl Physiol, 2000. **88**(3): p. 1127-32.

22. Lehman, W., et al., *Tropomyosin and actin isoforms modulate the localization of tropomyosin strands on actin filaments.* Journal of Molecular Biology, 2000. **302**(3): p. 593-606.

23. Labeit, S. and B. Kolmerer, *Titins: giant proteins in charge of muscle ultrastructure and elasticity.* Science, 1995. **270**(5234): p. 293-6.

24. Trinick, J., *Interaction of titin/connectin with the thick filament.* Advances in biophysics, 1996. **33**: p. 81-90.

25. Moncman, C.L. and K. Wang, *Nebulette: a 107 kD nebulin-like protein in cardiac muscle.* Cell Motil Cytoskeleton, 1995. **32**(3): p. 205-25.

26. Esham, M., et al., *Expression of nebulette during early cardiac development.* Cell Motility and the Cytoskeleton, 2007. **64**(4): p. 258-73.

27. Moncman, C.L. and K. Wang, *Targeted disruption of nebulette protein expression alters cardiac myofibril assembly and function.* Exp Cell Res, 2002. **273**(2): p. 204-18.

28. Purevjav, E., et al., *Nebulette mutations are associated with dilated cardiomyopathy and endocardial fibroelastosis.* Journal of the American College of Cardiology, 2010. **56**(18): p. 1493-502.

29. Moncman, C.L. and K. Wang, *Functional dissection of nebulette demonstrates actin binding of nebulin-like repeats and Z-line targeting of SH3 and linker domains.* Cell Motility and the Cytoskeleton, 1999. **44**(1): p. 1-22.

30. Bonzo, J.R., et al., *The nebulette repeat domain is necessary for proper maintenance of tropomyosin with the cardiac sarcomere.* Experimental Cell Research, 2008. **314**(19): p. 3519-3530.

31. Gokhin, D.S. and V.M. Fowler, *Tropomodulin capping of actin filaments in striated muscle development and physiology.* Journal of biomedicine & biotechnology, 2011. **2011**: p. 103069.

32. Tsukada, T., et al., *Leiomodin-2 is an antagonist of tropomodulin-1 at the pointed end of the thin filaments in cardiac muscle.* Journal of Cell Science, 2010. **123**(18): p. 3136-3145.

33. Chereau, D., et al., *Leiomodin is an actin filament nucleator in muscle cells.* Science, 2008. **320**(5873): p. 239-243.

34. Casella, J.F., et al., *Cap-Z(36-32), a Barbed End Actin-Capping Protein, Is a Component of the Z-Line of Skeletal-Muscle.* Journal of Cell Biology, 1987. **105**(1): p. 371-379.

35. Schafer, D.A., J.A. Waddle, and J.A. Cooper, *Localization of Capz during Myofibrillogenesis in Cultured Chicken Muscle.* Cell Motility and the Cytoskeleton, 1993. **25**(4): p. 317-335.

36. Schafer, D.A., C. Hug, and J.A. Cooper, *Inhibition of Capz during Myofibrillogenesis Alters Assembly of Actin-Filaments.* Journal of Cell Biology, 1995. **128**(1-2): p. 61-70.

37. Sellers, J.R., *Myosins: a diverse superfamily.* Biochimica Et Biophysica Acta-Molecular Cell Research, 2000. **1496**(1): p. 3-22.

38. Blankenfeldt, W., et al., *Crystal structures of human cardiac beta-myosin II S2-Delta provide insight into the functional role of the S2 subfragment.* Proc Natl Acad Sci U S A, 2006. **103**(47): p. 17713-7.

39. Jung, H.S., et al., *Head-head and head-tail interaction: a general mechanism for switching off myosin II activity in cells.* Mol Biol Cell, 2008. **19**(8): p. 3234-42.

40. Knappeis, G.G. and F. Carlsen, *The ultrastructure of the M line in skeletal muscle.* The Journal of cell biology, 1968. **38**(1): p. 202-11.

41. Wang, S.M., et al., *Role of M-line proteins in sarcomeric titin assembly during cardiac myofibrillogenesis.* Journal of Cellular Biochemistry, 1998. **71**(1): p. 82-95.

42. Xu, X.L., W. Huang, and R.L. Zhang, *Myofibrillogenesis in the developing zebrafish heart: A functional study of tnnt2.* Developmental Biology, 2009. **331**(2): p. 237-249.

43. Eppenberger, H.M., et al., *The Mr 165,000 M-protein myomesin: a specific protein of cross-striated muscle cells.* The Journal of cell biology, 1981. **89**(2): p. 185-93.

44. Grove, B.K., et al., *A new 185,000-dalton skeletal muscle protein detected by monoclonal antibodies.* The Journal of cell biology, 1984. **98**(2): p. 518-24.

45. van der Ven, P.F., et al., *Assignment of the human gene for endosarcomeric cytoskeletal M-protein (MYOM2) to 8p23.3.* Genomics, 1999. **55**(2): p. 253-5.

46. Price, M.G., *Skelemins - Cytoskeletal Proteins Located at the Periphery of M-Disks in Mammalian Striated-Muscle.* Journal of Cell Biology, 1987. **104**(5): p. 1325-1336.

47. Agarkova, I. and J.C. Perriard, *The M-band: an elastic web that crosslinks thick filaments in the center of the sarcomere.* Trends in Cell Biology, 2005. **15**(9): p. 477-485.

48. Fukuzawa, A., et al., *Interactions with titin and myomesin target obscurin and obscurin-like 1 to the M-band: implications for hereditary myopathies.* Journal of Cell Science, 2008. **121**(Pt 11): p. 1841-51.

49. Kontrogianni-Konstantopoulos, A., et al., *Muscle Giants: Molecular Scaffolds in Sarcomerogenesis.* Physiological Reviews, 2009. **89**(4): p. 1217-1267.

50. Schoenauer, R., et al., *Myomesin 3, a novel structural component of the M-band in striated muscle.* Journal of Molecular Biology, 2008. **376**(2): p. 338-351.

51. Hornemann, T., et al., *Muscle-type creatine kinase interacts with central domains of the M-band proteins myomesin and M-protein.* Journal of Molecular Biology, 2003. **332**(4): p. 877-87.

52. Obermann, W.M., et al., *The structure of the sarcomeric M band: localization of defined domains of myomesin, M-protein, and the 250-kD carboxy-terminal region of titin by immunoelectron microscopy.* The Journal of cell biology, 1996. **134**(6): p. 1441-53.

53. Will, R.D., et al., *Myomasp/LRRC39, a heart- and muscle-specific protein, is a novel component of the sarcomeric M-band and is involved in stretch sensing.* Circulation Research, 2010. **107**(10): p. 1253-64.

54. Lange, S., et al., *Dimerisation of myomesin: implications for the structure of the sarcomeric M-band.* Journal of Molecular Biology, 2005. **345**(2): p. 289-98.

55. van der Ven, P.F. and D.O. Furst, *Assembly of titin, myomesin and M-protein into the sarcomeric M band in differentiating human skeletal muscle cells in vitro.* Cell Structure and Function, 1997. **22**(1): p. 163-71.

56. Ehler, E., et al., *Myofibrillogenesis in the developing chicken heart: assembly of Z-disk, M-line and the thick filaments.* Journal of Cell Science, 1999. **112 (Pt 10)**: p. 1529-39.

57. Schoenauer, R., et al., *Myomesin is a molecular spring with adaptable elasticity.* Journal of Molecular Biology, 2005. **349**(2): p. 367-379.

58. Bertoncini, P., et al., *Study of the mechanical properties of myomesin proteins using dynamic force spectroscopy.* Journal of Molecular Biology, 2005. **348**(5): p. 1127-1137.

59. Pinotsis, N., et al., *Superhelical architecture of the Myosin filament-linking protein myomesin with unusual elastic properties.* PLoS biology, 2012. **10**(2): p. e1001261.

60. Lange, S., E. Ehler, and M. Gautel, *From A to Z and back? Multicompartment proteins in the sarcomere.* Trends in Cell Biology, 2006. **16**(1): p. 11-8.

61. Gautel, M., P. Young, and E. Ehler, *Obscurin, a giant sarcomeric Rho guanine nucleotide exchange factor protein involved in sarcomere assembly.* Journal of Cell Biology, 2001. **154**(1): p. 123-136.

62. Borisov, A.B., et al., *Essential role of obscurin in cardiac myofibrillogenesis and hypertrophic response: evidence from small interfering RNA-mediated gene silencing.* Histochemistry and Cell Biology, 2006. **125**(3): p. 227-238.

63. Kontrogianni-Konstantopoulos, A., et al., *Obscurin regulates the organization of myosin into A bands.* American Journal of Physiology-Cell Physiology, 2004. **287**(1): p. C209-C217.

64. Okagaki, T., et al., *The major myosin-binding domain of skeletal muscle MyBP-C (C protein) resides in the COOH-terminal, immunoglobulin C2 motif.* The Journal of cell biology, 1993. **123**(3): p. 619-26.

65. Freiburg, A. and M. Gautel, *A molecular map of the interactions between titin and myosin-binding protein C - Implications for sarcomeric assembly in familial hypertrophic cardiomyopathy.* European Journal of Biochemistry, 1996. **235**(1-2): p. 317-323.

66. Squire, J.M., P.K. Luther, and C. Knupp, *Structural evidence for the interaction of C-protein (MyBP-C) with actin and sequence identification of a possible actin-binding domain.* Journal of Molecular Biology, 2003. **331**(3): p. 713-24.

67. Weber, F.E., et al., *Complete sequence of human fast-type and slow-type muscle myosin-binding-protein C (MyBP-C). Differential expression, conserved domain structure and chromosome assignment.* European journal of biochemistry / FEBS, 1993. **216**(2): p. 661-9.

68. Gautel, M., et al., *Phosphorylation switches specific for the cardiac isoform of myosin binding protein-C: a modulator of cardiac contraction?* The EMBO journal, 1995. **14**(9): p. 1952-60.

69. Flashman, E., et al., *Cardiac myosin binding protein C: its role in physiology and disease.* Circulation Research, 2004. **94**(10): p. 1279-89.

70. Oakley, C.E., et al., *Myosin binding protein-C: enigmatic regulator of cardiac contraction.* The international journal of biochemistry & cell biology, 2007. **39**(12): p. 2161-6.

71. Sparrow, J.C. and F. Schock, *The initial steps of myofibril assembly: integrins pave the way.* Nature Reviews Molecular Cell Biology, 2009. **10**(4): p. 293-298.

72. Luther, P.K., *Three-dimensional reconstruction of a simple Z-band in fish muscle.* The Journal of cell biology, 1991. **113**(5): p. 1043-55.

73. Young, P., et al., *Molecular structure of the sarcomeric Z-disk: two types of titin interactions lead to an asymmetrical sorting of alpha-actinin.* Embo Journal, 1998. **17**(6): p. 1614-1624.

74. Balogh, J., et al., *Desmin filaments influence myofilament spacing and lateral compliance of slow skeletal muscle fibers.* Biophysical Journal, 2005. **88**(2): p. 1156-65.

75. Fuseler, J.W. and J.W. Shay, *The association of desmin with the developing myofibrils of cultured embryonic rat heart myocytes.* Developmental Biology, 1982. **91**(2): p. 448-57.

76. Samuel, J.L., et al., *Myofibrillar organization and desmin in rat heart myocytes.* Basic Research in Cardiology, 1985. **80 Suppl 2**: p. 119-22.

77. Hijikata, T., et al., *Plectin is a linker of intermediate filaments to Z-discs in skeletal muscle fibers.* Journal of Cell Science, 1999. **112**(6): p. 867-876.

78. Schroder, R., et al., *Association of plectin with Z-discs is a prerequisite for the formation of the intermyofibrillar desmin cytoskeleton.* Laboratory Investigation, 2000. **80**(4): p. 455-464.

79. Knoll, R., et al., *The cardiac mechanical stretch sensor machinery involves a Z disc complex that is defective in a subset of human dilated cardiomyopathy.* Cell, 2002. **111**(7): p. 943-955.

80. Meder, B., et al., *JunB-CBFbeta signaling is essential to maintain sarcomeric Z-disc structure and when defective leads to heart failure.* Journal of Cell Science, 2010. **123**(Pt 15): p. 2613-20.

81. Frey, N., et al., *Mice lacking calsarcin-1 are sensitized to calcineurin signaling and show accelerated cardiomyopathy in response to pathological biomechanical stress.* Nature Medicine, 2004. **10**(12): p. 1336-43.

82. Perriard, J.C., et al., *Myofibrillogenesis in the developing chicken heart: assembly of Z-disk, M-line and the thick filaments.* Journal of Cell Science, 1999. **112**(10): p. 1529-1539.

83. Carroll, S., et al., *N-RAP scaffolds I-Z-I assembly during myofibrillogenesis in cultured chick cardiomyocytes.* Journal of Cell Science, 2004. **117**(1): p. 105-114.

84. Boateng, S.Y. and P.H. Goldspink, *Assembly and maintenance of the sarcomere night and day.* Cardiovascular Research, 2008. **77**(4): p. 667-675.

85. Sanger, J.W., et al., *How to build a myofibril.* Journal of Muscle Research and Cell Motility, 2005. **26**(6-8): p. 343-354.

86. Sanger, J.W., et al., *Assembly and Dynamics of Myofibrils.* Journal of Biomedicine and Biotechnology, 2010.

87. Schultheiss, T., et al., *Differential Distribution of Subsets of Myofibrillar Proteins in Cardiac Nonstriated and Striated Myofibrils.* Journal of Cell Biology, 1990. **110**(4): p. 1159-1172.

88. Holtzer, H., et al., *Independent assembly of 1.6 microns long bipolar MHC filaments and I-Z-I bodies.* Cell Structure and Function, 1997. **22**(1): p. 83-93.

89. Ojima, K., et al., *Initiation and maturation of I-Z-I bodies in the growth tips of transfected myotubes.* Journal of Cell Science, 1999. **112 (Pt 22)**: p. 4101-12.

90. Rhee, D., J.M. Sanger, and J.W. Sanger, *The premyofibril: evidence for its role in myofibrillogenesis.* Cell Motil Cytoskeleton, 1994. **28**(1): p. 1-24.

91. Du, A., et al., *Myofibrillogenesis in the first cardiomyocytes formed from isolated quail precardiac mesoderm.* Developmental Biology, 2003. **257**(2): p. 382-94.

92. Lu, M.H., et al., *The vinculin/sarcomeric-alpha-actinin/alpha-actin nexus in cultured cardiac myocytes.* The Journal of cell biology, 1992. **117**(5): p. 1007-22.

93. Horowits, R., et al., *Krp1 (Sarcosin) promotes lateral fusion of myofibril assembly intermediates in cultured mouse cardiomyocytes.* Experimental Cell Research, 2008. **314**(5): p. 1177-1191.

94. Srikakulam, R. and D.A. Winkelmann, *Chaperone-mediated folding and assembly of myosin in striated muscle.* Journal of Cell Science, 2004. **117**(Pt 4): p. 641-52.

95. Lu, S.J. and R. Horowits, *Role of nonmuscle myosin IIB and N-RAP in cell spreading and myofibril assembly in primary mouse cardiomyocytes.* Cell Motility and the Cytoskeleton, 2008. **65**(9): p. 747-761.

96. Borisov, A.B., et al., *Dynamics of obscurin localization during differentiation and remodeling of cardiac myocytes: Obscurin as an integrator of myofibrillar structure.* Journal of Histochemistry & Cytochemistry, 2004. **52**(9): p. 1117-1127.

97. Burrows, M.T., *Rhythmical Activity of Isolated Heart Muscle Cells in Vitro.* Science, 1912. **36**(916): p. 90-2.

98. Mitcheson, J.S., J.C. Hancox, and A.J. Levi, *Cultured adult cardiac myocytes: future applications, culture methods, morphological and electrophysiological properties.* Cardiovascular Research, 1998. **39**(2): p. 280-300.

99. Welder, A.A., et al., *A Primary Culture System of Adult-Rat Heart-Cells for the Study of Toxicologic Agents.* In Vitro Cellular & Developmental Biology, 1991. **27**(12): p. 921-926.

100. Jacobson, S.L. and H.M. Piper, *Cell-Cultures of Adult Cardiomyocytes as Models of the Myocardium.* Journal of Molecular and Cellular Cardiology, 1986. **18**(7): p. 661-678.

101. Bugaisky, L.B. and R. Zak, *Differentiation of adult rat cardiac myocytes in cell culture.* Circ Res, 1989. **64**(3): p. 493-500.

102. Nag, A.C. and M.L. Lee, *Breakdown and rebuilding of myofibrils in cultured adult cardiac muscle cells.* Tsitologiia, 1997. **39**(10): p. 907-12.

103. Nag, A.C. and M. Cheng, *Adult mammalian cardiac muscle cells in culture.* Tissue & Cell, 1981. **13**(3): p. 515-523.

104. Nag, A.C., et al., *Long-term cell culture of adult mammalian cardiac myocytes: electron microscopic and immunofluorescent analyses of myofibrillar structure.* Journal of Molecular and Cellular Cardiology, 1983. **15**(5): p. 301-17.

105. Nag, A.C., M.L. Lee, and F.H. Sarkar, *Remodelling of adult cardiac muscle cells in culture: Dynamic process of disorganization and reorganization of myofibrils.* Journal of Muscle Research and Cell Motility, 1996. **17**(3): p. 313-334.

106. Guinamard, R., et al., *Characterization of a Ca2+-activated nonselective cation channel during dedifferentiation of cultured rat ventricular cardiomyocytes.* The Journal of membrane biology, 2002. **188**(2): p. 127-35.

107. Rosenblatt-Velin, N., et al., *Insulin resistance in adult cardiomyocytes undergoing dedifferentiation: role of GLUT4 expression and translocation.* Faseb Journal, 2004. **18**(3): p. 872-+.

108. Fares, N., J.P. Gomez, and D. Potreau, *T-type calcium current is expressed in dedifferentiated adult rat ventricular cells in primary culture.* Comptes Rendus De L Academie Des Sciences Serie Iii-Sciences De La Vie-Life Sciences, 1996. **319**(7): p. 569-576.

109. Spach, M.S. and J.P. Boineau, *Microfibrosis produces electrical load variations due to loss of side-to-side cell connections: A major mechanism of structural heart disease arrhythmias.* Pace-Pacing and Clinical Electrophysiology, 1997. **20**(2): p. 397-413.

110. New, R.B., et al., *Isolated left ventricular myocyte contractility in patients undergoing cardiac operations.* J Thorac Cardiovasc Surg, 1998. **116**(3): p. 495-502.

111. Ellingsen, O., et al., *Adult rat ventricular myocytes cultured in defined medium: phenotype and electromechanical function.* The American journal of physiology, 1993. **265**(2 Pt 2): p. H747-54.

112. Lipp, P., et al., *Spatially non-uniform Ca2+ signals induced by the reduction of transverse tubules in citrate-loaded guinea-pig ventricular myocytes in culture.* The Journal of Physiology, 1996. **497**: p. 9.

113. Kawai, M., M. Hussain, and C.H. Orchard, *Excitation-contraction coupling in rat ventricular myocytes after formamide-induced detubulation.* The American journal of physiology, 1999. **277**(2 Pt 2): p. H603-9.

114. Pavlovic, D., L.M. McLatchie, and M.J. Shattock, *The rate of loss of T-tubules in cultured adult ventricular myocytes is species dependent.* Experimental physiology, 2010. **95**(4): p. 518-527.

115. Kraushaar, U., et al., *A primary culture system for sustained expression of a calcium sensor in preserved adult rat ventricular myocytes.* Cell Calcium, 2008. **43**(1): p. 59-71.

116. Berger, H.J., et al., *Continual Electric-Field Stimulation Preserves Contractile Function of Adult Ventricular Myocytes in Primary Culture.* American Journal of Physiology, 1994. **266**(1): p. H341-H349.

117. Viero, C., et al., *A primary culture system for sustained expression of a calcium sensor in preserved adult rat ventricular myocytes.* Cell Calcium, 2008. **43**(1): p. 59-71.

118. Volz, A., et al., *Longevity of adult ventricular rat heart muscle cells in serum-free primary culture.* Journal of Molecular and Cellular Cardiology, 1991. **23**(2): p. 161-73.

119. Driesen, R.B., et al., *Structural adaptation in adult rabbit ventricular myocytes: influence of dynamic physical interaction with fibroblasts.* Cell Biochem Biophys, 2006. **44**(1): p. 119-28.

120. Ausma, J., et al., *Dedifferentiated cardiomyocytes from chronic hibernating myocardium are ischemia-tolerant.* Mol Cell Biochem, 1998. **186**(1-2): p. 159-68.

121. Dispersyn, G.D., et al., *Dissociation of cardiomyocyte apoptosis and dedifferentiation in infarct border zones.* Eur Heart J, 2002. **23**(11): p. 849-57.

122. Jopling, C., et al., *Zebrafish heart regeneration occurs by cardiomyocyte dedifferentiation and proliferation.* Nature, 2010. **464**(7288): p. 606-9.

123. Zhang, Y., et al., *Dedifferentiation and proliferation of mammalian cardiomyocytes.* Plos One, 2010. **5**(9): p. e12559.

124. Engel, F.B., et al., *p38 MAP kinase inhibition enables proliferation of adult mammalian cardiomyocytes.* Genes & development, 2005. **19**(10): p. 1175-87.

125. Dispersyn, G.D., et al., *Adult rabbit cardiomyocytes undergo hibernation-like dedifferentiation when co-cultured with cardiac fibroblasts.* Cardiovascular Research, 2001. **51**(2): p. 230-240.

126. Kubin, T., et al., *Oncostatin M Is a Major Mediator of Cardiomyocyte Dedifferentiation and Remodeling.* Cell Stem Cell, 2011. **9**(5): p. 420-432.

127. Russell, B., et al., *Mechanical stress-induced sarcomere assembly for cardiac muscle growth in length and width.* J Mol Cell Cardiol, 2010. **48**.

128. Van der Ven, P.F., et al., *Thick filament assembly occurs after the formation of a cytoskeletal scaffold.* J Muscle Res Cell Motil, 1999. **20**(5-6): p. 569-79.

129. Pizon, V., et al., *Transient association of titin and myosin with microtubules in nascent myofibrils directed by the MURF2 RING-finger protein.* Journal of Cell Science, 2002. **115**(Pt 23): p. 4469-82.

130. Plotnikov, S.V., et al., *Characterization of the myosin-based source for second-harmonic generation from muscle sarcomeres.* Biophysical Journal, 2006. **90**(2): p. 693-703.

131. Prent, N., et al., *Intermyofilament dynamics of myocytes revealed by second harmonic generation microscopy.* J Biomed Opt., 2008. **13**.

132. Pavone, F.S., et al., *Probing myosin structural conformation in vivo by second-harmonic generation microscopy.* Proceedings of the National Academy of Sciences of the United States of America, 2010. **107**(17): p. 7763-7768.

133. Barzda, V., et al., *Visualization of mitochondria in cardiomyocytes by simultaneous harmonic generation and fluorescence microscopy.* Optics Express, 2005. **13**(20): p. 8263-8276.

134. Kee, T.W., et al., *Second-harmonic generation and two-photon-excited autofluorescence microscopy of cardiomyocytes: quantification of cell volume and myosin filaments.* Journal of Biomedical Optics, 2008. **13**(6).

135. Spahr, R., et al., *Morphological Dedifferentiation of Adult Cardiac Myocytes in Coculture with Hepatocytes.* Basic Research in Cardiology, 1985. **80**: p. 83-86.

136. Horackova, M. and Z. Byczko, *Differences in the structural characteristics of adult guinea pig and rat cardiomyocytes during their adaptation and maintenance in long-term cultures: Confocal microscopy study.* Experimental Cell Research, 1997. **237**(1): p. 158-175.

137. Stephens, D.J. and V.J. Allan, *Light microscopy techniques for live cell imaging.* Science, 2003. **300**(5616): p. 82-6.

138. Robu, V.G., et al., *Localization of functional endothelin receptor signaling complexes in cardiac transverse tubules.* The Journal of biological chemistry, 2003. **278**(48): p. 48154-61.

139. Marcelle, C., J. Gros, and O. Serralbo, *WNT11 acts as a directional cue to organize the elongation of early muscle fibres.* Nature, 2009. **457**(7229): p. 589-U97.

140. So, P.T.C., et al., *Two-photon excitation fluorescence microscopy.* Annual Review of Biomedical Engineering, 2000. **2**: p. 399-429.

141. Decker, M.L., et al., *Morphometric evaluation of the contractile apparatus in primary cultures of rabbit cardiac myocytes*. Circ. Res. 1991. **69**: p. 86-94.

142. Svoboda, K. and R. Yasuda, *Principles of two-photon excitation microscopy and its applications to neuroscience.* Neuron, 2006. **50**(6): p. 823-39.

143. Zipfel, W.R., R.M. Williams, and W.W. Webb, *Nonlinear magic: multiphoton microscopy in the biosciences.* Nat Biotechnol, 2003. **21**(11): p. 1369-77.

144. Boulesteix, T., et al., *Second-harmonic microscopy of unstained living cardiac myocytes: measurements of sarcomere length with 20-nm accuracy.* Optics Letters, 2004. **29**(17): p. 2031-2033.

145. Recher, G., et al., *Three distinct sarcomeric patterns of skeletal muscle revealed by SHG and TPEF microscopy.* Optics Express, 2009. **17**(22): p. 19763-77.

146. Barzda, V., et al., *Visualization of mitochondria in cardiomyocytes by simultaneous harmonic generation and fluorescence microscopy.* Optics Express, 2005. **13**(20): p. 8263-76.

147. Dabiri, G.A., et al., *Myofibrillogenesis visualized in living embryonic cardiomyocytes.* Proceedings of the National Academy of Sciences of the United States of America, 1997. **94**(17): p. 9493-9498.

148. Yu, J.G. and B. Russell, *Cardiomyocyte remodeling and sarcomere addition after uniaxial static strain in vitro.* Journal of Histochemistry & Cytochemistry, 2005. **53**(7): p. 839-44.

149. Carroll, S., et al., *N-RAP scaffolds I-Z-I cardiomyocytes assembly during myofibrillogenesis in cultured chick cardiomyocytes.* Biophysical Journal, 2004. **86**(1): p. 70a-70a.

150. Carroll, S.L. and R. Horowits, *Expression of N-RAP, a nebulin-related LIM protein, during myofibrillogenesis in cultured chick cardiomyocytes.* Molecular Biology of the Cell, 1999. **10**: p. 169a-169a.

151. Dlugosz, A.A., et al., *The Relationship between Stress Fiber-Like Structures and Nascent Myofibrils in Cultured Cardiac Myocytes.* Journal of Cell Biology, 1984. **99**(6): p. 2268-2278.

152. Rhee, D., J.M. Sanger, and J.W. Sanger, *The Premyofibril - Evidence for Its Role in Myofibrillogenesis.* Cell Motility and the Cytoskeleton, 1994. **28**(1): p. 1-24.

153. Pizon, V., et al., *Transient association of titin and myosin with microtubules in nascent myofibrils directed by the MURF2 RING-finger protein.* Journal of Cell Science, 2002. **115**(23): p. 4469-4482.

154. Du, A.P., et al., *Myofibrillogenesis in the first cardiomyocytes formed from isolated quail precardiac mesoderm.* Developmental Biology, 2003. **257**(2): p. 382-394.

155. Liu, H., et al., *Myofibrillogenesis in live neonatal cardiomyocytes observed with hybrid two-photon excitation fluorescence-second harmonic generation microscopy.* Journal of Biomedical Optics, 2011. **16**(12): p. 126012.

156. Shao, Y.H., *3D myofibril imaging in live cardiomyocytes via hybrid SHG-TPEF microscopy* Proc. SPIE, 2011. **7903**.

157. Ma, Z., et al., *Laser-guidance-based cell deposition microscope for heterotypic single-cell micropatterning*. Biofabrication, 2011. **3**(3): p. 034107.

158. Sanger, J.M., et al., *Myofibrillogenesis in Living Cells Microinjected with Fluorescently Labeled Alpha-Actinin.* Journal of Cell Biology, 1986. **102**(6): p. 2053-2066.

159. Bray, M.A., S.P. Sheehy, and K.K. Parker, *Sarcomere alignment is regulated by myocyte shape.* Cell Motility and the Cytoskeleton, 2008. **65**(8): p. 641-651.

160. Walsh, K.B. and G.E. Parks, *Changes in cardiac myocyte morphology alter the properties of voltage-gated ion channels.* Cardiovasc Res, 2002. **55**(1): p. 64-75.

161. Dabiri, G.A., et al., *Use of green fluorescent proteins linked to cytoskeletal proteins to analyze myofibrillogenesis in living cells.* Green Fluorescent Protein, 1999. **302**: p. 171-186.

162. Vogel, M., et al., *Second Harmonic Generation Microscopy Probes Different States of Motor Protein Interaction in Myofibrils.* Biophysical Journal, 2010. **99**(6): p. 1842-1851.

163. Obermann, W.M., et al., *Molecular structure of the sarcomeric M band: mapping of titin and myosin binding domains in myomesin and the identification of a potential regulatory phosphorylation site in myomesin.* The EMBO journal, 1997. **16**(2): p. 211-20.

164. Dhume, A., S. Lu, and R. Horowits, *Targeted disruption of N-RAP gene function by RNA interference: a role for N-RAP in myofibril organization.* Cell Motility and the Cytoskeleton, 2006. **63**(8): p. 493-511.

165. Melkani, G.C., et al., *The UNC-45 Chaperone Is Critical for Establishing Myosin-Based Myofibrillar Organization and Cardiac Contractility in the Drosophila Heart Model.* Plos One, 2011. **6**(7).

166. Sugden, P.H., *An overview of endothelin signaling in the cardiac myocyte.* J Mol Cell Cardiol, 2003. **35**(8): p. 871-86.

167. Malekar, P., et al., *Wnt Signaling Is Critical for Maladaptive Cardiac Hypertrophy and Accelerates Myocardial Remodeling.* Hypertension, 2010. **55**(4): p. 939-U234.

168. Gautel, M., *The sarcomeric cytoskeleton: who picks up the strain?* Current Opinion in Cell Biology, 2011. **23**(1): p. 39-46.

169. Poling, J., et al., *The Janus face of OSM-mediated cardiomyocyte dedifferentiation during cardiac repair and disease.* Cell Cycle, 2012. **11**(3): p. 439-45.

170. Jacobson, S.L., *Culture of Spontaneously Contracting Myocardial-Cells from Adult Rats.* Cell Structure and Function, 1977. **2**(1): p. 1-9.

171. Powell, T. and V.W. Twist, *A rapid technique for the isolation and purification of adult cardiac muscle cells having respiratory control and a tolerance to calcium.* Biochem Biophys Res Commun, 1976. **72**(1): p. 327-33.

172. Berger, H.J., et al., *Continual electric field stimulation preserves contractile function of adult ventricular myocytes in primary culture.* The American journal of physiology, 1994. **266**(1 Pt 2): p. H341-9.